AEDC-TR-69-68

5(13

TRIPLE COLLISION EFFECTS IN THE THERMAL CONDUCTIVITY AND VISCOSITY OF MODERATELY DENSE GASES

J. V. Sengers
National Bureau of Standards
Washington, D. C.

March 1969

ARNOLD ENGINEERING DEVELOPMENT CENTER
AIR FORCE SYSTEMS COMMAND
ARNOLD AIR FORCE STATION, TENNESSEE

NOTICES

TRIPLE COLLISION EFFECTS IN THE THERMAL CONDUCTIVITY AND VISCOSITY OF MODERATELY DENSE GASES

J. V. Sengers
National Bureau of Standards
Washington, D. C.

FOREWORD

The research reported herein was sponsored by the Arnold Engineering Development Center (AEDC), Air Force Systems Command (AFSC), under Program Element 6144501F, Project 8951, Task 02. The research was conducted by the National Bureau of Standards, Washington, D. C. from February 1, 1966 to September 1, 1968 under delivery order (40-600) 66-494. Air Force project monitor for this project was 2nd Lt Michael G. Buja, AEDC (AELR). The manuscript was submitted for publication November 20, 1968.

Some of the results were reported in a paper entitled "Triple Collision Contribution to the Transport Coefficients of Gases", in Lectures in Theoretical Physics, Vol. IX C Kinetic Theory, W. E. Brittin, Editor, Gordon and Breach, New York, 1967, pp. 335-374. In addition, under the same delivery order a review was prepared entitled "Transport Properties of Compressed Gases", in Recent Advances in Engineering Science, Vol. 3, A. C. Eringen, Editor, Gordon and Breach, New York, 1969, pp. 153-196.

The author wants to thank Dr. M. S. Green, who suggested the subject of this research and enthusiastically encouraged its implementation. The author is indebted to Dr. J. R. Dorfman and Dr. E. G. D. Cohen for several valuable discussions which lead to the investigation of the logarithmic density dependence of the transport coefficients. He thanks Dr. S. Haber for his advice in selecting a numerical integration method and Mr. F. P. Karriker for his valuable assistance in carrying out the computations of the triple collision transport integrals. The research of Section 3.5 was carried out in cooperation with Dr. H. T. Wood. Chapter IV was prepared in collaboration with Dr. H. J. M. Hanley and Dr. R. D. McCarty; they also prepared Tables XIX and XX during this research effort.

This technical report has been reviewed and is approved.

Michael G. Buja
2nd Lt, USAF
Research Division
Directorate of Plans
and Technology

Edward R. Feicht
Colonel, USAF
Director of Plans
and Technology

ABSTRACT

A quantitative study is made of the effect of successive correlated binary collisions on the transport properties of gases. In particular, the triple collision transport integrals determining the first density coefficients of thermal conductivity and viscosity are derived for a gas of hard spherical molecules and estimates are presented for these integrals. By applying the method to a two dimensional gas of hard disks, a logarithmic density dependence of the transport coefficients is demonstrated.

In addition, an analysis is made of experimental data for the transport properties as a function of density. It is shown that the theoretically predicted density dependence is at least consistent with the experimental information. Experimental values for the first density coefficients of thermal conductivity and viscosity are reported, together with an assessment of their precision.

TABLE OF CONTENTS

LIST OF TABLES

LIST OF FIGURES

FIGURE PAGE

CHAPTER I
PURPOSE OF THE INVESTIGATION[+)]

1.1 INTRODUCTION

Transport properties of gases are directly related to the transfer of energy and momentum between colliding molecules. In dilute non-ionized gases the transport properties are independent of the density. Roughly speaking the number of molecules available for the transport of thermal energy and momentum is proportional to the density, but the distance over which this transport is effected, the mean free path, is in a dilute gas inversely proportional to the density.

The theoretical description of the transport coefficients of a dilute gas is based on the Boltzmann equation, which describes the rate of change of the molecular velocity distribution as a result of binary collisions between the molecules. Based on the Boltzmann equation the Chapman-Enskog theory provides a reliable procedure to obtain the transport coefficients of dilute gases.[1, 2] This theory is sufficiently well understood that in turn experimental transport coefficients of dilute gases are used to obtain information on the molecular interaction potential.[3]

Experience shows that the transport coefficients do vary with the density, when a gas is compressed. From a molecular point of view this density dependence has two origins. First, the effect of triple and higher order collisions on the transport properties can no longer be neglected.

+) For a survey of this report the reader is referred to the introductory Sections 1.1, 1.2, 3.1 and 4.1 and to the Sections 2.8, 3.6 and 4.5 which summarize the results (see table of contents).

Secondly, the difference in position of molecules involved in a collision (spatial inhomogeneity) leads to an additional density dependent contribution, sometimes referred to as collisional transfer.

Prediction of the density dependence of the transport properties is a task for statistical mechanics. For this purpose the Boltzmann equation has to be generalized to include the effects mentioned above. Up to the present approximate theories have been considered only. The oldest attempt is the theory of Enskog for hard spherical molecules.[4] In this theory the spatial correlation between the molecules is approximated by the equilibrium radial distribution function and the velocity correlation is disregarded. Recently, several approximate theories have been considered to describe the first density correction to the transport coefficients of gases.[5, 6, 7] All these theories attempt to describe the transport coefficients in terms of binary collisions and an explicit evaluation of the multiple collision dynamics is avoided. As a result it is difficult to assess the reliability and predictive power of such descriptions.

It is well known that the equation of state of a gas can be represented by a power series in the density ρ, the virial expansion:

$$pV = RT\,[1 + B\rho + C\rho^2 + \ldots]\ . \tag{1.1-1}$$

The various virial coefficients in this expansion can be related to molecular cluster integrals which are integrals over the configurations of n simultaneously interacting molecules. Thus the characteristic size determining these cluster integrals is the range of the molecular interaction.

To describe the density dependence of the transport coefficients a similar power series expansion was proposed by Bogoliubov.[8] To discuss the effect of multiple collisions we can distinguish between two types of multiple collisions:

1. Genuine multiple collisions in which all n molecules are interacting simultaneously. It is evident that such collisions contain again the size of the molecular interaction range as a characteristic length.

2. Multiple collisions that consist of a succession of correlated binary collisions between n particles. After a binary collision the velocities of two molecules will remain correlated until at least the next collision. Thus one can expect that the characteristic length associated with successive correlated binary collisions is no longer the interaction range, but the mean free path. However, in contrast to the interaction range, the mean free path is itself dependent on the density. As a result it is no longer evident that the effect of such multiple collisions can be represented by a power series in the density. Actually, as discussed in Chapter III, it turns out that these multiple collisions lead to a representation of the transport coefficients which contains terms logarithmic in the density ρ. In particular, for the thermal conductivity λ and the viscosity η we obtain

$$\begin{aligned} \lambda &= \lambda_o + \lambda_1\rho + \lambda_2'\rho^2 \ln\rho + \lambda_2\rho^2 + \ldots \\ \eta &= \eta_o + \eta_1\rho + \eta_2'\rho^2 \ln\rho + \eta_2\rho^2 + \ldots \quad . \end{aligned} \tag{1.1-2}$$

To predict the transport properties of a moderately dense gas it becomes our task to develop theories and procedures by which the various coefficients λ_i and η_i can be computed for a given molecular interaction potential.

1.2 SCOPE OF THIS RESEARCH

The present report describes the first results of an effort to obtain qualitative estimates of the effect of multiple collisions, in particular of triple collisions, on the transport properties. Evaluation of the triple collision effects is needed to predict the first density coefficients λ_1 and η_1 in (1.1-2). The analysis is highly desirable for a number of reasons:

(1) Reliable predictions of the density dependence of transport properties should be based on the rigorous statistical mechanical equations which contain the dynamics of multiple collisions.

(2) Quantitative information on the effect of multiple collisions, at least for some molecular models, is needed to make an assessment of the validity of any approximate theory.

(3) In order to study the effect of nonanalytic terms in the density expansion for the transport coefficients a quantitative estimate of the multiple collision effects is essential.

(4) As will be discussed in Chapter IV, the first density coefficient of viscosity, η_1 in (1.1-2), becomes negative at high temperatures. The sign of the corresponding coefficient λ_1 for the thermal conductivity at high temperatures is not definitely clear. These first density coefficients λ_1 and η_1 are the sum of two contributions: a collisional transfer contribution (related to binary collisions) which is usually positive and a triple collision contribution which is negative. Thus even to predict the sign of the first density correction at high temperatures in addition to the collisional transfer contribution a quantitative estimate of the triple collision term is very important.

Since a study of the effect of triple collisions turns out to be rather complicated, we limit ourselves in this report to a study of the effects for a very simple molecular model, namely two and three dimensional hard spheres.

The transport properties describe the linear response of the gas to the presence of gradients. The dilute gas values λ_o and η_o in (1.1-2) are obtained from the solution of the linearized Boltzmann equation. As a result they can be expressed in terms of binary collision integrals. (For hard spheres these results are summarized in Section 2.2). For repulsive intermolecular potentials the first density corrections are in principle to be determined by solving the Choh-Uhlenbeck integral equation which is a generalization of the linear Boltzmann equation to include the effect of triple collisions. In Chapter II we develop a procedure to solve this equation for a gas of hard spheres. The first density corrections λ_1 and η_1 are related to well defined triple collision transport integrals and preliminary values for these triple collision integrals are presented. The results are discussed in Section 2.8 and compared with the approximate predictions of the theory of Enskog.

To study the possible non-analytic density dependence of the transport coefficients, we consider in Chapter III a two dimensional model gas of hard disks. The advantage of this model is that the logarithmic density dependence can be evaluated with the same techniques as developed in Chapter II. The coefficient of the term logarithmic in the density is evaluated explicitly for this model and turns out to be non vanishing.

Finally, in Chapter IV we analyze experimental data for the transport coefficients of a number of gases. In this chapter we investigate whether the theoretically proposed density function (1.1-2) is consistent with the experimental data. Based on the analysis, first density coefficients of thermal conductivity and viscosity, together with an assessment of their precision, are reported as a function of temperature.

CHAPTER II
TRIPLE COLLISION CONTRIBUTION TO THE TRANSPORT COEFFICIENTS FOR A GAS OF HARD SPHERES

2.1 INTRODUCTION

In the kinetic theory of gases the transport coefficients are usually related to the velocity distribution function which specifies the state of the gas. This velocity distribution function $f(\vec{r},\vec{v};t)$ is defined such that $f(\vec{r},\vec{v};t)d\vec{v}d\vec{r}$ determines the number of molecules at a time t with position coordinates in the range $d\vec{r}$ around $\vec{r}$ and with velocities in the range $d\vec{v}$ around $\vec{v}$. The number density n and the mean velocity $\vec{u}$ at $\vec{r}$ and t are related to this distribution function by

$$n(\vec{r};t) = \int f(\vec{r},\vec{v};t)\, d\vec{v}\,, \tag{2.1-1}$$

$$n(\vec{r};t)\, \vec{u}(\vec{r};t) = \int \vec{v} f(\vec{r},\vec{v};t)\, d\vec{v}\,. \tag{2.1-2}$$

Denoting the thermal velocity of a molecule by $\vec{V} = \vec{v} - \vec{u}$, the average local kinetic energy is

$$\frac{3}{2}\, n(\vec{r};t)\, kT(\vec{r};t) = \int \frac{1}{2}\, mV^2\, f(\vec{r},\vec{v};t)\, d\vec{v}\,, \tag{2.1-3}$$

where m is the mass of the molecules. Since each molecule contributes $\frac{1}{2}\, mV^2\vec{V}$ to the flow of thermal energy, the total heat flux vector reads

$$\vec{Q} = \frac{1}{2}\, m \int V^2\, \vec{V}\, f(\vec{r},\vec{v};t)\, d\vec{v}\,. \tag{2.1-4}$$

The transport of momentum - or pressure tensor reads

$$\overleftrightarrow{P} = m \int \vec{V}\, \vec{V}\, f(\vec{r},\vec{v};t)\, d\vec{v}\,. \tag{2.1-5}$$

In the equilibrium state the distribution function reduces to the Maxwell-Boltzmann distribution

$$f(V) = n\, \left(\frac{m}{2\pi kT}\right)^{3/2} \exp\left[-\, \frac{mV^2}{2kT}\right]\,. \tag{2.1-6}$$

In equilibrium the heat flux vector (2.1-4) vanishes and the pressure tensor becomes diagonal

$$\overleftrightarrow{P} = p\,\overleftrightarrow{I}\ , \tag{2.1-7}$$

where $\overleftrightarrow{I}$ is the unit tensor and p the hydrostatic pressure.

When the gas is slightly out of equilibrium the heat flux vector and the off diagonal elements of the pressure tensor are proportional to the gradients in temperature T and fluid velocity $\vec{u}$, respectively:

$$\vec{Q} = -\lambda \nabla T = -\lambda \frac{\partial T}{\partial \vec{r}}\ , \tag{2.1-8}$$

$$\overleftrightarrow{P} = p\,\overleftrightarrow{I} - 2\eta\, \overline{\overline{\frac{\partial}{\partial \vec{r}}\vec{u}}}^{\,o}\ , \tag{2.1-9}$$

where $\overline{\overline{\frac{\partial}{\partial \vec{r}}\vec{u}}}^{\,o}$ is the symmetric traceless tensor derived from the dyadic $\frac{\partial}{\partial \vec{r}}\vec{u}$.[1] These linear relations define the coefficient of thermal conductivity λ and the coefficient of shear viscosity η +). On comparing these definitions with the molecular expressions (2.1-4) and (2.1-5) for the fluxes the transport coefficients are related to the distribution function f. For this purpose f is expanded in terms of the gradients of the macroscopic variables and only terms linear in the gradients are retained. In zeroth approximation f reduces to the local Maxwell distribution

$$f_o = n \left(\frac{m}{2\pi kT}\right)^{3/2} \exp\left[-\frac{m(\vec{v} - \vec{u})^2}{2kT}\right]\ , \tag{2.1-10}$$

where the macroscopic variables still depend on $\vec{r}$ and t. In first approximation

$$f = f_o(1 + \Phi)\ , \tag{2.1-11}$$

+) In this report we do not consider the bulk viscosity, since both its dilute gas value and its first density coefficient vanish.

where Φ is linear in the gradients of T and $\vec{u}$. For the time scale under consideration f, and consequently Φ, does not vary explicitly with time, but only via the dependence on the macroscopic variables $n(\vec{r};t)$, $\vec{u}(\vec{r};t)$ and $T(\vec{r};t)$:

$$\frac{\partial f}{\partial t} = \frac{\partial f}{\partial n}\frac{\partial n}{\partial t} + \frac{\partial f}{\partial \vec{u}}\cdot\frac{\partial \vec{u}}{\partial t} + \frac{\partial f}{\partial T}\frac{\partial T}{\partial t} \quad . \tag{2.1-12}$$

From the fact that Φ, like f itself, is a scalar function, one concludes that Φ must have the form

$$\Phi(\vec{V}) = -A(V)\,\vec{V}.\frac{\partial \ln T}{\partial \vec{r}} - B(V)\,\vec{V}^{o}\vec{V}:\frac{\partial}{\partial \vec{r}}\vec{u} \quad , \tag{2.1-13}$$

where A(V) and B(V) are scalar functions of the molecular velocity $\vec{V}$. To ascertain that n, $\vec{u}$ and T in f_o keep satisfying their definitions (2.1-1), (2.1-2) and (2.1-3) in the presence of gradients, the function Φ is subject to the auxiliary conditions

$$\int f_o\Phi\, d\vec{v} = 0 \quad , \tag{2.1-14}$$

$$\int \vec{V} f_o\Phi\, d\vec{v} = 0 \quad , \tag{2.1-15}$$

$$\int V^2 f_o\Phi\, d\vec{v} = 0 \quad . \tag{2.1-16}$$

Specifically, (2.1-15) implies that

$$\int f_o V^2 A(V)\, d\vec{v} = 0 \quad . \tag{2.1-17}$$

When we substitute this form of the distribution function into the molecular expressions (2.1-4) and (2.1-5) for the fluxes and compare the result with the definitions (2.1-8) and (2.1-9) of the transport coefficients, we obtain

$$\lambda = \frac{k}{3}\int d\vec{V}\, f_o(V)\, \left(\frac{mV^2}{2kT} - \frac{5}{2}\right) V^2 A(V) \quad , \tag{2.1-18}$$

$$\eta = \frac{m}{10}\int d\vec{V}\, f_o(V)\, \vec{V}^{o}\vec{V}:\vec{V}^{o}\vec{V}\, B(V) \quad . \tag{2.1-19}$$

Thus it becomes our task to assess the effect of the triple collisions on the functions A(V) and B(V).

2.2 TRANSPORT COEFFICIENTS IN THE DILUTE STATE

The first density correction to the transport coefficients is not only caused by a triple collision contribution to the kinetic fluxes (2.1-4) and (2.1-5), but also by an additional collisional transfer contribution from binary collisions. The latter term results from the difference in position of two molecules involved in a binary collision. For a gas of hard spheres the theory of Enskog presents an estimate for both contributions.[4] It turns out that the collisional transfer contribution to the first density contribution as evaluated by Enskog is exact.[9] Therefore, only the effect of triple collisions remains to be evaluated and it is sufficient for our present considerations to limit ourselves to the so called spatially homogeneous case. That is, the distribution function f is considered as a function of $\vec{v}$ and t and the gradients of the macroscopic variables, but its explicit dependence on the position $\vec{r}$ is disregarded.

Before discussing the effect of triple collisions we first summarize how the transport coefficients of a dilute gas are obtained when only binary collisions are taken into account. This will enable us to elucidate how the triple collision transport integrals are generalizations of the well known binary collision transport integrals.

In a dilute gas the time variation of f is described by the Boltzmann equation

$$\frac{\partial f(\vec{v}_1;t)}{\partial t} = J(ff) , \tag{2.2-1}$$

where the collision term J(ff) represents the effect of binary collisions. For a gas of hard spherical molecules this collision term J(ff) is given by[1]

$$J(ff) = \int d\vec{v}_2 \int d\vec{k}\ \sigma^2(\vec{v}_{21}.\vec{k})\ [f(\vec{v}_1';t)f(\vec{v}_2';t) - f(\vec{v}_1;t)f(\vec{v}_2;t)]\ . \qquad (2.2\text{-}2)$$

Here σ is the diameter of the molecules, $\vec{v}_{21}$ the relative velocity $\vec{v}_2 - \vec{v}_1$ and $\vec{k}$ the perihelion vector specifying the geometry of a binary collision between molecules 1 and 2. For hard spheres this perihelion vector $\vec{k}$ is the unit vector in the direction from the center of particle 2 to the center of particle 1 at the time of collision.

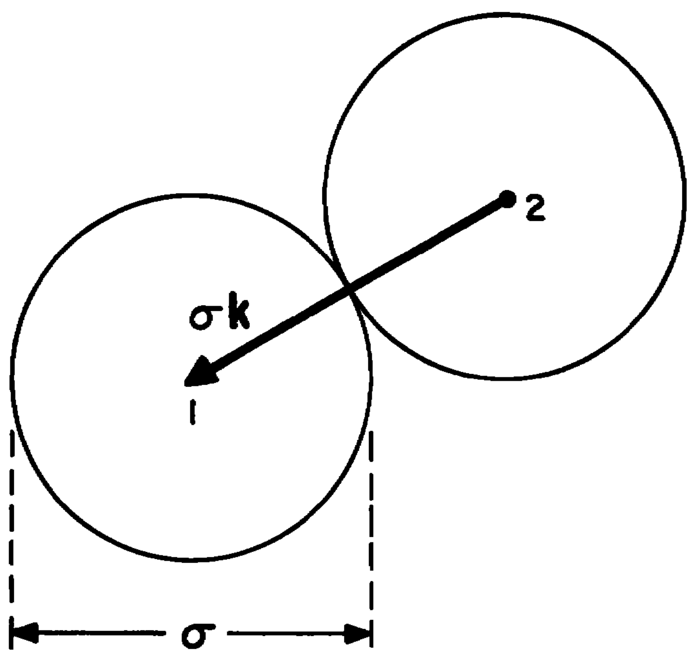

Figure 1. The perihelion vector $\vec{k}$ of a binary collision.

The distribution function $f(\vec{v}_1;t)$ changes with time, since during a time interval dt certain molecules with velocity $\vec{v}_1$ will collide with molecules with velocity $\vec{v}_2$. The number of such collisions with perihelion vector $\vec{k}$ will be proportional to $f(\vec{v}_1;t)f(\vec{v}_2;t)$ and the differential cross section $\sigma^2(\vec{v}_{21}.\vec{k})d\vec{k}$. On the other hand, molecules with velocities $\vec{v}_1'$ will collide with molecules $\vec{v}_2'$ such that after the collision their velocities will become $\vec{v}_1$ and $\vec{v}_2$. Thus $\vec{v}_1'$ and $\vec{v}_2'$ are the initial velocities for a binary collision with perihelion vector $\vec{k}$ and final velocities $\vec{v}_1$ and $\vec{v}_2$.

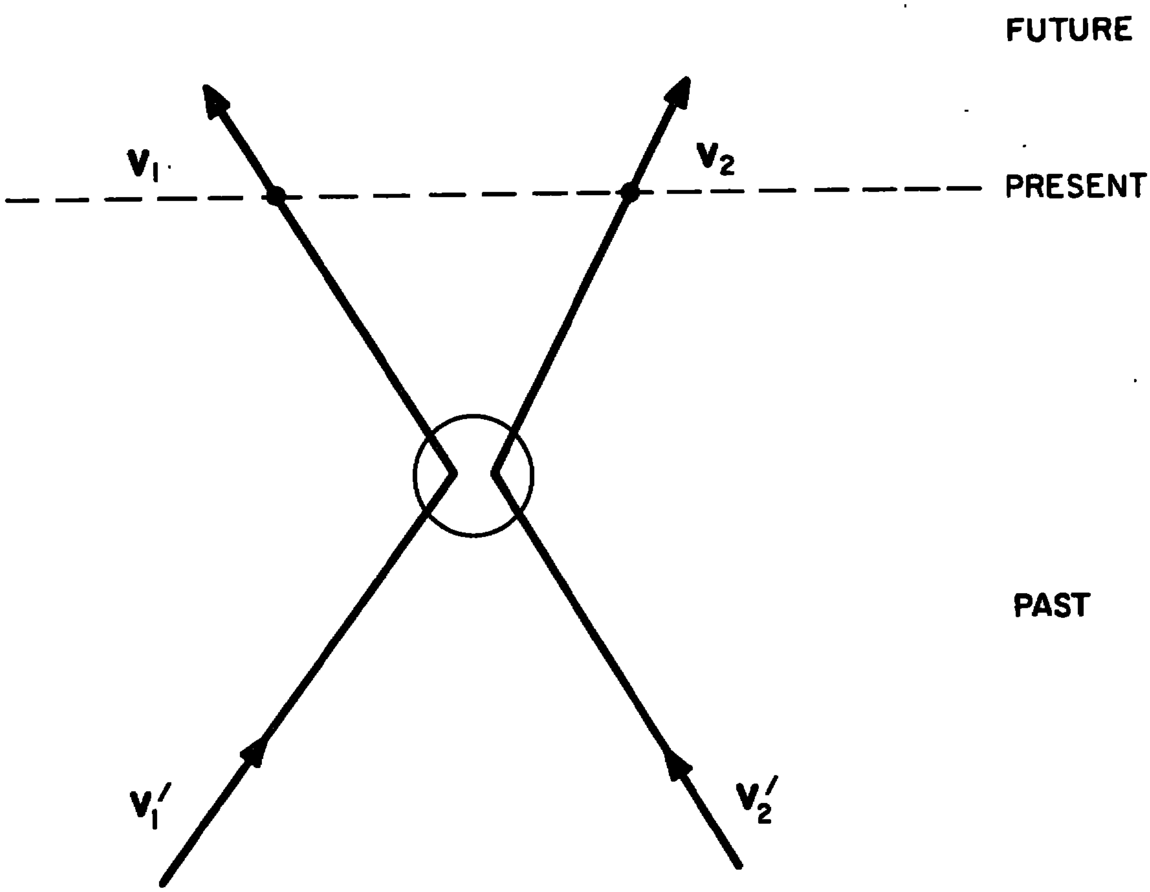

$V_1' = \mathcal{S}(12)\, V_1$ $\qquad$ $V_2' = \mathcal{S}(12)\, V_2$

Figure 2. Schematic representation of a binary collision. The lines represent the particle trajectories and the circle encloses a region in which a binary collision occurs.+)

It is convenient to relate the velocities $\vec{v}_i'$ to the velocities $\vec{v}_i$ by an operator $\mathcal{S}(12)$:

$$\vec{v}_1' = \mathcal{S}(12)\vec{v}_1 \; ; \; \vec{v}_2' = \mathcal{S}(12)\vec{v}_2 \; . \qquad (2.2\text{-}3)$$

+) Using the concept of inverse collisions one usually considers $\vec{v}_1'$, $\vec{v}_2'$ as the initial velocities for a binary collision with a perihelion vector $-\vec{k}$ and final velocities $\vec{v}_1$, $\vec{v}_2$. Since a generalization of the concept of inverse collisions to triple collisions is not obvious, we use here the Bogoliubov form[8] of the Boltzmann equation, in which the consideration of inverse encounters is avoided.

In general the substitution operator $\mathcal{S}(1. . .s)$ associated with s particles is defined as[8]

$$\mathcal{S}(1. . .s) = \lim_{t \to \infty} S_{-t}(1. . .s) \prod_{i=1}^{s} S_{+t}(i) , \qquad (2.2\text{-}4)$$

where $S_t(1. . .s)$ transforms the coordinates and the velocities of s particles into those at a time t later, if the s particles move under their mutual interaction. The effect of the operator $\mathcal{S}(12)$ on $\vec{v}_1$ and $\vec{v}_2$ is schematically represented by Fig. 2. If the positions and the velocities of the particles are such that they did not collide in the past, the operator $\mathcal{S}(12)$ reduces to one. The particles traverse the trajectories indicated in Fig. 2 from bottom to top. However, since the present is determined by the past, we actually retrace the history of the particles in the past+), that is, we read the diagrams always from top to bottom. The effect of the substitution operators related to triple collisions will be indicated later by similar diagrams. In terms of the substitution operator $\mathcal{S}(12)$ the Boltzmann equation can be written

$$\frac{\partial f(\vec{v}_1;t)}{\partial t} = \sigma^2 \int d\vec{v}_2 \int d\vec{k} (\vec{v}_{21} \cdot \vec{k}) \; T(12) f(\vec{v}_1;t) f(\vec{v}_2;t) , \qquad (2.2\text{-}5)$$

with

$$T(12) = \mathcal{S}(12) - 1 . \qquad (2.2\text{-}6)$$

For a derivation of the transport coefficients it is sufficient to consider the linearized Boltzmann equation. That is, we approximate f by $f_o(1 + \Phi)$ as in (2.1-11), eliminate the time derivatives of n, $\vec{u}$ and T in

---

+) This can be circumvented by changing the direction of time as will be done in a later stage.

(2.1-12) using the Euler equations and retain only terms linear in the gradients.[1] The resulting linearized Boltzmann equation which can be found in many places in the literature, reads

$$I_2(\Phi(\vec{V}_1)) = -f_o(V_1)\left[\left(\frac{mV_1^2}{2kT} - \frac{5}{2}\right)\vec{V}_1 \cdot \frac{\partial \ln T}{\partial \vec{r}_1} + \frac{m}{kT}\,\overset{\rightarrow o}{V_1}\vec{V}_1 : \frac{\partial}{\partial \vec{r}_1}\vec{u}\right], \qquad (2.2\text{-}7)$$

where I_2 is a linearized binary collision integral operator

$$I_2(\Phi(\vec{V}_1)) = -\sigma^2 \int d\vec{V}_2 \int d\vec{k}(v_{21}\cdot\vec{k})\ f_o(V_1)\ f_o(V_2)\ T(12)[\Phi(\vec{V}_1) + \Phi(\vec{V}_2)]\,. \qquad (2.2\text{-}8)$$

Since the total kinetic energy is invariant under a binary collision, the operator $T(12)$ commutes with $f_o(V_1)f_o(V_2)$.

Using the specific form (2.1-13) for the perturbation function Φ we obtain linearized integral equations for the functions $A(V_1)$ and $B(V_1)$

$$I_2(\vec{V}_1 A^{(o)}(V_1)) = f_o(V_1)\left(\frac{mV_1^2}{2kT} - \frac{5}{2}\right)\vec{V}_1\,,$$

$$I_2(\overset{\rightarrow o}{V_1}\vec{V}_1 B^{(o)}(V_1)) = f_o(V_1)\frac{m}{kT}\overset{\rightarrow o}{V_1}\vec{V}_1\,, \qquad (2.2\text{-}9)$$

where the superscript (o) indicates that we consider only the contribution of zeroth order in the density here.

To solve these integral equations one customarily approximates the solution by a finite sum of Sonine polynomials $S_n^{(m)}$:

$$A^{(o)}(V_1) = -\frac{15}{32}\frac{1}{n\sigma^2}\left(\frac{m}{\pi kT}\right)^{1/2}\sum_{k=1}^{N} a_k^{(o)}(N)\ S_{3/2}^{(k)}(W_1^2)\,,$$

$$B^{(o)}(V_1) = \frac{5}{16}\frac{1}{n\sigma^2}\left(\frac{m}{\pi kT}\right)^{1/2}\frac{m}{kT}\sum_{k=o}^{N-1} b_k^{(o)}(N)\ S_{5/2}^{(k)}(W_1^2)\,, \qquad (2.2\text{-}10)$$

where we have introduced a dimensionless velocity

$$\vec{W}_i = \left(\frac{m}{2kT}\right)^{1/2}\vec{V}_i\,. \qquad (2.2\text{-}11)$$

The Sonine polynomial $S_n^{(m)}(x)$ is defined as the coefficient of t^m in the expansion

$$\sum_{m=o}^{\infty} S_n^{(m)}(x)\ t^m = \frac{1}{(1-t)^{n+1}} \exp\{-\frac{xt}{1-t}\}\ . \tag{2.2-12}$$

They become the eigenfunctions of the linearized Boltzmann operator I_2 when the molecular interaction potential obeys an inverse fourth power law (Maxwell molecules). The number N of Sonine polynomials taken into account in the approximate solution (2.2-10) is referred to as the order of the Enskog approximation. If we substitute the solution (2.2-10) into the expressions (2.1-18) and (2.1-19) for the transport coefficients, we obtain

$$\begin{aligned} \lambda_o &= \lambda_o(N) = \frac{75}{64\sigma^2} \left(\frac{k^3T}{m\pi}\right)^{1/2} a_1^{(o)}(N)\ , \\ \eta_o &= \eta_o(N) = \frac{5}{16\sigma^2} \left(\frac{mkT}{\pi}\right)^{1/2} b_o^{(o)}(N)\ . \end{aligned} \tag{2.2-13}$$

The values of the coefficients $a_k^{(o)}(N)$ and $b_k^{(o)}(N)$ are determined by a variational method[2]; they should satisfy a set of linear equations

$$\begin{aligned} &\sum_{k=1}^{N} a_k^{(o)}(N)\ a_{k\ell}^{(o)} = \delta_{\ell 1} \quad (\ell = 1, \ldots, N)\ , \\ &\sum_{k=o}^{N-1} b_k^{(o)}(N)\ b_{k\ell}^{(o)} = \delta_{\ell o} \quad (\ell = 0, \ldots, N-1)\ , \end{aligned} \tag{2.2-14}$$

where $\delta_{\ell m}$ is the Kronecker delta and where $a_{k\ell}^{(o)}$ and $b_{k\ell}^{(o)}$ are matrix elements representing inner products associated with the linearized Boltzmann operator:

$$\begin{aligned} a_{k\ell}^{(o)} &= \frac{1}{2\sqrt{2\pi}}\ \frac{kT}{mn^2\sigma^2} \int d\vec{W}_1 \vec{W}_1\ S_{3/2}^{(k)}(W_1^2) . I_2(\vec{W}_1 S_{3/2}^{(\ell)}(W_1^2))\ , \\ b_{k\ell}^{(o)} &= \frac{1}{2\sqrt{2\pi}}\ \frac{kT}{mn^2\sigma^2} \int d\vec{W}_1\ \vec{W}_1^o\vec{W}_1\ S_{5/2}^{(k)}(W_1^2)\ :\ I_2(\vec{W}_1^o\vec{W}_1 S_{5/2}^{(\ell)}(W_1^2))\ . \end{aligned} \tag{2.2-15}$$

The equations have been normalized such that for hard spheres $a_1^{(o)}(1) = b_o^{(o)}(1) = a_{11}^{(1)} = b_{oo}^{(1)} = 1$. The operator I_2 is a symmetric operator, so that

$$a_{k\ell}^{(o)} = a_{\ell k}^{(o)} \quad ; \quad b_{k\ell}^{(o)} = b_{\ell k}^{(o)} . \qquad (2.2\text{-}16)$$

For hard spheres the matrix elements can be readily evaluated. Using the generating function (2.2-12) for $S_n^{(m)}(W_1^2)$, the elements $a_{k\ell}^{(o)}$ and $b_{k\ell}^{(o)}$ are the coefficients of $s^k t^\ell$ in the expansions[10]

$$\sum_{k=1}^{\infty} \sum_{\ell=1}^{\infty} a_{k\ell}^{(o)} s^k t^\ell = \{1 - \tfrac{1}{2}(s + t)\}^{1/2} st(1-st)^{-3} - \tfrac{1}{4}\{1 - \tfrac{1}{2}(s + t)\}^{-1/2} s^2 t^2 (1 - st)^{-2},$$

$$\sum_{k=o}^{\infty} \sum_{\ell=o}^{\infty} b_{k\ell}^{(o)} s^k t^\ell = \qquad (2.2\text{-}17)$$

$$\{1 - \tfrac{1}{2}(s + t)\}^{1/2}(1 + \tfrac{2}{3}st + \tfrac{1}{3}s^2t^2)(1 - st)^{-4} - \tfrac{1}{3}\{1 - \tfrac{1}{2}(s + t)\}^{-1/2} st(1 - st)^{-3}$$

$$- \tfrac{1}{48}\{1 - \tfrac{1}{2}(s + t)\}^{-3/2} s^2 t^2 (1 - st)^{-2} .$$

The coefficients up to the third Enskog approximation are listed in Table I and the corresponding corrections $a_1^{(o)}$ and $b_o^{(o)}$ to the transport coefficients in Table II. For Maxwell molecules the first Enskog approximation would suffice. From Table II it is evident that the expansion still converges fast for hard spheres; the second Enskog approximation amounts to only a few percents. For more realistic molecular interactions the convergence is even faster.[2]

Table I

The matrix elements $a_{k\ell}^{(o)}$ and $b_{k\ell}^{(o)}$, defined by (2.2-15) for hard spheres[11]

$a_{11}^{(o)} = 1$	$a_{12}^{(o)} = -\frac{1}{4}$	$a_{13}^{(o)} = -\frac{1}{32}$
	$a_{22}^{(o)} = \frac{45}{16}$	$a_{23}^{(o)} = -\frac{103}{128}$
		$a_{33}^{(o)} = \frac{5657}{1024}$
$b_{00}^{(o)} = 1$	$b_{01}^{(o)} = -\frac{1}{4}$	$b_{02}^{(o)} = -\frac{1}{32}$
	$b_{11}^{(o)} = \frac{205}{48}$	$b_{12}^{(o)} = -\frac{163}{128}$
		$b_{22}^{(o)} = \frac{11889}{1024}$

Table II

The successive approximations $a_k^{(o)}(N)$ and $b_k^{(o)}(N)$ determining the solution of the linearized Boltzmann equation for hard spheres

First Enskog approximation: $N = 1$

$$a_1^{(o)}(1) = 1 \qquad b_o^{(o)}(1) = 1$$

Second Enskog approximation: $N = 2$

$$a_1^{(o)}(2) = 1 + \frac{1}{44} \qquad b_o^{(o)}(2) = 1 + \frac{3}{202}$$

$$a_2^{(o)}(2) = \frac{1}{11} \qquad b_1^{(o)}(2) = \frac{6}{101}$$

Third Enskog approximation: $N = 3$

$$a_1^{(o)}(3) = 1 + \frac{1}{44} + \frac{(37)^2}{88 \times 7439} \qquad b_o^{(o)}(3) = 1 + \frac{3}{202} + \frac{(347)^2}{808 \times 145043}$$

$$a_2^{(o)}(3) = \frac{1}{11} + \frac{481}{11 \times 7439} \qquad b_1^{(o)}(3) = \frac{6}{101} + \frac{42681}{101 \times 145043}$$

$$a_3^{(o)}(3) = \frac{148}{7439} \qquad b_2^{(o)}(3) = \frac{1388}{145043}$$

2.3 THE THEORY OF ENSKOG

The transport coefficients λ_o and η_o deduced from the Boltzmann equation are independent of the density. A first attempt to generalize the Boltzmann equation to account for the density dependence of the transport coefficients was made by Enskog.[4] Strictly speaking, the number of molecules experiencing a binary collision with perihelion vector $\vec{k}$ will be proportional to the pair distribution function $f^{(2)}(\vec{r}_1,\vec{v}_1,\vec{r}_1-\sigma\vec{k},\vec{v}_2;t)$. In equilibrium the pair distribution function $f_o^{(2)}$ is related to the one particle distribution function $f_o^{(1)} = f_o$ by

$$f_o^{(2)}\ (\vec{r}_1,\vec{v}_1,\vec{r}_1 - \sigma\vec{k},\vec{v}_2) = g(\sigma)\ f_o(v_1)f_o(v_2)\ , \tag{2.3-1}$$

where $g(\sigma)$ is the equilibrium radial distribution function at a separation σ. This equilibrium radial distribution function is independent of the velocities and depends only on the relative distance r_{21}(= σ at a collision). Enskog assumed the same relationship between the pair distribution function and f, when the system is not in equilibrium[9]:

$$f^{(2)}(\vec{r}_1,\vec{v}_1,\vec{r}_1 - \sigma\vec{k},\vec{v}_2;t) = g(\sigma)f(\vec{v}_1;t)f(\vec{v}_2;t)\ , \tag{2.3-2}$$

where $g(\sigma)$ is now the local equilibrium radial distribution function depending on the local density and temperature. Thus, again disgarding the spatial dependence of the velocity distribution function f in our present discussion, Enskog generalized the collision term J(ff) in (2.2-1) to

$$J^E(ff) = \sigma^2 g(\sigma)\int d\vec{v}_2\int d\vec{k}(\vec{v}_{21}.\vec{k})\ T(12)f(\vec{v}_1;t)f(\vec{v}_2;t) = g(\sigma)J(ff)\ . \tag{2.3-3}$$

If we consider **again** a perturbation linear in the gradients

$$f = f_o(1 + \Phi)\ , \tag{2.3-4}$$

the linearized Boltzmann equation (2.2-7) is to be replaced with

$$g(\sigma)I_2(\Phi^E(\vec{V}_1)) = -f_o(V_1)\left[\left(\frac{mV_1^2}{2kT} - \frac{5}{2}\right)\vec{V}_1 \cdot \frac{\partial \ln T}{\partial \vec{r}} + \frac{m}{kT}\,\vec{V}_1^o\vec{V}_1 : \frac{\partial}{\partial \vec{r}_1}\vec{u}\right] . \qquad (2.3\text{-}5)$$

This equation is identical to (2.2-7), if we identify $\Phi^E(\vec{V}_1)$ with $g^{-1}(\sigma)\Phi(\vec{V}_1)$. Consequently, the theory of Enskog predicts that the (kinetic) transport of a dense gas of hard spheres are related to the dilute gas values by

$$\lambda^E = \frac{\lambda_o}{g(\sigma)} \; : \; \eta^E = \frac{\eta_o}{g(\sigma)} \; . \qquad (2.3\text{-}6)$$

The value $g(\sigma)$ of the radial distribution function is directly related to the equation of state

$$p = nkT\{1 + b\rho g(\sigma)\} \; , \qquad (2.3\text{-}\;)$$

where

$$b\rho = \frac{2\pi}{3}\, n\sigma^3 \; , \qquad (2.3\text{-}8)$$

is the covolume of the spheres. The pressure p, as well as $g(\sigma)$ can be expanded into a power series in terms of the density

$$g(\sigma) = 1 + \frac{5}{8}\, b\rho + \ldots \quad . \qquad (2.3\text{-}9)$$

The coefficient of the first density dependent correction term in $g(\sigma)$ is determined by the so-called excluded volume of a third particle; that is, the volume where a third particle would overlap with the two particles 1 and 2 simultaneously.

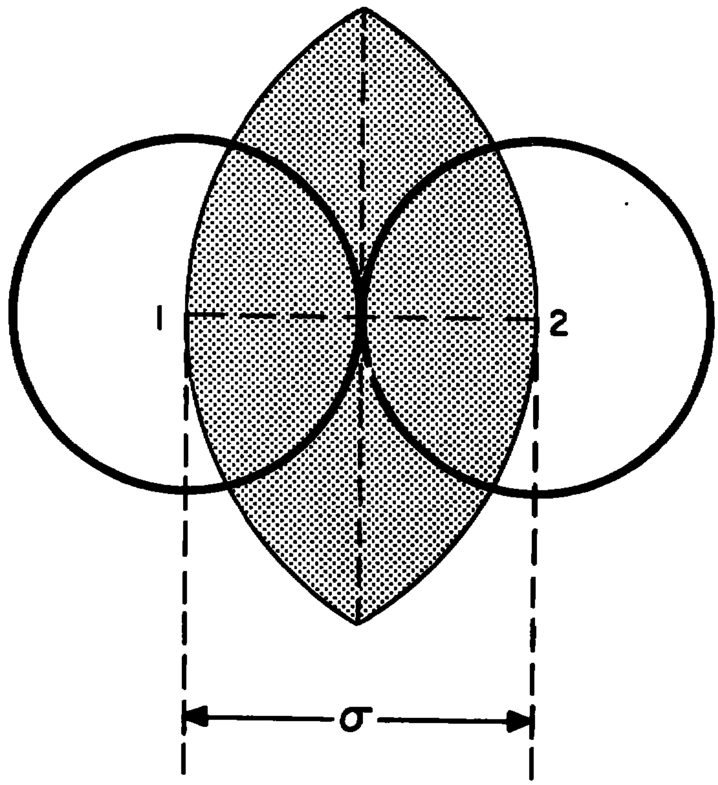

Figure 3. The excluded volume determining the first density correction to $g(\sigma)$.

The power series (2.3-9) implies a power series for the transport coefficients (2.3-6):

$$\lambda = \lambda_o + \lambda_1 b\rho + \ldots \quad ,$$
$$\eta = \eta_o + \eta_1 b\rho + \ldots \quad . \tag{2.3-10}$$

In the sequel we shall refer to λ_1 and λ_1 as the first density coefficient of thermal conductivity, resp. viscosity. From (2.3-6) and (2.3-9) it is evident that in the Enskog theory λ_1 and η_1 are approximated by

$$\lambda_1^E = -\frac{5}{8}\lambda_o \quad ; \quad \eta_1^E = -\frac{5}{8}\eta_o \quad , \tag{2.3-11}$$

independent of the order of the Enskog approximation in λ_o and η_o.

2.4 THE CHOH-UHLENBECK INTEGRAL EQUATION

The Enskog theory was based on an ad hoc assumption (2.3-2). A systematic procedure to take into account successive higher order contributions in the density was proposed by Bogoliubov.[8] For the first density correction the theory was worked out by Choh and Uhlenbeck[12] and further elucidated by Green[13] and Cohen.[14] Limiting ourselves to the first density correction, the Boltzmann equation (2.2-1) is to be replaced with

$$\frac{\partial f(\vec{v}_1;t)}{\partial t} = J(ff) + K(fff) , \tag{2.4-1}$$

where K(fff) represents the effects of triple collisions and is related to the product of <u>three</u> one particle distribution functions:

$$K(fff) = \int d\vec{v}_2 d\vec{v}_3 \int d\vec{r}_2 d\vec{r}_3 \theta_{12} \tau(12;3) f(\vec{v}_1;t) f(\vec{v}_2;t) f(\vec{v}_3;t) . \qquad (2.4\text{-}2)$$

Here θ_{12} is an differential operator introduced by Choh and Uhlenbeck[12]

$$\theta_{12} = \frac{1}{m}\frac{\partial\phi_{12}}{\partial\vec{r}_1} \cdot \frac{\partial}{\partial\vec{v}_1} + \frac{1}{m}\frac{\partial\phi_{12}}{\partial\vec{r}_2} \cdot \frac{\partial}{\partial\vec{v}_2} , \qquad (2.4\text{-}2)$$

where ϕ_{12} is the intermolecular potential between particles 1 and 2. For hard spheres ϕ_{12} is a step function and consequently θ_{12} contains a δ-function. The operator $\tau(12;3)$ is a combination of substitution operators[13, 14]

$$\tau(12;3) = \mathcal{S}(123) - \mathcal{S}(12)\,\mathcal{S}(13) - \mathcal{S}(12)\mathcal{S}(23) + \mathcal{S}(12) , \tag{2.4-4}$$

where $\mathcal{S}(123)$, defined by (2.2-4), is a generalization of the two particle substitution operator $\mathcal{S}(12)$ and includes the interaction between three particles. Apart from neglecting collisions between three particles that actually occur, the Boltzmann equation took into account some binary collisions that actually will not occur, due to the interference of a third particle. Thus in $\tau(12;3)$ we subtract certain combinations of two particle streaming operators.

To derive the transport coefficients we again linearize the equation by substituting $f = f_o(1 + \Phi)$. As a result the linearized Boltzmann equation (2.2-7) is replaced with

$$I_2(\Phi(\vec{V}_1)) + b\rho I_3(\Phi(\vec{V}_1)) = -f_o(V_1)\left[\left(\frac{mV_1^2}{2kT} - \frac{5}{2}\right)\vec{V}_1\cdot\frac{\partial \ln T}{\partial \vec{r}_1} + \frac{m}{kT}\vec{V}_1^{o}\vec{V}_1 : \frac{\partial}{\partial \vec{r}_1}\vec{u}\right], \quad (2.4\text{-}5)$$

where I_3 is a linearized ternary collision integral operator

$$I_3(\Phi(\vec{V}_1)) = -\frac{1}{b\rho}\int d\vec{v}_2 d\vec{v}_3 \int d\vec{r}_2 d\vec{r}_3 \theta_{12}\tau(12;3) f_o(V_1) f_o(V_2) f_o(V_3)\ [\Phi(\vec{V}_1)+\Phi(\vec{V}_2)+\Phi(\vec{V}_3)]\ . \quad (2.4\text{-}6)$$

For convenience a factor $(b\rho)^{-1}$ has been entered in the definition of I_3, so that I_3 has the same dimension as I_2. From the right hand side of (2.4-5) it is evident that $\Phi(\vec{V}_1)$ will have again the form (2.1-13). To solve the equation we expand the functions $A(V_1)$ and $B(V_1)$ in terms of the density:

$$A(V_1) = A^{(o)}(V_1) + b\rho A^{(1)}(V_1)\ ,$$
$$B(V_1) = B^{(o)}(V_1) + b\rho B^{(1)}(V_1)\ . \quad (2.4\text{-}7)$$

The corresponding expansion for the transport coefficients was introduced in (2.3-10). From the expressions (2.1-18) and (2.1-19) we see that the first density coefficients λ_1 and η_1 are given by

$$\lambda_1 = \frac{k}{3}\int d\vec{V}_1 f_o(V_1)\left(\frac{mV_1^2}{2kT} - \frac{5}{2}\right)V^2 A^{(1)}(V_1)\ ,$$
$$\eta_1 = \frac{m}{10}\int d\vec{V}_1 f_o(V_1)\ \vec{V}_1^{o}\vec{V}_1 : \vec{V}_1^{o}\vec{V}_1 B^{(1)}(V_1)\ . \quad (2.4\text{-}8)$$

The integral equations for $A^{(1)}(V_1)$ and $B^{(1)}(V_1)$ are derived by substituting (2.4-7) into (2.1-13) and (2.4-5). Since $A^{(o)}(V_1)$ and $B^{(o)}(V_1)$ satisfy the linearized Boltzmann equation (2.2-9), we obtain

$$
\begin{aligned}
I_2(\vec{V}_1 A^{(1)}(V_1)) &= - I_3(\vec{V}_1 A^{(o)}(V_1)) \ , \\
I_3(\overset{\rightarrow o}{V_1}\vec{V}_1 B^{(1)}(V_1)) &= -I_3(\overset{\rightarrow o}{V_1}\vec{V}_1 B^{(o)}(V_1)) \ ,
\end{aligned}
\tag{2.4-9}
$$

neglecting terms quadratic in the density. In these equations, to which we refer as Choh-Uhlenbeck integral equation, the new ternary collision operator I_3 operates on the functions $A^{(o)}(V_1)$ and $B^{(o)}(V_1)$ that are known from the solution of the linearized Boltzmann equation. The kernel of the Choh-Uhlenbeck integral equation is the same as that of the linearized Boltzmann equation. In principle, one could solve this equation by expanding $A^{(1)}$ and $B^{(1)}$ again in terms of Sonine polynomials.[15] However, we are not interested in $A^{(1)}$ and $B^{(1)}$ as such, but only in the moments (2.4-8) of these functions, which can be written explicitly in terms of $A^{(o)}$ and $B^{(o)}$ +). For this purpose we substitute (2.2-9) into (2.4-8)

$$
\begin{aligned}
\lambda_1 &= \frac{k}{3} \int d\vec{V}_1 \ \vec{V}_1 A^{(1)}(V_1) . I_2(\vec{V}_1 A^{(o)}(V_1)) \ , \\
\eta_1 &= \frac{kT}{10} \int d\vec{V}_1 \overset{\rightarrow o}{V_1}\vec{V}_1 \ B^{(1)}(V_1) : I_2(\overset{\rightarrow o}{V_1}\vec{V}_1 B^{(o)}(V_1)) .
\end{aligned}
\tag{2.4-10}
$$

+) The author is indebted to Dr. M. H. Ernst for this remark.

Since I_2 is a symmetric operator, we can interchange $A^{(o)}$ and $A^{(1)}$, resp. $B^{(o)}$ and $B^{(1)}$, in (2.4-10). Thus it follows from (2.4-9) that λ_1 and η_1 are related to $A^{(o)}$ and $B^{(o)}$ by

$$\boxed{\begin{aligned} \lambda_1 &= -\frac{k}{3} \int d\vec{V}_1 \vec{V}_1 A^{(o)}(V_1) . I_3(\vec{V}_1 A^{(o)}(V_1)) \ , \\ \eta_1 &= -\frac{kT}{10} \int d\vec{V}_1 \overset{\rightarrow o \rightarrow}{V_1 V_1} B^{(o)}(V_1) : I_3(\overset{\rightarrow o \rightarrow}{V_1 V_1} B^{(o)}(V_1)). \end{aligned}} \tag{2.4-11}$$

By substituting the Sonine polynomial expansion (2.2-10) for $A^{(o)}$ and $B^{(o)}$ (with known coefficients) into (2.4-11) we can evaluate λ_1 and η_1 in successive Enskog approximations. Introducing again dimensionless velocities $\vec{W}_i = (m/2kT)^{1/2}\vec{V}_i$, we obtain in the Nth Enskog approximation

$$\begin{aligned} \frac{\lambda_1(N)}{\lambda_o(1)} &= -\sum_{k=1}^{N} \sum_{\ell=1}^{N} a_k^{(o)}(N)\ a_\ell^{(o)}(N)\ a_{k\ell}^{(1)} \ , \\ \frac{\eta_1(N)}{\eta_o(1)} &= -\sum_{k=0}^{N-1} \sum_{\ell=o}^{N-1} b_k^{(o)}(N)\ b_\ell^{(o)}(N)\ b_{k\ell}^{(1)} \ . \end{aligned} \tag{2.4-12}$$

The new matrix elements $a_{k\ell}^{(1)}$ and $b_{k\ell}^{(1)}$ are inner products associated with the linearized triple collision integral operator I_3:

$$\begin{aligned} a_{k\ell}^{(1)} &= \frac{1}{2\sqrt{2\pi}} \frac{kT}{mn^2\sigma^2} \int d\vec{W}_1\ \vec{W}_1 S_{3/2}^{(k)}(W_1^2) . I_3(\vec{W}_1 S_{3/2}^{(\ell)}(W_1^2)) \ , \\ b_{k\ell}^{(1)} &= \frac{1}{2\sqrt{2\pi}} \frac{kT}{mn^2\sigma^2} \int d\vec{W}_1\ \overset{\rightarrow o \rightarrow}{W_1 W_1} S_{5/2}^{(k)}(W_1^2) : I_3(\overset{\rightarrow o \rightarrow}{W_1 W_1} S_{5/2}^{(\ell)}(W_1^2)) \ . \end{aligned} \tag{2.4-13}$$

These matrix elements are the immediate generalizations of the matrix elements $a_{k\ell}^{(o)}$ and $b_{k\ell}^{(o)}$, defined by (2.2-15), that determine the dilute gas values λ_o and η_o; they were first introduced in a previous publication.[15] For convenience, we have divided the first density coefficients $\lambda_1(N)$ and $\eta_1(N)$

by the dilute gas values $\lambda_o(1)$ and $\eta_o(1)$, so that the ratios in (2.4-12) are independent of the temperature.

It is convenient to symmetrize the integrands in (2.4-13). The operator I_3 can be symmetrized as shown by Green[16]

$$I_3(\phi(\vec{V}_1)) = -\frac{1}{2b\rho}\int d\vec{V}_2 d\vec{V}_3 O(123) f_o(V_1) f_o(V_2) f_o(V_3) \sum_{n=1}^{3} \phi(\vec{V}_n) , \tag{2.4-14}$$

where O(123) is a configurational triple collision integral operator

$$O(123) = \int d\vec{r}_2 d\vec{r}_3 [\theta_{12}\tau(12;3) + \theta_{13}\tau(13;2) + \theta_{23}\tau(23;1)] . \tag{2.4-15}$$

The integrands in (2.4-13) can be further symmetrized by interchanging the velocity variables. Thus we obtain

$$\begin{aligned} a_{k\ell}^{(1)} &= -\frac{1}{32\pi^6\sigma^5}\left(\frac{m}{kT}\right)^{1/2} \int d\vec{W}_1 d\vec{W}_2 d\vec{W}_3 \exp\,[-(W_1^2 + W_2^2 + W_3^2)] \\ &\quad \cdot \sum_{m=1}^{3} \vec{W}_m S_{3/2}^{(k)}(W_m^2) \cdot O(123) \sum_{n=1}^{3} \vec{W}_n S_{3/2}^{(\ell)}(W_n^2) , \\ b_{k\ell}^{(1)} &= -\frac{1}{32\pi^6\sigma^5}\left(\frac{m}{kT}\right)^{1/2} \int d\vec{W}_1 d\vec{W}_2 d\vec{W}_3 \exp[-(W_1^2 + W_2^2 + W_3^2)] \\ &\quad \cdot \sum_{m=1}^{3} \overset{\circ}{\vec{W}_m\vec{W}_m} S_{5/2}^{(k)}(W_m^2) : O(123) \sum_{n=1}^{3} \overset{\circ}{\vec{W}_n\vec{W}_n} S_{5/2}^{(\ell)}(W_n^2) , \end{aligned} \tag{2.4-16}$$

where we used the property that O(123) commutes with the kinetic energy and therefore with the product of the Maxwell distributions.[15]

There exists a simple relationship between the rigorous expressions (2.4-11) for λ_1 and η_1 and the approximate expressions (2.3-11) given by the theory of Enskog. The operator I_3, defined in (2.4-6), contains an integration over all possible positions $\vec{r}_3$ of particle 3. If we limit this integration to those values of $\vec{r}_3$ for which both $r_{13}<\sigma$ and $r_{23}<\sigma$, that is, the excluded

volume of Fig. 3, the operator I_3 reduces to $\frac{5}{8}I_2$ as shown in a previous paper.[15] Thus the rigorous expressions (2.4-11) reduce to the values predicted by Enskog, when the configurational integral is restricted to those configurations that determine in equilibrium the first dentity correction to the radial distribution function $g(\sigma)$.

2.5 CLASSIFICATION OF THE TRIPLE COLLISION EVENTS

The transport coefficients λ_o and η_o in the dilute state were determined by the binary collision integrals (2.2-15). To obtain the first density corrections λ_1 and η_1 we need to evaluate the triple collision integrals (2.4-16). Apart from the fact that the dynamics of triple collisions is more complicated than that of an individual binary collision, there is another major difference between the two sets of transport collision integrals. In the binary collision integral operator I_2, defined in (2.2-8), the configurational integration does not extend over all possible positions $\vec{r}_2$ of particle 2, but the integration is restricted to a two dimensional surface, specified by the perihelion vector $\vec{k}$. For a given $\vec{k}$ the operator T(12) in (2.2-8) can be evaluated at any point along the trajectories of the two particles (provided that the two particles are receding), since one needs only the velocities before and after the binary collision. On the other hand, the triple collision integral operator O(123), defined in (2.4-15) is still a six dimensional integral and contains the differential operators θ_{ij}; it has not yet been expressed in terms of the velocities of the particles before and after certain collision events. It is possible to convert the six

dimensional triple collision integral (2.4-15) into a five dimensional surface integral which is much more similar to the two dimensional surface integral form of the binary collision integral operator I_2.[15, 16] A derivation of the surface integral form of the triple collision integral operator is presented in Appendix A.

It turns out that the triple collision integral can be decomposed into a sum of six surface integral operators, each of which is associated with a particular triple collision event. To elucidate this result we give first a description of the six triple collision events which are schematically represented in Fig. 4. The positions of the particles (on the five dimensional surface) over which the integration has to be carried out are indicated by the black dots. The direction of the velocities is indicated by the arrows. The lines represent trajectories and are labeled with the corresponding particle number. The circles represent (binary) collisions between the particles whose trajectories are enclosed. The operators in (2.4-15) transform the present phases of the particles into the phases that the particles would have had in the previous past according to a particular dynamical history. Therefore, we retrace the motion backwards in time and we shall always read the diagrams from top to bottom, just as for the binary collision diagram of Fig. 2. The sequence of successive binary collisions will be ordered as they are encountered in this procedure.

Following Green[13] we distinguish between real and hypothetical collisions. Any binary collision encountered when we retrace the trajectories of the particles taking into account the interaction between all three particles is called a <u>real</u> collision. Any binary collision that is encountered

only when the effect of some other collision on the trajectories of the particles is disregarded is called a hypothetical collision. In addition, we distinguish between interacting and non-interacting collisions. In a non-interacting collision the particles are aimed to collide, but we continue the free trajectories of the particles without taking into account the interaction between the particles. In fig. 4, non-interacting collisions are indicated by a dotted circle. It is evident from the definition that all collisions encountered in the diagrams of Fig. 4 after a non-interacting collision are hypothetical collisions.

With this nomenclature the triple collision events of Fig. 4 can be described as follows (always reading the diagrams from top to bottom!).

R1 (Recollision of the first kind):

A real collision between 1 and 2 is followed by a real collision between 1 and 3, followed by a real collision between 1 and 2 again.

R2 (Recollision of the second kind):

A real non-interacting collision between 1 and 2 is followed by a hypothetical interacting collision between 1 and 3, followed by a hypothetical collision between 1 and 2.

C1 (Cyclic collision of the first kind):

A real collision between 1 and 2 is followed by a real collision between 1 and 3, followed by a real collision between 2 and 3.

C2 (Cyclic collision of the second kind):

A real non-interacting collision between 1 and 2 is followed by a hypothetical interacting collision between 1 and 3, followed by a hypothetical collision between 2 and 3.

H1 (Hypothetical cyclic collision of the first kind):

A real collision between 1 and 2 is followed by a real non-interacting

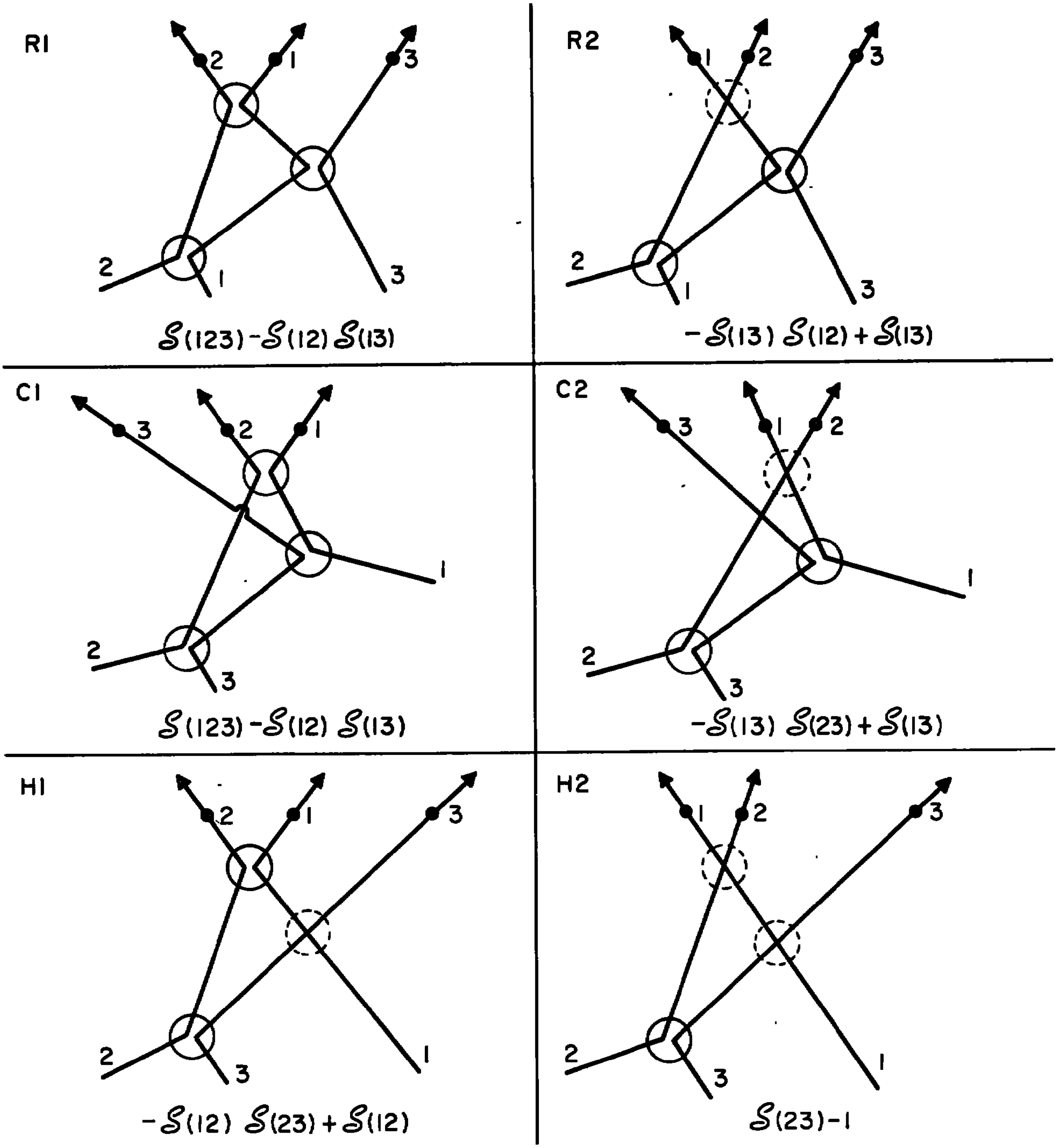

Figure 4. The six triple collision events.

collision between 1 and 3, followed by a hypothetical collision between 2 and 3.

H2 (Hypothetical cyclic collision of the second kind):

A real non-interacting collision between 1 and 2 is followed by a hypothetical non-interacting collision between 1 and 3, followed by a hypothetical collision between 2 and 3.

As shown in Appendix A the configurational triple collision operator O(123), introduced in (2.4-14), can be replaced with

$$O(123) = 6 \cdot O(12;13) , \qquad (2.5\text{-}1)$$

with O(12;13) given by (A-30)

$$O(12;13) = \sigma^4 \int d\vec{k}_1 d\vec{k}_2 \int d\tau \; \vec{V}_{21} \cdot \vec{k}_1 \vec{V}_{31}(1) \cdot \vec{k}_2 \sum_{\mu} T_{\mu}(12;13) . \qquad (2.5\text{-}2)$$

The points on the five dimensional surface are specified by the variables $\vec{k}_1$, $\vec{k}_2$ and τ; $\vec{k}_1$ is the perihelion vector of the first collision (between 1 and 2), $\vec{k}_2$ the perihelion vector of the second collision (between 1 and 3) and τ the time between the first and the second collision. $\vec{V}_{31}(1)$ is the relative velocity of 3 with respect to 1 between the first and the second collision. The summation over μ in (2.5-2) has to be taken over the diagrams μ = R1, R2, C1, C2, H1, H2. The operator $T_{\mu}(12;13)$ is only different from zero for phase points whose dynamical history can be represented by the diagram μ. For such phase points the definition of $T_{\mu}(12;13)$ is given in Table III.

Table III

The triple collision operators $T_{\mu}(12;13)$

μ	$T_{\mu}(12;13)$
R1	$\mathcal{S}(123) - \mathcal{S}(12)\mathcal{S}(13)$
R2	$-\mathcal{S}(13)\mathcal{S}(12) + \mathcal{S}(13)$
C1	$\mathcal{S}(123) - \mathcal{S}(12)\mathcal{S}(13)$
C2	$-\mathcal{S}(13)\mathcal{S}(23) + \mathcal{S}(13)$
H1	$-\mathcal{S}(12)\mathcal{S}(23) + \mathcal{S}(12)$
H2	$\mathcal{S}(23) - 1$

These expressions for the operators $T_{\mu}(12;13)$ in terms of the streaming operators $\mathcal{S}$ are presented in Fig. 4 below each diagram; they are direct generalizations of the operator T(12), defined in (2.2-6), for the binary collision term. Operating on any function of the velocities, $T_{\mu}(12;13)$ transforms that function into the difference between its value for the final velocities at the bottom of the diagram and its value for the velocities between the second and the third collision. The effect of the operator has the opposite sign, when the number of non-interacting collisions is odd. Note that in R1 and C1 a fourth collision may occur;[17,18] in that case the trajectories have to be retraced until this fourth collision has also been completed. We consider only those diagrams for which the first collision refers to particles 1 and 2 and the second collision to particles 1 and 3. Any other diagram obtained by permutation of the particle numbers is accounted for by the factor 6 in (2.5-1).

In the previous Section we pointed out that the expression for λ_1 and η_1 reduce to the predictions of Enskog, if the configurational integral is restricted to the excluded volume of particle 3. To ascertain which triple collision events are taken into account in the Enskog theory, we consider

diagram H2 in some detail. In this diagram the first collision (between 1 and 2) is a non-interacting collision. Such a non-interacting collision implies that during a certain time interval particles 1 and 2 move inside each other, when their free trajectories are followed from top to bottom. We call such configurations overlapping configurations. When the time between the first and the second collision is sufficiently small, particle 3 will be aimed to collide with 1, while 1 and 2 are still overlapping. Since the collision between 1 and 3 is also non-interacting, 1 and 3 overlap during a short time interval after the second collision. When in addition the time between the second and the third collision is small, it is possible that 3 will collide with 2, while particles 1 and 2 as well as particles 1 and 3 are still overlapping. Thus, such a collision process leads to the excluded volume configuration (Fig. 3 if we interchange 1 and 3) considered in the Enskog theory. Therefore, as mentioned in a previous paper,[15] it can be concluded that the Enskog theory neglects all triple collision events shown in Fig. 4, except for some collisions of the type H2. Among all collisions H2, the theory of Enskog includes only those for which the time between the first and the last collision is so small that, when 3 starts to collide with 2, 1 and 2 as well as 1 and 3 are still overlapping.

The surface integral form (2.5-1) for O(123) should be substituted into the expressions (2.4-16) for $a_{k\ell}^{(1)}$ and $b_{k\ell}^{(1)}$. In doing so we take the diameter σ of the spheres as the unit of length. Since the velocity was expressed in units $(2kT/m)^{1/2}$, the corresponding dimensionless time τ^* is

$$\tau^* = \frac{1}{\sigma}\left(\frac{2kT}{m}\right)^{1/2}\tau \quad . \tag{2.5-3}$$

Thus the integrals (2.4-16) for $a_{k\ell}^{(1)}$ and $b_{k\ell}^{(1)}$ become in dimensionless form

$$a_{k\ell}^{(1)} = -\frac{3\sqrt{2}}{16\pi^6}\int d\vec{W}_1 d\vec{W}_2 d\vec{W}_3 \exp[-(W_1^2 + W_2^2 + W_3^2)]$$

$$\cdot \sum_{m=1}^{3} \vec{W}_m S_{3/2}^{(k)}(W_m^2) \cdot 0^*(12;13) \sum_{n=1}^{3} \vec{W}_n S_{3/2}^{(\ell)}(W_n^2) \;,$$

$$b_{k\ell}^{(1)} = -\frac{3\sqrt{2}}{16\pi^6}\int d\vec{W}_1 d\vec{W}_2 d\vec{W}_3 \exp[-(W_1^2 + W_2^2 + W_3^2)] \tag{2.5-4}$$

$$\cdot \sum_{m=1}^{3} \vec{W}_m^{\circ}\vec{W}_m S_{5/2}^{(k)}(W_m^2) : 0^*(12;13) \sum_{n=1}^{3} \vec{W}_n^{\circ}\vec{W}_n S_{5/2}^{(\ell)}(W_n^2) \;,$$

with

$$0^*(12;13) = \sum_{\mu}\int d\vec{k}_1 d\vec{k}_2 \int d\tau^* \;\; \vec{W}_{21}\cdot\vec{k}_1 \; \vec{W}_{31}(1)\cdot\vec{k}_2 \; T_{\mu}(12;13) \;. \tag{2.5-5}$$

For the evaluation of these triple collision integrals it is more convenient to describe the collisions between the molecules in terms of forward motion, rather than retracing the motion backwards in time. Such a description is obtained if we change the sign of all velocities. The integrands are symmetric in the velocities and therefore invariant under this transformation, provided that we replace t with -t in the definition (2.2-4) of the operators. For the diagrams in Fig. 4 it means that we change the direction of the velocities as shown in Fig. 5, but still read the diagrams from top to bottom. In the sequel of this chapter we shall refer to Fig. 5 in discussing the triple collision events.

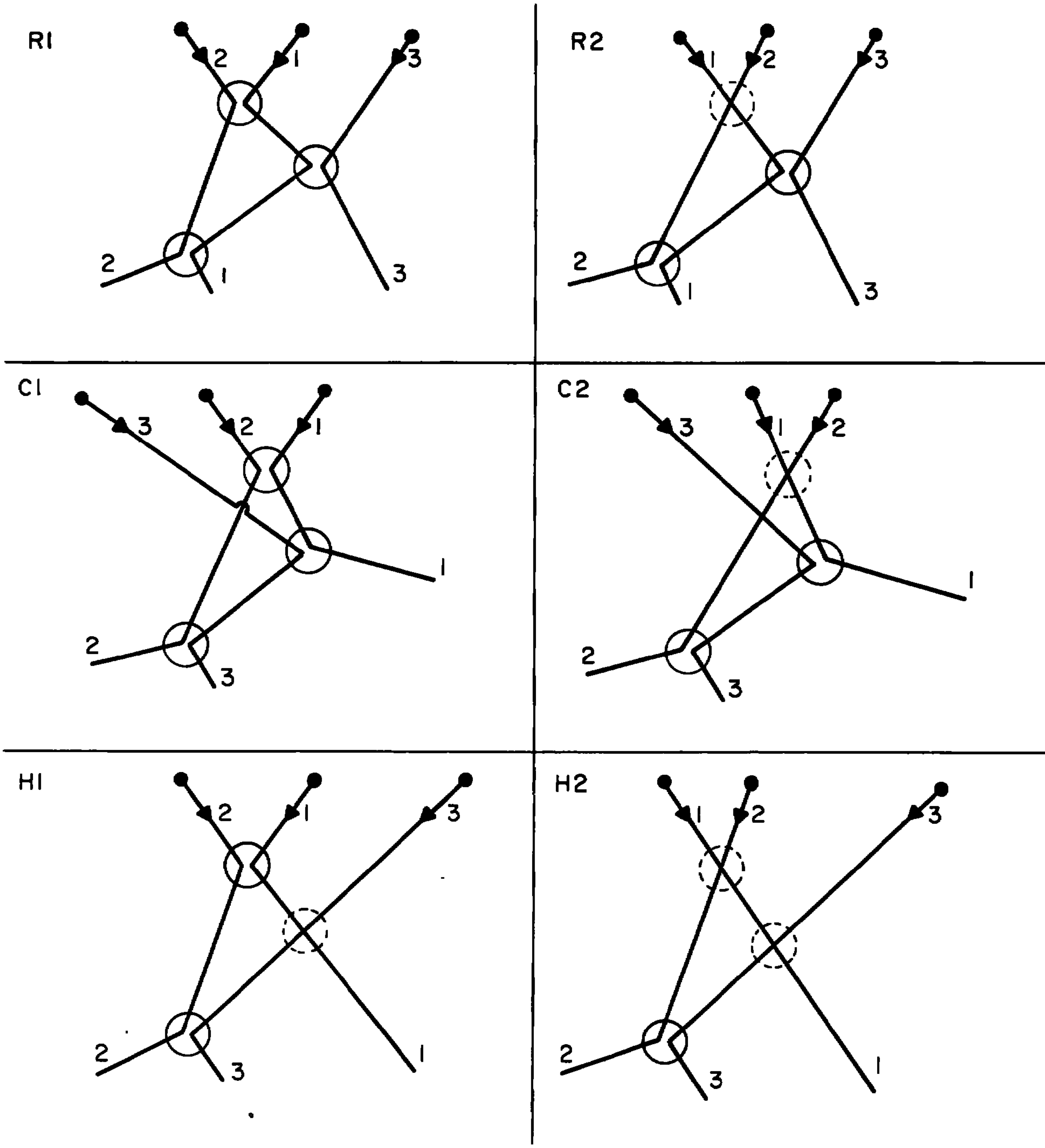

Figure 5. The six triple collision events after changing the direction of the velocities and time.

2.6 ANALYSIS OF THE TRIPLE COLLISION TRANSPORT INTEGRALS

In the preceding Section the triple collision integral was decomposed into a sum of integrals associated with the six triple collision events of Fig. 5. However, there exists a close relationship between the diagrams of the first kind (R1, C1 and H1) and those of the second kind (R2, C2, H2). If in R1, C1 or H1 the velocities after the first collision are taken as the initial velocities, we obtain the diagrams of the second kind. Minor exceptions to this correspondence will be discussed later. Using this relationship we can combine the contributions from the diagrams of the first kind with those of the second kind.[15]

As an example let us consider the recollision events R1 and R2 in Fig. 5. To specify the effect of the T_μ operators, we indicate the velocities after the i-th collision in R1 by $\vec{W}_m(i)$ $(m = 1,2,3)$. Thus the initial velocities are $\vec{W}_m(0)$, the velocities after the first collision $\vec{W}_m(1)$, the velocities after the second collision $\vec{W}_m(2)$, the velocities after the third collision $\vec{W}_m(3_R)$ and after a fourth collision, if that occurs, $\vec{W}_m(4_R)$. The index R indicates that the velocities are related to the integration variables by a recollision event. With this notation we can write for any pair of functions $\phi^{(k)}(\vec{W}_m)$ and $\phi^{(\ell)}(\vec{W}_n)$

$$\phi^{(k)}(\vec{W}_m).T_{R1}(12;13)\ \phi^{(\ell)}(\vec{W}_n) =$$

$$= \phi^{(k)}(\vec{W}_m(0)).[\phi^{(\ell)}(\vec{W}_n(j_R)) - \phi^{(\ell)}(\vec{W}_n(2))]\ . \qquad (2.6\text{-}1)$$

If (as usually) only three real collisions occur j = 3: if four collisions occur j = 4. The velocities in R2 are indicated by the same notation, except that the initial velocities are no longer $\vec{W}_m(0)$ but are identified with $\vec{W}_m(1)$. Thus

$$\Phi^{(k)}(\vec{W}_m).T_{R2}(12;13)\ \Phi^{(\ell)}(\vec{W}_n) = \qquad (2.6\text{-}2)$$
$$= -\ \Phi^{(k)}(\vec{W}_m(1)).[\Phi^{(\ell)}(\vec{W}_n(3_R)) - \Phi^{(\ell)}(\vec{W}_n(2))]\ .$$

In order to combine these two terms we refer to the coordinate system of Fig. 6 for a description of the collision process R1. Particle 1 is taken at rest at the origin after the first collision. The Z-axis is taken in the direction of $\vec{W}_{21}(1) = \vec{W}_2(1) - \vec{W}_1(1)$. The X-axis is chosen such that the perihelion vector $\vec{k}_1$ of the first collision is in the XZ plane as indicated in the figure; θ_1 is the angle between $-\vec{k}_1$ and the Z-axis. The perihelion vector $\vec{k}_2$ of the second collision lies in general outside the XZ plane. In this coordinate system particle 2 came originally from A. At the time of the first collision particle 2 is at B and particle 3 at C with relative position vectors+)

$$\vec{r}_{21}(1) = -\vec{k}_1\ ;\ \vec{r}_{31}(1) = -\vec{k}_2 - \tau^*\vec{W}_{31}(1);$$
$$\vec{r}_{32}(1) = \vec{k}_1 - \vec{k}_2 - \tau^*\vec{W}_{31}(1)\ . \qquad (2.6\text{-}3)$$

In order for a recollision to occur, particle 3 should collide with 1 at D after a time τ^* such that particle 1 will collide again with 2.

+) In this report $\vec{W}_{ij} = \vec{W}_i - \vec{W}_j$ and $\vec{r}_{ij} = \vec{r}_i - \vec{r}_j$.

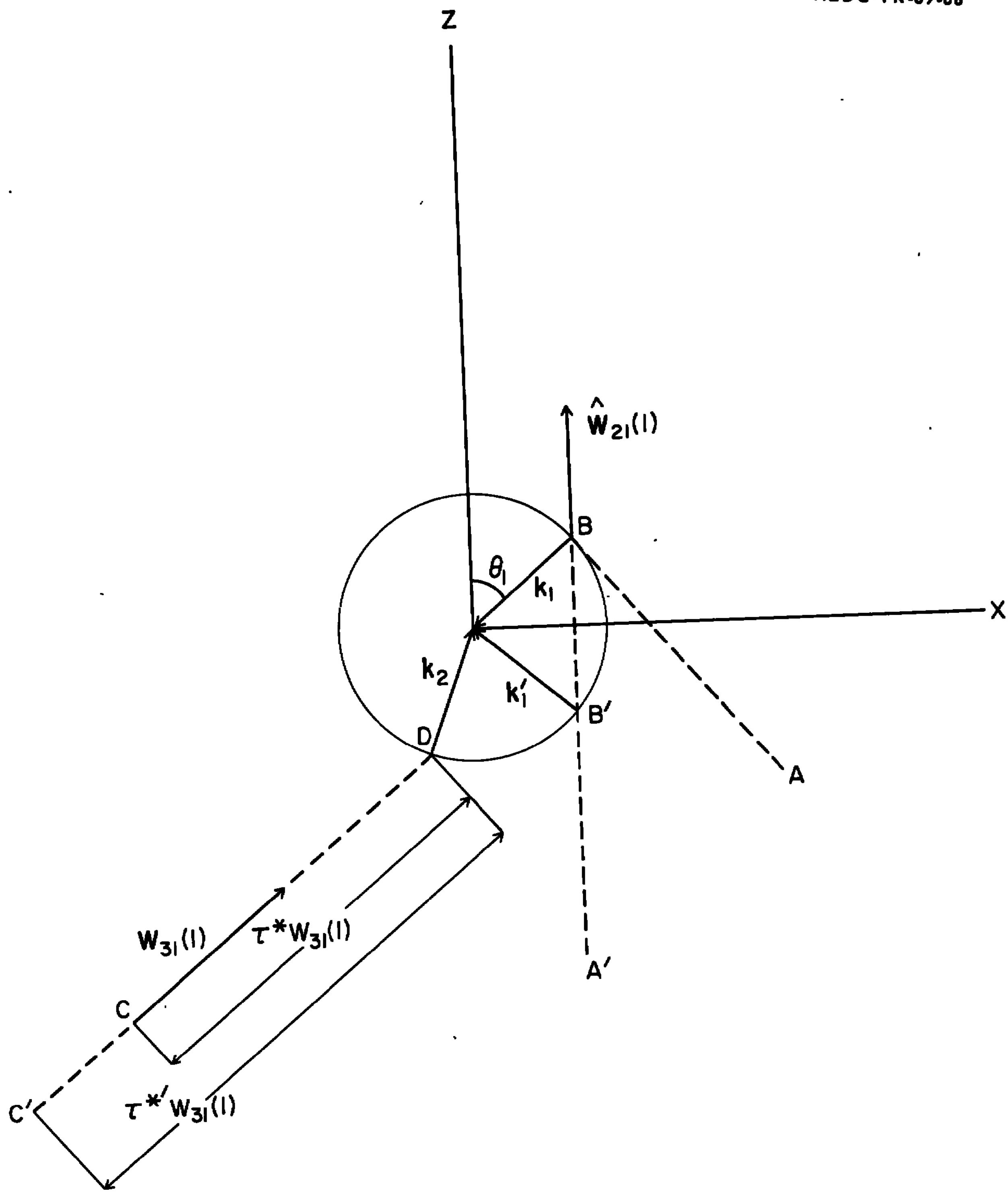

Figure 6. Coordinate system for the triple collision events.

The figure represents the situation immediately after the first collision.

In the collision event R2 the first collision is a non-interacting collision. Let the perihelion vector of this non-interacting collision be $\vec{k}'_1$, and the time between the first and the second collision $\tau^{*\prime}$. This implies that in Fig. 6 particle 2 came originally from A'. The relative position vectors at the time that the first collision begins are now indicated by $\vec{r}_{ij}(0)$. Thus

$$\vec{r}_{21}(0) = -\vec{k}'_1 \ ; \ \vec{r}_{31}(0) = -\vec{k}_2 - \tau^{*\prime}\vec{W}_{31}(1) \ ;$$

$$\vec{r}_{32}(0) = \vec{k}'_1 - \vec{k}_2 - \tau^{*\prime}\vec{W}_{31}(1) . \tag{2.6-4}$$

We require that particle 3 collides with 1 at D such that 1 and 2 will collide again. The same event as that described earlier is obtained if $\vec{k}'_1$ and $\tau^{*\prime}$ are chosen such that+)

$$\vec{k}'_1 = \vec{k}_1 - 2\,\hat{\vec{W}}_{21}(1).\vec{k}_1 \ ; \ \tau^{*\prime} = \tau^* + \tau_o^* , \tag{2.6-5}$$

with

$$\tau_o^* = \frac{2|\hat{\vec{W}}_{21}(1).\vec{k}_1|}{W_{21}(1)} . \tag{2.6-6}$$

This implies for the initial positions $\vec{r}_{ij}(0)$ in (2.6-4)

$$\vec{r}_{21}(0) = -\vec{k}_1 + 2\,\hat{\vec{W}}_{21}(1).\vec{k}_1 \ ; \ \vec{r}_{31}(0) = -\vec{k}_2 - (\tau^* + \tau_o^*)\vec{W}_{31}(1) \ ;$$

$$\vec{r}_{32}(0) = \vec{r}_{31}(0) - \vec{r}_{21}(0) . \tag{2.6-7}$$

We take $\vec{k}_1$ and τ^*, defined by (2.6-5) as the new integration variables for the integrals associated with the diagrams of the second kind. Then the velocities $\vec{W}_m(i)$ in (2.6-2) are the same functions of the integration variables

+) In this report a superscript indicates a unit vector: $\hat{\vec{a}} = \vec{a}/a$.

as those in (2.6-1) and one does not need to retrace the diagrams R1 and R2 separately.

The integrands associated with the other diagrams of the first and second kind can be combined by the same procedure. Using the velocities $\vec{W}_m(1)$ after the first collision as integration variables we obtain

$$a_{k\ell}^{(1)} = -\frac{3\sqrt{2}}{16\pi^6}\int d\vec{W}_1(1)d\vec{W}_2(1)d\vec{W}_3(1)\ \exp\ [-(W_1^2(1) + W_2^2(1) + W_3^2(1)]$$

$$\cdot \int d\vec{k}_1 d\vec{k}_2 \int d\tau^* |\vec{W}_{21}(1).\vec{k}_1|\vec{W}_{31}(1).\vec{k}_2 \sum_{m=1}^{3}\sum_{n=1}^{3} \tag{2.6-8}$$

$$[\vec{W}_m(0)S_{3/2}^{(k)}(W_m^2(0))\ .\ \{\vec{W}_n(j_R)S_{3/2}^{(\ell)}(W_n^2(j_R)) - \vec{W}_n(2)S_{3/2}^{(\ell)}(W_n^2(2))\} + \tag{R1}$$

$$- \vec{W}_m(1)S_{3/2}^{(k)}(W_m^2(1)).\ \{\vec{W}_n(3_R)S_{3/2}^{(\ell)}(W_n^2(3_R)) - \vec{W}_n(2)S_{3/2}^{(\ell)}(W_n^2(2))\} + \tag{R2}$$

$$+ \vec{W}_m(0)S_{3/2}^{(k)}(W_m^2(0)).\ \{\vec{W}_n(j_C)S_{3/2}^{(\ell)}(W_n^2(j_C)) - \vec{W}_n(2)S_{3/2}^{(\ell)}(W_n^2(2))\} + \tag{C1}$$

$$- \vec{W}_m(1)S_{3/2}^{(k)}(W_m^2(1)).\ \{\vec{W}_n(3_C)S_{3/2}^{(\ell)}(W_n^2(3_C)) - \vec{W}_n(2)S_{3/2}^{(\ell)}(W_n^2(2))\} + \tag{C2}$$

$$- \vec{W}_m(0)S_{3/2}^{(k)}(W_m^2(0)).\ \{\vec{W}_n(3_H)S_{3/2}^{(\ell)}(W_n^2(3_H)) - \vec{W}_n(1)S_{3/2}^{(\ell)}(W_n^2(1))\} + \tag{H1}$$

$$+ \vec{W}_m(1)S_{3/2}^{(k)}(W_m^2(1)).\ \{\vec{W}_n(3_H)S_{3/2}^{(\ell)}(W_n^2(3_H)) - \vec{W}_n(1)S_{3/2}^{(\ell)}(W_n^2(1))\}]\ , \tag{H2}$$

and a similar expression for $b_{k\ell}^{(1)}$.

To evaluate the various terms in the integrand we only have to retrace three triple collision events to which we refer as recollisions, cyclic collisions and hypothetical cyclic collisions. Nevertheless, we specify in (2.6-8) whether a term is associated with a diagram μ1 of the first kind or

$\mu 2$ of the second kind. The reason is that there are some differences in the region of integration over the variables. For instance, in C2 and H2 it is possible that 3 starts to collide with 1 while 1 and 2 are still overlapping. This phenomenon occurs when $0<\tau^{*\prime}<\tau^*_o$. For such a phase point there exists no diagram of the first kind as a counter part. Thus it follows from (2.6-5) that negative values of τ^* such that $-\tau_o^*<\tau^*<0$ are to be included in the contribution from C2 and H2, but not in any of the other terms. Apart from the phase points leading to overlapping configurations, the integration region associated with a diagram of the second kind is very similar to that associated with the corresponding diagram of the first kind. The remaining differences arise from the effect of various possible fourth collisions between the three particles, the effect of which is small.

The integration region will be specified by formulating the conditions that the integration variables should satisfy. Some of these conditions should be imposed on all integrals, namely

$$\vec{W}_{21}(1).\vec{k}_1<0 \quad , \tag{2.6-9}$$

$$\vec{W}_{31}(1).\vec{k}_2>0 \quad . \tag{2.6-10}$$

Condition (2.6-9) guarantees that the first collision and (2.6-10) that the second collision will take place. Furthermore as noted above

$$\tau^* > -\tau_o^* \; (\mu = C2,\ H2) \tag{2.6-11}$$

and

$$\tau^*>0 \ (\mu = R1, R2, C1, H1) \ . \tag{2.6-12}$$

(A negative value of τ^* is not allowed for R2, since it implies that the third collision would precede the second collision).

The requirement that a third collision should take place leads to a second class of conditions. They differ, of course, whether we consider a recollision, a cyclic collision or a hypothetical cyclic collision and are most conveniently expressed in terms of the positions and velocities at (just after) the time of the second collision. The initial positions for a diagram of the first kind were given by (2.6-3) and those for a diagram of the second kind by (2.6-7). The positions at the time of the second collision are the same for all diagrams:

$$\vec{r}_{21}(2) = -\vec{k}_1 + \tau^*\vec{W}_{21}(1) \ ; \ \vec{r}_{31}(2) = -\vec{k}_2 \ ; \ \vec{r}_{32}(2) = \vec{k}_1 - \vec{k}_2 - \tau^*\vec{W}_{21}(1) \ . \tag{2.6-13}$$

The basic equations describing a collision between two hard spheres are presented in Appendix B. Applying the inequalities (B-3) and B-4) we see that for <u>recollisions</u> (μ = R1, R2)

$$\{\vec{W}_{21}(2) \times \vec{r}_{21}(2)\}^2 - W_{21}^2(2) < 0 \ , \tag{2.6-14}$$

$$\vec{W}_{21}(2) . \vec{r}_{21}(2) < 0 \ , \tag{2.6-15}$$

for <u>cyclic</u> collisions (μ = C1, C2)

$$\{\vec{W}_{32}(2) \times \vec{r}_{32}(2)\}^2 - W_{32}^2(2) < 0 \ , \tag{2.6-16}$$

$$\vec{W}_{32}(2) . \vec{r}_{32}(2) < 0 \ , \tag{2.6-17}$$

and for <u>hypothetical cyclic</u> collisions (μ = H1, H2)

$$\{\vec{W}_{32}(1) \times \vec{r}_{32}(2)\}^2 - W_{32}^2(1) < 0 \ , \tag{2.6-18}$$

$$\vec{W}_{32}(1) . \vec{r}_{32}(2) < 0 \ . \tag{2.6-19}$$

For recollisions condition (2.6-15) combined with (2.6-10) can be reduced to

$$\vec{k}_1 . \vec{k}_2 < 0 \quad , \tag{2.6-20}$$

$$\vec{W}_{31}(1) . \vec{k}_2 > \frac{\vec{W}_{21}(1) . \vec{k}_1}{\vec{k}_1 . \vec{k}_2} \quad , \tag{2.6-21}$$

as pointed out by Weinstock.[19]

The initial phases should be such that particles 2 and 3 are not overlapping. Thus

$$r_{32}^2(1) > 1 \quad (\mu = R1,\ C1,\ H1) \quad , \tag{2.6-22}$$

$$r_{32}^2(0) > 1 \quad (\mu = R2,\ C2,\ H2) \quad . \tag{2.6-23}$$

For the cyclic and hypothetical cyclic collisions, particles 2 and 3 should also not overlap at the time of the second collision, since the third collision should not precede the second one.

$$r_{32}^2(2) > 1 . \tag{2.6-24}$$

The triple collision events were defined in Section 2.5 together with a distinction between real and hypothetical collisions. This distinction leads to some minor additional conditions:

i) In order that the first collision be real, the initial phases in Fig. 5 should be such that the particles did not experience a collision in their past history.

ii) In order that in R1, C1 and H1 the second collision be real, particle 3 should not collide with 2 before colliding with 1.

iii) In order that in R1 and C1 the third collision be real, no other collision should interfere along the path of particle 2.

Although these conditions together guarantee the proper triple collision events, some of them are redundant. Therefore, not all conditions need to be imposed explicitly. For instance, when in R1 the phases of the particles are such that the third collision (between 1 and 2) will occur it is no longer possible for 3 to collide with 2 before the second collision. On the other hand, in C1 this possibility has to be excluded explicitly.

We made an effort to reduce the number of conditions to be imposed. The conditions retained are presented in Table IV. The conditions (μ-1) through (μ-5) determine the basic phenomenon. The remaining conditions exclude possible fourth collisions that would interfere with the triple collision series desired.

We note that the integration regions associated with R1 and R2 are identical, except for the exclusion of a possible fourth collision in the previous past ((R1-6) and (R2-6)), the probability of which is very small.[18,20] The related integrands in (2.6-8) only differ in the possibility of a fourth collision succeeding the third one. Except for possible negative values of τ^*, the integrations associated with C1 and C2, resp. H1 and H2, are also very similar.

The position vectors $\vec{r}_{ij}(n)$ are related to the integration variables by (2.6-3), (2.6-7) and (2.6-13). The velocities $\vec{W}_{ij}(0)$ and $\vec{W}_{ij}(2)$ are related to the integration variables $\vec{k}_1$, $\vec{k}_2$ and $\vec{W}_i(1)$ by

$$\begin{aligned}
\vec{W}_{21}(0) &= \vec{W}_{21}(1) - 2\vec{W}_{21}(1).\vec{k}_1\vec{k}_1 \quad , \\
\vec{W}_{31}(0) &= \vec{W}_{31}(1) - \vec{W}_{21}(1).\vec{k}_1\vec{k}_1 \quad , \qquad (2.6\text{-}25) \\
\vec{W}_{32}(0) &= \vec{W}_{32}(1) + \vec{W}_{21}(1).\vec{k}_1\vec{k}_1 \quad ,
\end{aligned}$$

and

$$\vec{W}_{21}(2) = \vec{W}_{21}(1) - \vec{W}_{31}(1).\vec{k}_2\vec{k}_2 \;,$$

$$\vec{W}_{31}(2) = \vec{W}_{31}(1) - 2\vec{W}_{31}(1).\vec{k}_2\vec{k}_2 \;, \tag{2.6-26}$$

$$\vec{W}_{32}(2) = \vec{W}_{32}(1) - \vec{W}_{31}(1).\vec{k}_2\vec{k}_2 \;.$$

The integrals (2.6-8) together with the conditions of Table IV specify the triple collision transport integrals to be evaluated.

Table IV

Conditions specifying the integration region for the triple collision transport integrals.

Recollisions of the first kind R1

$$\tau^* > 0 \tag{R1-1}$$

$$\vec{W}_{21}(1).\vec{k}_1 < 0 \tag{R1-2}$$

$$\vec{k}_1.\vec{k}_2 < 0 \tag{R1-3}$$

$$\vec{W}_{31}(1).\vec{k}_2 > \frac{\vec{W}_{21}(1).\vec{k}_1}{\vec{k}_1.\vec{k}_2} \tag{R1-4}$$

$$\{\vec{W}_{21}(2) \times \vec{r}_{21}(2)\}^2 - W_{21}^2(2) < 0 \tag{R1-5}$$

$$\vec{W}_{32}(0).\vec{r}_{32}(1) < 0 \text{ or } \{\vec{W}_{32}(0) \times \vec{r}_{32}(1)\}^2 - W_{32}^2(0) > 0 \tag{R1-6}$$

Recollisions of the second kind R2

$$\tau^* > 0 \tag{R2-1}$$

$$\vec{W}_{21}(1).\vec{k}_1 < 0 \tag{R2-2}$$

$$\vec{k}_1.\vec{k}_2 < 0 \tag{R2-3}$$

$$\vec{W}_{31}(1).\vec{k}_2 > \frac{\vec{W}_{21}(1).\vec{k}_1}{\vec{k}_1.\vec{k}_2} \tag{R2-4}$$

$$\{\vec{W}_{21}(2) \times \vec{r}_{21}(2)\}^2 - W_{21}^2(2) < 0 \tag{R2-5}$$

$$\vec{W}_{32}(1).\vec{r}_{32}(0) < 0 \text{ or } \{\vec{W}_{32}(1) \times \vec{r}_{32}(0)\}^2 - W_{32}^2(1) > 0 \tag{R2-6}$$

Table IV (continued)

Cyclic collisions of the first kind C1

$$\tau^* > 0 \tag{C1-1}$$

$$\vec{W}_{21}(1)\cdot\vec{k}_1 < 0 \tag{C1-2}$$

$$\vec{W}_{31}(1)\cdot\vec{k}_2 > 0 \tag{C1-3}$$

$$\vec{W}_{32}(2)\cdot\vec{r}_{32}(2) < 0 \tag{C1-4}$$

$$\{\vec{W}_{32}(2) \times \vec{r}_{32}(2)\}^2 - W_{32}^2(2) < 0 \tag{C1-5}$$

$$r_{32}^2(1) > 1 \tag{C1-6}$$

$$\vec{W}_{31}(0)\cdot\vec{r}_{31}(1) < 0 \text{ or } \{\vec{W}_{31}(0) \times \vec{r}_{31}(1)\}^2 - W_{31}^2(0) > 0 \tag{C1-7}$$

3 should not collide with 2 before colliding with 1 (C1-8)

2 should not recollide with 1 before colliding with 3 (C1-9)

Cyclic collisions of the second kind C2

$$\tau^* > -\tau_o^* \tag{C2-1}$$

$$\vec{W}_{21}(1)\cdot\vec{k}_1 < 0 \tag{C2-2}$$

$$\vec{W}_{31}(1)\cdot\vec{k}_2 > 0 \tag{C2-3}$$

$$\vec{W}_{32}(2)\cdot\vec{r}_{32}(2) < 0 \tag{C2-4}$$

$$\{\vec{W}_{32}(2) \times \vec{r}_{32}(2)\}^2 - W_{32}^2(2) < 0 \tag{C2-5}$$

$$r_{32}^2(0) > 1 \tag{C2-6}$$

$$r_{32}^2(2) > 1 \tag{C2-7}$$

$$\vec{W}_{32}(1)\cdot\vec{r}_{32}(0) < 0 \text{ or } \{\vec{W}_{32}(1) \times \vec{r}_{32}(0)\}^2 - W_{32}^2(1) > 0 \tag{C2-8}$$

Table IV (continued)

Hypothetical cyclic collisions of the first kind H1

$$\tau^* > 0 \quad \text{(H1-1)}$$

$$\vec{W}_{21}(1).\vec{k}_1 < 0 \quad \text{(H1-2)}$$

$$\vec{W}_{31}(1).\vec{k}_2 > 0 \quad \text{(H1-3)}$$

$$\vec{W}_{32}(1).\vec{r}_{32}(2) < 0 \quad \text{(H1-4)}$$

$$\{\vec{W}_{32}(1) \times \vec{r}_{32}(2)\}^2 - W_{32}^2(1) < 0 \quad \text{(H1-5)}$$

$$r_{32}^2(1) > 1 \quad \text{(H1-6)}$$

$$r_{32}^2(2) > 1 \quad \text{(H1-7)}$$

$$\vec{W}_{31}(0).\vec{r}_{31}(1) < 0 \text{ or } \{\vec{W}_{31}(0) \times \vec{r}_{31}(1)\}^2 - W_{31}^2(0) > 0 \quad \text{(H1-8)}$$

$$\vec{W}_{32}(0).\vec{r}_{32}(1) < 0 \text{ or } \{\vec{W}_{32}(0) \times \vec{r}_{32}(1)\}^2 - W_{32}^2(0) > 0 \quad \text{(H1-9)}$$

Hypothetical cyclic collisions of the second kind H2

$$\tau^* > -\tau_o^* \quad \text{(H2-1)}$$

$$\vec{W}_{21}(1).\vec{k}_1 < 0 \quad \text{(H2-2)}$$

$$\vec{W}_{31}(1).\vec{k}_2 > 0 \quad \text{(H2-3)}$$

$$\vec{W}_{32}(1).\vec{r}_{32}(2) < 0 \quad \text{(H2-4)}$$

$$\{\vec{W}_{32}(1) \times \vec{r}_{32}(2)\}^2 - W_{32}^2(1) < 0 \quad \text{(H2-5)}$$

$$r_{32}^2(0) > 1 \quad \text{(H2-6)}$$

$$r_{32}^2(2) > 1 \quad \text{(H2-7)}$$

2.7 EVALUATION OF THE TRIPLE COLLISION TRANSPORT INTEGRALS IN THE FIRST ENSKOG APPROXIMATION

The triple collision integrals (2.6-8) which contain still fourteenintegrations, can be reduced to seven dimensional integrals. First, the operators $T_\mu(12;13)$ commute with the total momentum and the conditions of Table IV, specifying the integration region, are independent of the total momentum. Thus we can integrate over the total momentum or velocity and express the resulting integrals in terms of the relative velocities $\vec{W}_{21}(1)$ and $\vec{W}_{31}(1)$. Secondly, the integrand is a scalar, invariant under rotations of the coordinate system. Thus we can integrate over all possible directions of $\vec{W}_{21}(1)$ and evaluate the resulting integrand with $\vec{W}_{21}(1)$ taken in the Z-direction as in Fig. 6. Furthermore, we can integrate over all directions of the component of $\vec{k}_1$ in the XY plane and take $\vec{k}_1$ in the XZ plane as in Fig. 6. Finally, for hard spheres the angle of deflection, caused by a binary collision, is independent of the magnitude of the relative velocity. This enables us to integrate over all values $W_{21}(1)$ $(=|\vec{W}_{21}(1)|)$ and to evaluate the resulting integrand for collision events for which $\hat{\vec{W}}_{21}(1)$, is a unit vector.

For the matrix elements $a_{11}^{(1)}$ and $b_{oo}^{(1)}$, determining the first Enskog approximations $\lambda_1(1)$ and $\eta_1(1)$ in (2.4-12), this reduction was carried out in a previous paper.[15] Denoting the angle between $-\vec{k}_1$ and the Z-axis by θ_1 (see Fig. 6) we obtain

$$\frac{\lambda_1(1)}{\lambda_o(1)} = -a_{11}^{(1)} = \frac{2}{3}\frac{\eta_1(1)}{\eta_o(1)} + \frac{385}{\pi^2}\frac{3^7}{2^{14}}\int d\vec{W}_{31}(1)\int_o^{\pi/2} d\theta_1 \sin\theta_1 \int d\vec{k}_2 \int d\tau \cos\theta_1$$

$$\vec{W}_{31}(1).\vec{k}_2 E^{-13/2} \sum_\mu \vec{K} \cdot T_\mu(12;13)\, \vec{K} \quad , \tag{2.7-1}$$

$$\frac{\eta_1(1)}{\eta_o(1)} = -b_{oo}^{(1)} = \frac{35}{\pi^2}\frac{3^6}{2^{10}}\int d\vec{W}_{31}(1)\int_o^{\pi/2} d\theta_1 \sin\theta_1 \int d\vec{k}_2 \int d\tau \cos\theta_1$$

$$\vec{W}_{31}(1).\vec{k}_2 E^{-11/2} \sum_\mu \overleftrightarrow{L} : T_\mu(12;13)\, \overleftrightarrow{L} \ .$$

For convenience, we have introduced the abbreviations

$$E = W_{21}^2 + W_{31}^2 - \vec{W}_{21}.\vec{W}_{31} \ , \tag{2.7-2}$$

$$\vec{K} = \vec{W}_{21}(W_{21}^2 - \tfrac{2}{3}E) + \vec{W}_{31}(W_{31}^2 - \tfrac{2}{3}E) \ , \tag{2.7-3}$$

$$\overleftrightarrow{L} = \vec{W}_{21}\vec{W}_{21} + \vec{W}_{31}\vec{W}_{31} - \tfrac{1}{2}(\vec{W}_{21}\vec{W}_{31} + \vec{W}_{31}\vec{W}_{21}) \ . \tag{2.7-4}$$

The operators $T_\mu(12;13)$ commute with E which represents the kinetic energy. In (2.7-1) τ is the scaled dimensionless time $t^*W_{21}(1)$ (see [15]). Just as in (2.6-8) the effect of the $T_\mu(12;13)$ operators can be written explicitly as

$$\begin{aligned}
\sum_\mu \vec{K} \cdot T_\mu(12;13)\, \vec{K} = {} & \vec{K}(0) \ . \ \{\vec{K}(j_R) - \vec{K}(2)\} + && \text{(R1)} \\
& - \vec{K}(1) \ . \ \{\vec{K}(3_R) - \vec{K}(2)\} + && \text{(R2)} \\
& + \vec{K}(0) \ . \ \{\vec{K}(j_C) - \vec{K}(2)\} + && \text{(C1)} \\
& - \vec{K}(1) \ . \ \{\vec{K}(3_C) - \vec{K}(2)\} + && \text{(C2)} \\
& - \vec{K}(0) \ . \ \{\vec{K}(3_H) - \vec{K}(1)\} + && \text{(H1)} \\
& + \vec{K}(1) \ . \ \{\vec{K}(3_H) - \vec{K}(1)\} \ , && \text{(H2)}
\end{aligned} \tag{2.7-5}$$

$$\sum_{\mu} \overleftrightarrow{L} : T_\mu(12{:}13)\,\overleftrightarrow{L} = \overleftrightarrow{L}(0) : \{\overleftrightarrow{L}(j_R) - \overleftrightarrow{L}(2)\} + \qquad \text{(R1)}$$

$$- \overleftrightarrow{L}(1) : \{\overleftrightarrow{L}(3_R) - \overleftrightarrow{L}(2)\} + \qquad \text{(R2)}$$

$$+ \overleftrightarrow{L}(0) : \{\overleftrightarrow{L}(j_C) - \overleftrightarrow{L}(2)\} + \qquad \text{(C1)} \qquad (2.7\text{-}6)$$

$$- \overleftrightarrow{L}(1) : \{\overleftrightarrow{L}(3_C) - \overleftrightarrow{L}(2)\} + \qquad \text{(C2)}$$

$$- \overleftrightarrow{L}(0) : \{\overleftrightarrow{L}(3_H) - \overleftrightarrow{L}(1)\} + \qquad \text{(H1)}$$

$$+ \overleftrightarrow{L}(1) : \{\overleftrightarrow{L}(3_H) - \overleftrightarrow{L}(1)\}\,, \qquad \text{(H2)}$$

where again each term has to be integrated subject to the conditions of Table IV. The argument n in $\vec{K}(n)$ and $\overleftrightarrow{L}(n)$ indicates for which velocities $\vec{W}_{21}(n)$, $\vec{W}_{31}(n)$ these quantities should be evaluated. The kinetic energy E is invariant during the collision process and thus independent of n.

We specify the perihelion vector $\vec{k}_2$ by its polar angle θ_2 with the Z-axis (see Fig. 7) and by its azimuthal angle ϕ with the XZ plane as initial plane. Hence

$$k_{2x} = \sin\theta_2\cos\phi,\ k_{2y} = \sin\theta_2\sin\phi\ ,\ k_{2z} = \cos\theta_2\ , \qquad (2.7\text{-}7)$$

and

$$d\vec{k}_2 = \sin\theta_2 d\theta_2 d\phi\ . \qquad (2.7\text{-}8)$$

The velocity $\vec{W}_{31}(1)$ is specified by its magnitude w, its polar angle θ_3 with the Z-axis and the aximuthal angle ψ in the XY plane, measured with respect to the plane through $\vec{k}_2$ and the Z-axis as initial plane. Thus

$$W_{31}(1)_x = w\sin\theta_3\ \cos(\phi + \psi)\ ,$$

$$W_{31}(1)_y = w\sin\theta_3\ \sin(\phi + \psi)\ , \qquad (2.7\text{-}9)$$

$$W_{31}(1)_z = w\cos\theta_3\ ,$$

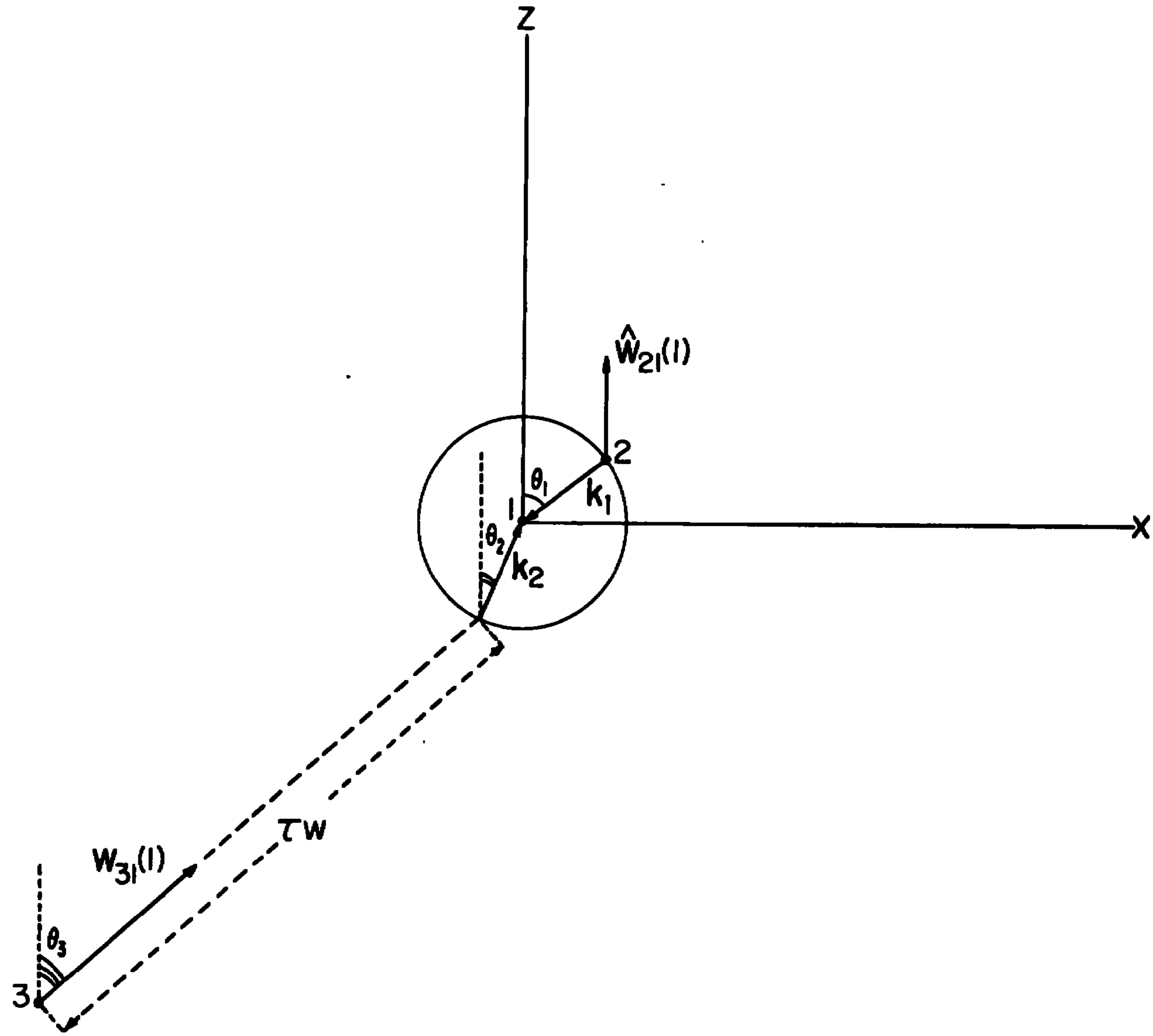

Figure 7. Coordinate system for the evaluation of the triple collision integrals. The figure represents the situation immediately after the first collision.

and

$$d\vec{W}_{31}(1) = w^2 \sin\theta_3 dw d\theta_3 d\psi \,. \tag{2.7-10}$$

As a consequence

$$\vec{W}_{31}(1).\vec{k}_2 = w(\cos\theta_2\cos\theta_3 + \sin\theta_2\sin\theta_3\cos\psi), \tag{2.7-11}$$

and condition (2.6-10) becomes

$$\cos\theta_{23} \equiv \cos\theta_2\cos\theta_3 + \sin\theta_2\sin\theta_3\cos\psi > 0 \,. \tag{2.7-12}$$

In terms of these variables the triple collision integrals (2.7-1) read

$$\frac{\lambda_1(1)}{\lambda_o(1)} = \frac{2}{3}\frac{\eta_1(1)}{\eta_o(1)} + \frac{385}{\pi^2}\frac{3^7}{2^{14}}\int_o^{\pi/2} d\theta_1 \int_o^{\pi} d\theta_2 \int_o^{\pi} d\theta_3 \int_o^{2\pi} d\phi \int_o^{2\pi} d\psi \int_o^{\infty} dw \int_{-\tau_o}^{\infty} d\tau$$

$$w^3 \sin\theta_1\cos\theta_1\sin\theta_2\sin\theta_3\cos\theta_{23} E^{-13/2} \sum_\mu \vec{K} \,.\, T_\mu(12;13)\,\vec{K} \,,$$

(2.7-13)

$$\frac{\eta_1(1)}{\eta_o(1)} = \frac{35}{\pi^2}\frac{3^6}{2^{10}}\int_o^{\pi/2} d\theta_1 \int_o^{\pi} d\theta_2 \int_o^{\pi} d\theta_3 \int_o^{2\pi} d\phi \int_o^{2\pi} d\psi \int_o^{\infty} dw \int_{-\tau_o}^{\infty} d\tau$$

$$w^3 \sin\theta_1\cos\theta_1\sin\theta_2\sin\theta_3\cos\theta_{23}\, E^{-11/2} \sum_\mu \vec{L} \,.\, T_\mu(12;13)\,\vec{L} \,,$$

with

$$E = 1 + w^2 - w\cos\theta_3 \,. \tag{2.7-14}$$

Of course, in addition the integration variables are still subject to the conditions of Table IV.

It does not seem feasible to reduce the number of integrations further analytically without making approximations. Therefore, to carry out the remaining seven integrations we take resort to a numerical procedure.

The integration over the velocity w extends to infinity. In addition, the time τ between collisions can also become infinite, when two of the molecules are moving in parallel directions. In order to apply a numerical integration procedure, we transform the integral into an integral over a finite integration region. For large values of w the integrand decreases as w^{-4}; this suggests the transformation

$$u = \frac{1}{1 + w^3} , \tag{2.7-15}$$

where $0<u<1$. To reduce the integration over τ to a finite interval we proceed as follows. For a given $\vec{k}_1$, $\vec{k}_2$ and $\vec{W}_{31}(1)$ (θ_1, θ_2, θ_3, ϕ, ψ and w in (2.7-13)) we solve the inequalities ($\mu - 4$) and ($\mu - 5$) in Table IV for the variable τ (together with the requirement $\tau > - \tau_o$):

$$\begin{aligned} T_{R,Min} &< \tau < T_{R,Max} (\mu = R1, R2) , \\ T_{C,Min} &< \tau < T_{C,Max} (\mu = C1, C2) , \\ T_{H,Min} &< \tau < T_{H,Max} (\mu = H1, H2) . \end{aligned} \tag{2.7-16}$$

These inequalities determine the range of τ values for which a third collision can occur when $\vec{k}_1$, $\vec{k}_2$ and $\vec{W}_{31}(1)$ are specified. It turns out that $T_{R,Min}=0$ independent of the other variables. As a new integration variable we take $\tilde{\tau}$ such that

$$\tau = T_{\nu,Min} + \tilde{\tau}\, \Delta T_{\nu} \quad (\nu = R, C, H) , \tag{2.7-17}$$

where

$$\Delta T_{\nu} = T_{\nu,Max} - T_{\nu,Min} . \tag{2.7-18}$$

Hence

$$\frac{\lambda_1(1)}{\lambda_o(1)} = \frac{2}{3}\frac{\eta_1(1)}{\eta_o(1)} + \frac{385}{\pi^2}\frac{3^6}{2^{14}}\int_0^{\pi/2} d\theta_1 \int_0^{\pi} d\theta_2 \int_0^{\pi} d\theta_3 \int_0^{2\pi} d\phi \int_0^{2\pi} d\psi \int_0^1 du \int_0^1 d\tilde{\tau}$$

$$\cdot \frac{\sin\theta_1 \cos\theta_1 \sin\theta_2 \sin\theta_3 w \cos\theta_{23}}{u^2 E^{13/2}} \sum_{\mu} \Delta T_{\mu}\, \vec{K} \cdot T_{\mu}(12;13)\, \vec{K} \;, \tag{2.7-19}$$

$$\frac{\eta_1(1)}{\eta_o(1)} = \frac{35}{\pi^2} \cdot \frac{3^5}{2^{10}} \int_0^{\pi/2} d\theta_1 \int_0^{\pi} d\theta_2 \int_0^{\pi} d\theta_3 \int_0^{2\pi} d\phi \int_0^{2\pi} d\psi \int_0^1 du \int_0^1 d\tilde{\tau}$$

$$\cdot \frac{\sin\theta_1 \cos\theta_1 \sin\theta_2 \sin\theta_3 w \cos\theta_{23}}{u^2 E^{11/2}} \sum_{\mu} \Delta T_{\mu}\, \overset{\leftrightarrow}{L} : T_{\mu}(12;13)\, \overset{\leftrightarrow}{L} \;,$$

where $\Delta T_{R1} = \Delta T_{R2} = \Delta T_R$, etc.

As mentioned earlier the time intervals ΔT_μ become infinite for certain points in the integration region. For recollisions this happens when $\theta_2 \to 0$, where

$$\Delta T_R \propto \frac{1}{\vec{W}_{21}(2) \times \vec{W}_{21}(1)} \propto \frac{1}{\sin\theta_2} \;;$$

for hypothetical cyclic collisions when $\theta_3 \to 0$, where

$$\Delta T_H \propto \frac{1}{\vec{W}_{31}(1) \times \vec{W}_{21}(1)} \propto \frac{1}{\sin\theta_3} \;;$$

and for cyclic collisions when ζ, the angle between $\vec{W}_{32}(2)$ and $\vec{W}_{21}(1)$ approaches zero

$$\Delta T_C \propto \frac{1}{\vec{W}_{32}(2) \times \vec{W}_{21}(1)} \propto \frac{1}{\sin\zeta} \,.$$

The behavior of the integrand near these singularities can be characterized by

$$\sin\theta_2 \sin\theta_3 \left(\frac{a_R}{\sin\theta_2} + \frac{a_C}{\sin\zeta} + \frac{a_H}{\sin\theta_3}\right) .$$

The coordinate system introduced was designed to remove any singular behavior of the integrand for $\theta_2 = 0$ and $\theta_3 = 0$. However, although the integral is convergent (see Section 3.1), the integrand is singular near ζ=0 and therefore not yet suitable for numerical integration. Since

$$\lim_{\zeta\to 0} \sin\zeta = \lim_{\theta_2\to\pi/2} \lim_{\phi\to 0} \{(\frac{\pi}{2} - \theta_2)^2 \cos^2\theta_3 + \psi^2 \sin^2\theta_3\}^{1/2} ,$$

the singularity can be removed by the transformation

$$\begin{aligned} \rho\cos\chi &= \pi - 2\theta_2 , \\ \rho\sin\chi &= \frac{1}{2}\psi . \end{aligned} \tag{2.7-20}$$

ρ and χ are the polar coordinates associated with the variables $\pi - 2\theta_2$ and $\psi/2$.

$$\int_o^\pi d\theta_2 \int_o^{2\pi} d\psi = \int_o^\pi d\chi \int_o^{\rho_{Max}} \rho d\rho , \tag{2.7-21}$$

with

$$\rho_{Max} = \mathrm{Min}\{\frac{\pi}{\sin\chi}, \frac{\pi}{|\cos\chi|}\} . \tag{2.7-22}$$

Thus the limiting behavior of the integrand around $\zeta = 0$ or $\rho = 0$ becomes

$$\frac{d\theta_2 d\psi}{\sin\zeta} = \frac{d\chi d\rho}{\{\frac{1}{4}\cos^2\chi\cos^2\theta_3 + 4\sin^2\chi\sin^2\theta_3\}^{1/2}} \quad ,$$

which is well behaved for any value of χ. Introducing ρ such that

$$\rho = \tilde{\rho}\, \rho_{Max} \quad , \tag{2.7-23}$$

the final form of the triple collision integrals to be considered for numerical evaluation becomes

$$\frac{\lambda_1(1)}{\lambda_o(1)} - \frac{2}{3}\frac{\eta_1(1)}{\eta_o(1)} = \frac{385}{\pi^2}\,\frac{3^6}{2^{14}} \int_0^{\pi/2} d\theta_1 \int_0^{\pi} d\theta_3 \int_0^{2\pi} d\phi \int_0^{\pi} d\chi \int_0^1 d\tilde{\rho} \int_0^1 du \int_0^1 d\tilde{\tau}$$

$$\cdot \frac{\tilde{\rho}\,\rho_{Max}\sin\theta_1\cos\theta_1\sin\theta_2\sin\theta_3\; w\cos\theta_{23}}{u^2\; E^{13/2}} \sum_\mu \Delta T_\mu\, \vec{K} \cdot T_\mu(12;13)\, \vec{K} \quad ,$$

$$\frac{\eta_1(1)}{\eta_1(1)} = \frac{35}{\pi^2}\,\frac{3^5}{2^{10}} \int_0^{\pi/2} d\theta_1 \int_0^{\pi} d\theta_3 \int_0^{2\pi} d\phi \int_0^{\pi} d\chi \int_0^1 d\tilde{\rho} \int_0^1 du \int_0^1 d\tilde{\tau} \tag{2.7-24}$$

$$\cdot \frac{\tilde{\rho}\,\rho_{Max}\sin\theta_1\cos\theta_1\sin\theta_2\sin\theta_3\; w\cos\theta_{23}}{u^2\; E^{11/2}} \sum_\mu \Delta T_\mu\, \vec{\vec{L}} : T_\mu\,(12;13)\, \vec{\vec{L}} \quad .$$

The seven dimensional integration region is specified by

$$\begin{aligned} 0 &< \theta_1 < \pi/2 \; , \\ 0 &< \theta_3 < \pi \; , \\ 0 &< \phi < 2\pi \; , \\ 0 &< \chi < \pi \; , \\ 0 &< \tilde{\rho} < 1 \; , \\ 0 &< u < 1 \; , \\ 0 &< \tilde{\tau} < 1 \; . \end{aligned} \tag{2.7-25}$$

Condition (μ-2) in Table IV is taken care of by $0 < \theta_1 < \pi/2$. Conditions (μ-4) and (μ-5) are satisfied by $0<\tau<1$ (together with $\tau>0$ for R and $\tau>-\tau_o$ for C and H). The remaining conditions will be imposed explicitly. When one of these conditions is violated the corresponding term in the integrand will be taken to be zero. We remark that the triple collision transport integrals (2.6-8) together with the conditions of Table IV represent a complete solution of the Choh-Uhlenbeck integral equation for λ_1 and η_1, in which all dynamical effects are taken into account. Since we did not have any reliable a priori estimate of the effects of the various triple collision events, we retained the complete collision integrals (2.7-24) together with all conditions of Table IV in the numerical integration. From the results obtained we can suggest a posteriori approximations that would not change the values significantly as will be discussed later.

A computer program was devised that yields the value of the integrand for any point of the integration region (2.7-25). The following checks were included in the computer program:

1. For each triple collision event we verified conservation of kinetic energy.

2. For each triple collision event we verified conservation of angular momentum.

3. For each triple collision event subject to the conditions of Table IV we verified that all other (redundant) conditions mentioned in Section 2.6 were satisfied as well.

To obtain an estimate for the integrals we need to select a sampling procedure. At first we tried a method of Haselgrove for numerical integration.[21] However, we did not obtain a satisfactory convergence for the estimates. As an alternative we decided upon a modified Monte Carlo quadrature suggested by

Haber.[22+)] Consider the integral

$$I = \int_0^1 \cdot \cdot \cdot \cdot \int_0^1 f(\vec{x})\, d\vec{x} \quad , \tag{2.7-26}$$

over the n dimensional vector $\vec{x}$. The n dimensional integration region is to be pictured as divided into $N = k^n$ subcubes. In the i-th subcube two independent random points are chosen $\vec{x}_i$ and $\vec{y}_i$. In addition we consider the points $\vec{x}_i'$ and $\vec{y}_i'$ which are, respectively, the points symmetrically opposite to $\vec{x}_i$ and $\vec{y}_i$ in the subcube. A first estimate of the integral I is

$$J_1(k) = \frac{1}{2N} \sum_{i=1}^{N} \{f(\vec{x}_i) + f(\vec{y}_i)\} \quad , \tag{2.7-27}$$

with an estimated standard deviation

$$\sigma_1 = \frac{1}{2N} \left[\sum_{i=1}^{N} \{f(\vec{x}_i) - f(\vec{y}_i)\}^2 \right]^{1/2} . \tag{2.7-28}$$

A second better estimate is obtained by

$$J_2(k) = \frac{1}{2N} \sum_{i=1}^{N} \left\{ \frac{f(\vec{x}_i) + f(\vec{x}_i')}{2} + \frac{f(\vec{y}_i) + f(\vec{y}_i')}{2} \right\} , \tag{2.7-29}$$

with an estimated standard deviation

$$\sigma_2 = \frac{1}{2N} \left[\sum_{i=1}^{N} \left\{ \frac{f(\vec{x}_i) + f(\vec{x}_i')}{2} - \frac{f(\vec{y}_i) + f(\vec{y}_i')}{2} \right\}^2 \right]^{1/2} . \tag{2.7-30}$$

+) The author is indebted to Dr. S. Haber for his advice and to Mr. F. P. Karriker for his assistance in carrying out the computations.

To test the reliability of this procedure for our triple collision transport integrals, we first evaluate the seven dimensional integrals associated with diagram H2 with the additional conditions $r_{21}^2(3) < 1$ and $r_{31}^2(3) < 1$ at the time of the third collision. As pointed out in Section 2.5 under these conditions we should regain the values predicted by Enskog. Thus for these integrals we can compare the estimates with the exact answer. The results obtained for k = 2, 3, 4, 5 and 6 are presented in Table V together with the corresponding standard deviations. It turns out that the estimates k = 2 and k = 3 are not yet reliable which is not surprising. However, the estimates for k > 4 are all within each others standard deviations and do agree with the exact result.

Subsequently, we applied this procedure to the complete triple collision integrals (2.7-24). In practice, we subtract from H2 the contributions contained in the Enskog theory and compute directly the difference between the complete triple collision integral and the value predicted by Enskog. Since we expect possible cancellations between the contributions of different diagrams (confirmed by the results) we combine for each phase point all six terms of the integrand to obtain a maximum precision for the total integral. From the test calculation we conclude that we should disregard the estimates for k = 2 and k = 3. In the preliminary computations reported here, we obtained four successive estimates $J_1(4)$, $J_2(4)$, $J_1(5)$, $J_2(5)$, indicated respectively by i = 1, 2, 3, 4 in Tables VI and VII. The results obtained for the total triple collision integrals are presented in Table VI. In addition, we made an estimate of the contributions of the six individual triple collision events; these results are reported in Table VII. We see that the four different estimates agree with each other, as was the case for

the test calculation in Table V. Thus we conclude that our preliminary calculations seem to yield a fair estimate for the triple collision transport integrals.

Table V

Test of the numerical integration procedure

	$\left[\frac{\lambda_1(1)}{\lambda_1(1)} - \frac{2}{3}\frac{\eta_1(1)}{\eta_o(1)}\right]_{\text{Enskog}}$	$\left[\frac{\eta_1(1)}{\eta_o(1)}\right]_{\text{Enskog}}$
$J_1(2)$	-0.32 ± 0.29	-0.53 ± 0.35
$J_2(2)$	-0.13 ± 0.15	-0.49 ± 0.21
$J_1(3)$	-0.16 ± 0.02	-0.54 ± 0.05
$J_2(3)$	-0.17 ± 0.04	-0.55 ± 0.06
$J_1(4)$	-0.203 ± 0.017	-0.634 ± 0.025
$J_2(4)$	-0.211 ± 0.012	-0.634 ± 0.019
$J_1(5)$	-0.215 ± 0.008	-0.637 ± 0.011
$J_2(5)$	-0.213 ± 0.007	-0.634 ± 0.009
$J_1(6)$	-0.213 ± 0.007	-0.629 ± 0.009
exact	-0.208	-0.625

Table VI

Estimates for the triple collision transport integrals

i	$\frac{\lambda_1(1)}{\lambda_o(1)} - \frac{2}{3}\frac{\eta_1(1)}{\eta_o(1)}$	$\frac{\eta_1(1)}{\eta_o(1)}$
1	-0.191 ± 0.010	-0.612 ± 0.012
2	-0.199 ± 0.010	-0.614 ± 0.010
3	-0.190 ± 0.004	-0.598 ± 0.005
4	-0.192 ± 0.004	-0.601 ± 0.004

Table VII

Estimates for the contributions of the separate triple collision events.

μ	i	$\frac{\lambda_1(1)}{\lambda_o(1)} - \frac{2}{3} \cdot \frac{\eta_1(1)}{\eta_o(1)}$	$\frac{\eta_1(1)}{\eta_o(1)}$
R1	1	-0.048 ± 0.007	-0.042 ± 0.006
R1	2	-0.050 ± 0.005	-0.039 ± 0.004
R1	3	-0.051 ± 0.003	-0.039 ± 0.003
R1	4	-0.049 ± 0.002	-0.040 ± 0.002
R2	1	+0.044 ± 0.006	+0.035 ± 0.007
R2	2	+0.045 ± 0.005	+0.032 ± 0.004
R2	3	+0.047 ± 0.003	+0.033 ± 0.003
R2	4	+0.046 ± 0.002	+0.032 ± 0.002
C1	1	-0.023 ± 0.003	-0.036 ± 0.004
C1	2	-0.028 ± 0.006	-0.039 ± 0.005
C1	3	-0.035 ± 0.006	-0.037 ± 0.002
C1	4	-0.032 ± 0.004	-0.037 ± 0.002
C2	1	+0.057 ± 0.004	+0.147 ± 0.006
C2	2	+0.064 ± 0.007	+0.152 ± 0.006
C2	3	+0.069 ± 0.006	+0.151 ± 0.003
C2	4	+0.069 ± 0.004	+0.152 ± 0.003

Table VII (continued)

μ	i	$\frac{\lambda_1(1)}{\lambda_o(1)} - \frac{2}{3} \cdot \frac{\eta_1(1)}{\eta_o(1)}$	$\frac{\eta_1(1)}{\eta_o(1)}$
H1	1	+0.135 ± 0.016	+0.197 ± 0.018
H1	2	+0.141 ± 0.012	+0.206 ± 0.013
H1	3	+0.150 ± 0.008	+0.219 ± 0.009
H1	4	+0.145 ± 0.006	+0.211 ± 0.007
H2	1	-0.355 ± 0.017	-0.913 ± 0.021
H2	2	-0.371 ± 0.014	-0.926 ± 0.016
H2	3	-0.370 ± 0.008	-0.924 ± 0.010
H2	4	-0.370 ± 0.006	-0.920 ± 0.008

2.8 DISCUSSION OF THE RESULTS

In this chapter we have shown how the first density coefficients of the transport coefficients are related to triple collision transport integrals. In the preceding Section we obtained preliminary numerical estimates for these integrals. Retaining the best estimates we conclude+)

$$\frac{\lambda_1(1)}{\lambda_o(1)} = -0.593 \pm 0.014, \qquad \frac{\eta_1(1)}{\eta_o(1)} = -0.601 \pm 0.008 , \tag{2.8-1}$$

where, for the error estimate, we have replaced the standard deviation by a 95 percent confidence interval.

The triple collision integrals could be decomposed into integrals associated with the six triple collision events of Fig. 5. The best estimates for the contributions of the separate events are

(2.8-2)

μ	$\frac{\lambda_1(1)}{\lambda_o(1)}$	$\frac{\eta_1(1)}{\eta_o(1)}$
R1	-0.076 ± 0.007	-0.040 ± 0.004
R2	$+0.067 \pm 0.007$	$+0.033 \pm 0.004$
C1	-0.057 ± 0.011	-0.037 ± 0.004
C2	$+0.172 \pm 0.012$	$+0.152 \pm 0.006$
H1	$+0.286 \pm 0.021$	$+0.211 \pm 0.015$
H2	-0.983 ± 0.023	-0.920 ± 0.015 .

The theory of Enskog neglects the effects of all diagrams except for a piece of diagram H2. To facilitate a comparison with the Enskog prediction -5/8 (2.3-11) we rewrite (2.8-1) as

$$\frac{\lambda_1(1)}{\lambda_o(1)} = -0.625[1 - (5 \pm 2.2)\%]; \quad \frac{\eta_1(1)}{\eta_o(1)} = -0.625[1 - (4 \pm 1.3)\%] . \tag{2.8-3}$$

+) In addition, there is a collisional transfer contribution +6/5 to λ_1/λ_o and +4/5 to η_1/η_o.

Thus, as a first conclusion, we see that despite the approximations involved, the theory of Enskog presents a surprisingly good estimate for the first density coefficient, namely within 5%. From (2.8-2) it appears that the complete contribution from diagram H2 would have overestimated the triple collision integrals by as much as 50%. Somehow, this additional contribution is cancelled against contributions from the remaining diagrams.

Secondly, the difference between the results (2.8-3) obtained from the Choh-Uhlenbeck integral equation and those from the Enskog theory are larger than the error estimates. Thus we confirm the theoretical expectation that the theory of Enskog is not strictly correct. Recently, Alder and Wainwright obtained an estimate for the first density coefficient of self diffusion from molecular dynamics calculations.[23] The deviations from the theory of Enskog found here for the thermal conductivity and viscosity have the same sign as the deviation found by Alder and Wainwright for the self diffusion. We have extended the method of this report to include the self diffusion; preliminary calculations carried out so far are in substantial agreement with the molecular dynamics results.

As pointed out in Section 2.6 the integrals associated with R1 and R2 could not be combined into one single integral due to the effect of a possible fourth collision preceding or succeeding the three correlated binary collisions. In a quantitative analysis Cohen, Murphy and Foch concluded that in a succession of three real collisions pertaining to our diagrams R1 and C1, the probability of a fourth collision is only of the order of one or two parts in a thousand.[24] Our computer results confirm that the probability of a fourth collision is rather small both for real and hypothetical collisions. Thus to a good approximation, certainly within the present

precision, we can combine these two integrals and forget the fourth collisions. Similarly, we expect that in first approximation we could combine C1 and C2, resp. H1 and H2, provided we exclude the overlapping configurations which should be treated separately. However, we have not made an explicit quantitative investigation of the contributions to C2 and H2 when the overlapping configurations are excluded.

The results (2.8-2) reveal an appreciable difference between the contributions R1, R2 and C1 on one hand and the contributions C2, H1 and H2 on the other hand. We note that in C2, H1 and H2 a binary collision can occur, while two other particles are overlapping (see Fig. 5). In C2 1 and 3 are allowed to collide while 1 and 2 are still inside each other. In H1 particle 2 and 3 are allowed to collide while 1 and 3 are overlapping. In H2 particles 1 and 3 are allowed to collide while 1 and 2 are overlapping, and 2 and 3 are allowed to collide while 1 and 2 and/or 1 and 3 are overlapping. Collisions with such overlapping configurations are not included in R1, R2 and C1. Our computations indicate that the probability for triple collision events with overlapping configurations is rather large and they determine the major contributions to the triple collision integrals. On the other hand, the contributions from successive correlated binary collisions that are spatially separated are very small. In (2.8-2) this is illustrated by the results for R1 and R2 which do not include overlapping configurations and whose contributions almost cancel each other.

These results suggest _a posteriori_ that the Enskog values could be considered as a valid _first_ approximation to the triple collision integrals; this first approximation is determined by those events in H2, where in the third collision 2 and 3 are colliding, while both 2 and 3 are overlapping

with particle 1. As a second approximation those triple collision events suggest themselves which contain collisions between two particles while one of them is overlapping with the third particle. This second approximation contains contributions from C2, H1 and H2. As a third approximation one could then consider the effect of three successive binary collisions for which all pairs are spatially separated. The various effects of possible fourth collisions could be treated as an even higher order correction. A theoretical formulation of such an expansion procedure is presently being proposed by Ernst and Van Beijeren+).

We should remark that we have evaluated λ_1 and η_1 only in the first Enskog approximation, that is, we have taken only the first Sonine polynomial contribution. As discussed in Section 2.2, the first Enskog approximation is a good one in the case of the dilute gas values λ_o and η_o, obtained from the linearized Boltzmann equation. In Section 3.5 we shall make some study of the effect of the higher order Enskog approximation on the solution of the Choh-Uhlenbeck equation for the two dimensional model. The preliminary results lead us to expect that this expansion is suitable to obtain the first density coefficients λ_1 and η_1. Since the Enskog values -5/8 are independent of the Enskog approximation, we only need the expansion into Sonine polynomials for the term determining the deviation from the Enskog theory. We expect that the second Enskog approximation would not change the values (2.8-1) by more than a few tenths of a percent. To justify this suggestion we hope to obtain better estimates for the triple collision integrals, including the effect of the second Enskog approximation, in the future.

+) The author is indebted to Dr. M. H. Ernst for a valuable discussion on this point.

CHAPTER III
LOGARITHMIC DENSITY DEPENDENCE OF THE TRANSPORT COEFFICIENTS FOR A GAS OF HARD DISKS

3.1 INTRODUCTION

Up to this point the treatment of the density dependence of the transport properties was based on the theory of Bogoliubov. In this procedure the transport properties are expanded in a power series in the density ρ

$$\lambda = \lambda_o + \lambda_1\rho + \tilde{\lambda}_2\rho^2 + \ldots ,$$
$$\eta = \eta_o + \eta_1\rho + \tilde{\eta}_2\rho^2 + \ldots . \tag{3.1-1}$$

For hard spheres we prefer to use $b\rho$ as a dimensionless density. In this expansion the coefficients λ_i and η_i are, at least in part, determined by transport integrals related to successive correlated binary collisions between the molecules. The coefficients λ_1 and η_1 were related to collision events between three molecules. As mentioned in Section 2.7 the time between two successive collisions among three particles can become very large. If one analyzes the triple collision events of Fig. 5 for large values of the time τ between collisions, it turns out that the probability of such an event decreases as τ^{-2}. The reason is that, in order that for large values of τ a third collision will occur, the perihelion vector $\hat{k}_2$ of the second collision must be restricted to a solid angle proportional to σ^2/τ^2. If we then integrate over all values of τ up to a maximum value T, the collision integrals converge as T^{-1}, when T goes to infinity:

$$\lambda_1, \eta_1 = \text{constant} + \lim_{T\to\infty} \frac{c}{T} , \tag{3.1-2}$$

where the constant term represents the finite value obtained for the triple collision integrals.

In an actual gas triple collisions with very large times between the separate binary collisions will not occur, since for times larger than the mean free time $\bar{\tau}$ a collision with another molecule would interfere and destroy the triple collision correlation. Such an interference with another molecule is not accounted for in this expansion, since a power series expansion in the density amounts to an expansion in terms of the properties of groups of isolated molecules of 2, 3 . . . etc. particles. One would expect that the other molecules would exert a so called collisional damping on the triple collision correlation, so that the upper limit T in (3.1-2) should be identified with the mean free time $\bar{\tau}$+).

$$\lambda_1, \eta_1 = \text{constant} + \frac{c}{\bar{\tau}} \quad . \tag{3.1-3}$$

Since the mean free time $\bar{\tau}$ is in first approximation inversely proportional to the density ρ, the difference between (3.1-2) and (3.1-3) does not affect the first density coefficients λ_1 and η_1, but is of higher order in the density and would affect the next coefficients $\tilde{\lambda}_2$ and $\tilde{\eta}_2$ in (3.1-1).

The second density coefficients $\tilde{\lambda}_2$ and $\tilde{\eta}_2$ contain contributions from correlated collisions between four particles. It was discovered by Dorfman and Cohen[25], by Weinstock[26] and Goldman and Frieman[27] that the probability of such events no longer would decrease as τ^{-2}, but as τ^{-1}. A similar situation is encountered in the triple collision integrals for a two dimensional gas, since in two dimensions for large values of τ the perihelion vector $\vec{k}_2$ is restricted to a planar angle proportional to σ/τ. As a consequence, after

---

+) Strictly speaking the collisional damping modifies the probability of a multiple collision by a factor $e^{-\tau/\bar{\tau}}$ which leads to the same result.

integration over all values of τ, these integrals contain a contribution that would diverge as $\ln T$. For the reasons mentioned above it is to be expected that in reality the upper limit T should be identified with the mean free time $\bar{\tau}$ which is proportional to ρ^{-1}. Thus it was suggested in a previous paper[28] that $\tilde{\lambda}_2$ and $\tilde{\eta}_2$ should be replaced by $\lambda_2' \ln\rho + \lambda_2$ and $\eta_2' \ln\rho + \eta_2$ so that

$$\begin{aligned} \lambda &= \lambda_o + \lambda_1\rho + \lambda_2'\rho^2 \ln\rho + \lambda_2\rho^2 + \ldots \quad , \\ \eta &= \eta_o + \eta_1\rho + \eta_2'\rho^2 \ln\rho + \eta_2\rho^2 + \ldots \quad , \end{aligned} \tag{3.1-4}$$

for a three dimensional gas, and

$$\begin{aligned} \lambda &= \lambda_o + \lambda_1'\rho\ln\rho + \lambda_1\rho + \ldots \quad , \\ \eta &= \eta_o + \eta_1'\rho\ln\rho + \eta_1\rho + \ldots \quad , \end{aligned} \tag{3.1-5}$$

for a two dimensional gas. This conjecture was confirmed by a partial resummation of the formal density series.[26,29,30]

An evaluation of the coefficients λ_2' and η_2' of the logarithmic contribution requires an analysis of four body collisions which is rather cumbersome. For a two dimensional gas, however, the same physical effect can be studied from an analysis of the triple collision integrals developed in the previous Chapter. For this reason we have made an evaluation of the logarithmic density dependence of the transport coefficients for a two dimensional model gas consisting of hard disks.

3.2 SOLUTION OF THE LINEARIZED BOLTZMANN EQUATION FOR HARD DISKS

To obtain the transport coefficients for this model gas we consider again a perturbation to the velocity distribution linear in the gradients

$$f = f_o(1 + \Phi) , \tag{3.2-1}$$

where f_o is the (two dimensional) local Maxwell distribution

$$f = n \frac{m}{2\pi kT} \exp[-\frac{m(\vec{v} - \vec{u})^2}{2kT}] , \tag{3.2-2}$$

and $\Phi(\vec{V})$ has again the form (2.1-13)

$$\Phi(\vec{V}) = -A(V)\ \vec{V}\cdot \frac{\partial \ln T}{\partial \vec{r}} - B(V)\ \vec{V}^{o}\vec{V}:\frac{\partial}{\partial \vec{r}}\vec{u} . \tag{3.2-3}$$

The local density $n(\vec{r};t)$ and average velocity $\vec{u}(\vec{r};t)$ are again related to the distribution function f by (2.1-1) and (2.1-2). Since in two dimensions the molecules have only two degrees of freedom, the average kinetic energy per molecule is kT. Thus the expression (2.1-3) for the local temperature $T(\vec{r};t)$ has to be replaced with

$$n(\vec{r};t)\ T(\vec{r};t) = \int \frac{1}{2} mV^2 f(r;\vec{v};t)d\vec{v} . \tag{3.2-4}$$

Substitution of (3.2-3) into the expressions (2.1-4) and (2.1-5) for the fluxes yields for the two dimensional transport coefficients:

$$\lambda = \frac{k}{2} \int d\vec{V}\ f_o(V)\ (\frac{mV^2}{2kT} - 2)\ V^2 A(V) , \tag{3.2-5}$$

$$\eta = \frac{m}{4} \int d\vec{V}\ f_o(V)\ \vec{V}^{o}\vec{V}:\vec{V}^{o}\vec{V}\ B(V) . \tag{3.2-6}$$

Just as in (2.1-18), we have added in (3.2-5) a term which is zero according to the auxiliary condition (2.1-17).

Before studying the logarithmic density contribution (λ_1' and η_1' in (3.1-5)), we first should obtain the dilute gas values λ_o and η_o. As in three dimensions we limit our discussion to the spatially homogeneous case. For a two dimensional gas of hard disks with diameter σ the Boltzmann equation reads

$$\frac{\partial f(\vec{v}_1;t)}{\partial t} = \sigma\int d\vec{v}_2\int d\vec{k}(\vec{v}_{21}.\vec{k})\ T(12)f(\vec{v}_1;t)f(\vec{v}_2;t)\ . \qquad (3.2\text{-}7)$$

Using the same Chapman-Enskog procedure as in three dimensions we obtain for the linearized perturbation (3.2-3)

$$I_2(\vec{V}_1A^{(o)}(V_1)) = f_o(V_1)\ (\frac{mV_1^2}{2kT} - 2)\vec{V}_1\ , \qquad (3.2\text{-}8)$$

$$I_2(\vec{V}_1^o\vec{V}_1B^{(o)}(V_1)) = f_o(V_1)\ \frac{m}{kT}\ \vec{V}_1^o\vec{V}_1\ ,$$

to be compared with (2.2-9). Here I_2 is the two dimensional linearized binary collision operator

$$I_2(\Phi(\vec{V}_1)) = -\sigma\int d\vec{V}_2\int d\vec{k}(\vec{v}_{21}.\vec{k})f_o(V_1)f_o(V_2)T(12)[\Phi(\vec{V}_1) + \Phi(\vec{V}_2)]\ . \qquad (3.2\text{-}9)$$

To solve the linearized Boltzmann equation (3.2-8) we approximate again the solution by a finite sum of the appropriate Sonine polynomials

$$A^{(o)}(V_1) = -\frac{1}{n\sigma}\ (\frac{m}{\pi kT})^{1/2}\ \sum_{k=1}^{N} a_k^{(o)}(N)S_1^{(k)}(W_1^2)\ ,$$

$$B^{(o)}(V_1) = \frac{1}{n\sigma}\ (\frac{m}{\pi kT})^{1/2}\frac{m}{2kT}\ \sum_{k=o}^{N-1} b_k^{(o)}(N)S_2^{(k)}(W_1^2)\ . \qquad (3.2\text{-}10)$$

so that from (3.2-5) and (3.2-6)

$$\lambda_o = \lambda_o(N) = \frac{2}{\sigma}\left(\frac{k^3T}{m\pi}\right)^{1/2} a_1^{(o)}(N) ,$$
$$\eta_o = \eta_o(N) = \frac{1}{2\sigma}\left(\frac{mkT}{\pi}\right)^{1/2} b_o^{(o)}(N) . \tag{3.2-11}$$

The coefficients $a_k^{(o)}(N)$ and $b_k^{(o)}(N)$ are again determined by the equations (2.2-14):

$$\sum_{k=1}^{N} a_k^{(o)}(N)\, a_{k\ell}^{(o)} = \delta_{\ell 1} \quad (\ell = 1, \ldots, N) ,$$
$$\sum_{k=0}^{N-1} b_k^{(o)}(N)\, b_{k\ell}^{(o)} = \delta_{\ell 0} \quad (\ell = 0, \ldots, N-1) , \tag{3.2-12}$$

where the matrix elements $a_{k\ell}^{(o)}$ and $b_{k\ell}^{(o)}$ are now two dimensional binary collision integrals

$$a_{k\ell}^{(o)} = \frac{1}{n^2\sigma}\left(\frac{kT}{m\pi}\right)^{1/2} \int d\vec{W}_1 \vec{W}_1 S_1^{(k)}(W_1^2) \cdot I_2(\vec{W}_1 S_1^{(\ell)}(W_1^2)) ,$$
$$b_{k\ell}^{(o)} = \frac{1}{n^2\sigma}\left(\frac{kT}{m\pi}\right)^{1/2} \int d\vec{W}_1 \overset{o}{\vec{W}_1\vec{W}_1} S_2^{(k)} : I_2(\overset{o}{\vec{W}_1\vec{W}_1} S_2^{(\ell)}(W_1^2)) . \tag{3.2-13}$$

If we represent the Sonine polynomials by the generating function (2.2-12) and carry out the integrations we obtain

$$\sum_{k=1}^{\infty}\sum_{\ell=1}^{\infty} a_{k\ell}^{(o)} s^k t^\ell = \frac{1}{2}\left(1 - \frac{s+t}{2}\right)^{1/2}\left[3(1 - st)^{-5/2} - 2(1 - st)^{-2} - (1 - st)^{-3/2}\right]$$

$$- \frac{1}{4}\left(1 - \frac{s+t}{2}\right)^{-1/2}\left[(1 - st)^{-3/2} - st(1 - st)^{-1} - (1 - st)^{-1/2}\right] ,$$

$$\sum_{k=o}^{\infty}\sum_{\ell=o}^{\infty} b_{k\ell}^{(o)} s^k t^\ell = \tag{3.2-14}$$

$$\frac{1}{8}\left(1 - \frac{s+t}{2}\right)^{1/2}\left[15(1 - st)^{-7/2} - 8(1 - st)^{-3} - 3(1 - st)^{-5/2} + 2(1 - st)^{-2} + 2(1 - st)^{-3/2}\right]$$

$$- \frac{1}{8}\left(1 - \frac{s+t}{2}\right)^{-1/2}\left[3(1 - st)^{-5/2} - 2(1 - st)^{-2} - (1 - st)^{-3/2}\right]$$

$$- \frac{1}{32}\left(1 - \frac{s+t}{2}\right)^{-3/2}\left[(1 - st)^{-3/2} - st(1 - st)^{-1} - (1 - st)^{-1/2}\right] .$$

The resulting values for the matrix elements are listed in Table VIII up to the third Enskog approximation, and the resulting corrections $a_k^{(o)}(N)$ and $b_k^{(o)}(N)$ in Table IX. It turns out that the expansion procedure is again very satisfactory. The convergence is almost as rapid as in three dimensions, as is shown in Table X.

Table VIII

The matrix elements $a_{k\ell}^{(o)}$ and $b_{k\ell}^{(o)}$ defined by (3.2-14) for hard disks.

$$a_{11}^{(o)} = 1 \qquad a_{12}^{(o)} = -\frac{1}{4} \qquad a_{13}^{(o)} = -\frac{1}{32}$$

$$a_{22}^{(o)} = \frac{39}{16} \qquad a_{23}^{(o)} = -\frac{91}{128}$$

$$a_{33}^{(o)} = \frac{4433}{1024}$$

$$b_{00}^{(o)} = 1 \qquad b_{01}^{(o)} = -\frac{1}{4} \qquad b_{02}^{(o)} = -\frac{1}{32}$$

$$b_{11}^{(o)} = \frac{51}{16} \qquad b_{12}^{(o)} = -\frac{123}{128}$$

$$b_{22}^{(o)} = \frac{7569}{1024}$$

Table IX

The successive approximations $a_k^{(o)}(N)$ and $b_k^{(o)}(N)$ determining the solution of the linearized Boltzmann equation for hard disks.

First Enskog approximation: N = 1

$$a_1^{(o)}(1) = 1 \qquad b_o^{(o)}(1) = 1$$

Second Enskog approximation: N = 2

$$a_1^{(o)}(2) = 1 + \frac{1}{38} \qquad b_o^{(o)}(2) = 1 + \frac{1}{50}$$

$$a_2^{(o)}(2) = \frac{2}{19} \qquad b_1^{(o)}(2) = \frac{2}{25}$$

Third Enskog approximation: N = 3

$$a_1^{(o)}(3) = 1 + \frac{1}{38} + \frac{65^2}{152 \times 9997} \qquad b_o^{(o)}(3) = 1 + \frac{1}{50} + \frac{29^2}{200 \times 2521}$$

$$a_2^{(o)}(3) = \frac{2}{19} + \frac{23 \times 65}{19 \times 9997} \qquad b_1^{(o)}(3) = \frac{2}{25} + \frac{31 \times 29}{75 \times 2521}$$

$$a_3^{(o)}(3) = \frac{4 \times 65}{9997} \qquad b_2^{(o)}(3) = \frac{4 \times 29}{3 \times 2521}$$

Table X

Convergence of the Sonine polynomial expansion in determining the dilute gas values of the transport coefficients

	hard spheres		hard disks	
N	$\frac{\lambda_o(N)}{\lambda_o(1)}$	$\frac{\eta_o(N)}{\eta_o(1)}$	$\frac{\lambda_o(N)}{\lambda_o(1)}$	$\frac{\eta_o(N)}{\eta_o(1)}$
1	1.000	1.000	1.000	1.000
2	1.023	1.015	1.026	1.020
3	1.025	1.016	1.029	1.022

3.3 ASYMPTOTIC SOLUTION OF THE CHOH-UHLENBECK INTEGRAL EQUATION

To obtain the first density correction to the transport coefficients we start with a formal density expansion

$$\lambda = \lambda_o + \tilde{\lambda}_1 b\rho \ ,$$
$$\eta = \eta_o + \tilde{\eta}_1 b\rho \ , \qquad (3.3\text{-}1)$$

where $b\rho$ is the co-area

$$b\rho = \frac{1}{2}\pi n\sigma^2 \ . \qquad (3.3\text{-}2)$$

This density expansion is a formal one and the coefficients $\tilde{\lambda}_1$ and $\tilde{\eta}_1$ will turn out to depend logarithmically on the density. Pursuing first the formal procedure, we consider the related expansion for the functions A(V) and B(V) in (3.2-5) and (3.2-6)

$$A(V) = A^{(o)}(V) + b\rho\, \tilde{A}^{(1)}(V) \ , \qquad (3.3\text{-}3)$$

$$B(V) = B^{(o)}(V) + b\rho\, \tilde{B}^{(1)}(V) \ .$$

$\tilde{A}^{(1)}(V)$ and $\tilde{B}^{(1)}(V)$ are again determined by the Choh-Uhlenbeck integral equation (2.4-9)

$$I_2(\vec{V}_1\tilde{A}^{(1)}(V_1)) = -\tilde{I}_3(\vec{V}_1 A^{(o)}(V_1)) \ ,$$
$$I_2(\vec{V}_1^{\,o}\vec{V}_1\tilde{B}^{(1)}(V_1)) = -\tilde{I}_3(\vec{V}_1^{\,o}\vec{V}_1 B^{(o)}(V_1)) \ , \qquad (3.3\text{-}4)$$

where $\tilde{I}_3$ is the linearized ternary collision integral operator in two dimensions

$$\tilde{I}_3(\Phi(\vec{V}_1)) = -\frac{1}{b\rho}\int d\vec{V}_2 d\vec{V}_3 \int d\vec{r}_2 d\vec{r}_3\, \theta_{12}\, \tau(12;3) f_o(V_1) f_o(V_2) f_o(V_3) \sum_{m=1}^{3} \Phi(\vec{V}_m) \ . \qquad (3.3\text{-}5)$$

Substituting (3.2-8) into (3.2-5) and (3.2-6) and using the symmetry of the operator I_2, we obtain similarly to (2.4-11)

$$\lambda_1 = -\frac{k}{2}\int d\vec{V}_1\ \vec{V}_1 A^{(o)}(V_1).\tilde{I}_3(\vec{V}_1 A^{(o)}(V_1)) ,$$

$$\eta_1 = -\frac{kT}{4}\int d\vec{V}_1\ \vec{V}_1^{o}\vec{V}_1 B^{(o)}(V_1):\tilde{I}_3(\vec{V}_1^{o}\vec{V}_1 B^{(o)}(V_1)) . \qquad (3.3\text{-}6)$$

Using the solution (3.2-10) of the linearized Boltzmann equation we obtain in the Nth Enskog approximation

$$\frac{\lambda_1(N)}{\lambda_o(1)} = -\sum_{k=1}^{N}\sum_{\ell=1}^{N} a_k^{(o)}(N)\ a_\ell^{(o)}(N)\ \tilde{a}_{k\ell}^{(1)} ,$$

$$\frac{\eta_1(N)}{\eta_o(1)} = -\sum_{k=o}^{N-1}\sum_{\ell=o}^{N-1} b_k^{(o)}(N)\ a_\ell^{(o)}(N)\ \tilde{b}_{k\ell}^{(1)} , \qquad (3.3\text{-}7)$$

where $\tilde{a}_{k\ell}^{(1)}$ and $\tilde{b}_{k\ell}^{(1)}$ are now two dimensional triple collision integrals

$$\tilde{a}_{k\ell}^{(1)} = \frac{1}{n^2\sigma}\left(\frac{kT}{m\pi}\right)^{1/2}\int d\vec{W}_1\ \vec{W}_1 S_1^{(k)}(W_1^2).\tilde{I}_3(\vec{W}_1 S_1^{(\ell)}(W_1^2)) ,$$

$$\tilde{b}_{k\ell}^{(1)} = \frac{1}{n^2\sigma}\left(\frac{kT}{m\pi}\right)^{1/2}\int d\vec{W}_1\ \vec{W}_1^{o}\vec{W}_1 S_1^{(k)}(W_1^2):\tilde{I}_3(\vec{W}_1^{o}\vec{W}_1 S_2^{(\ell)}(W_1^2)) . \qquad (3.3\text{-}8)$$

They can be reduced again to the surface integral form (2.5-4)

$$\tilde{a}_{k\ell}^{(1)} = -\frac{1}{\pi^4}\sqrt{\frac{2}{\pi}}\int d\vec{W}_1 d\vec{W}_2 d\vec{W}_3 \exp[-(W_1^2 + W_2^2 + W_3^2)]$$
$$.\sum_{m=1}^{3}\vec{W}_m S_1^{(k)}(W_m^2).\tilde{O}^*(12;13)\sum_{n=1}^{3}\vec{W}_n S_1^{(\ell)}(W_n^2) ,$$

$$\tilde{b}_{k\ell}^{(1)} = -\frac{1}{\pi^4}\sqrt{\frac{2}{\pi}}\int d\vec{W}_1 d\vec{W}_2 d\vec{W}_3 \exp[-(W_1^2 + W_2^2 + W_3^2)]$$
$$.\sum_{m=1}^{3}\vec{W}_m^{o}\vec{W}_m S_2^{(k)}(W_m^2):\tilde{O}^*(12;13)\sum_{n=1}^{3}\vec{W}_n^{o}\vec{W}_n S_2^{(\ell)}(W_n^2) , \qquad (3.3\text{-}9)$$

with $\tilde{O}^*(12;13)$ defined by (2.5-5)

$$\tilde{O}^*(12;13) = \sum_{\mu} \int d\tau^* \int d\hat{k}_1 d\hat{k}_2 \; \vec{W}_{21}\cdot\hat{k}_1 \; \vec{W}_{31}(1)\cdot\hat{k}_2 \; T_\mu(12;13) \,. \tag{3.3-10}$$

To obtain the coefficient of the logarithmic contribution, we evaluate the integrand in the triple collision integrals for large values of the time τ^*. For this purpose the integrand is expanded in terms of $1/\tau^*$ and only the leading terms of first order in $1/\tau^*$ are retained. The triple collision integrals are again a sum of integrals over the six triple collision events specified by the conditions of Table IV, just as in (2.6-8). However, for the leading terms in $1/\tau^*$ we can neglect the difference in integration region between the diagrams of the first and second kind. Part of this difference was related to the effect of overlapping configurations for small values of τ^* which clearly do not affect the asymptotic behavior for large values of τ^*. The remaining differences were related to possible fourth collisions interfering with the three successive binary collisions; these effects lead to contributions of higher order in $1/\tau^*$ as was shown in a previous publication.[31] Thus for an asymptotic analysis it is sufficient to consider

$$\begin{aligned} \tilde{a}^{(1)}_{k\ell} = & -\frac{1}{\pi^4}\sqrt{\frac{2}{\pi}} \int d\tau^* \int d\vec{W}_1(1) d\vec{W}_2(1) d\vec{W}_3(1) \exp[-W_1^2(1) + W_2^2(1) + W_3^2(1))] \\ & d\hat{k}_1 d\hat{k}_2 |\vec{W}_{21}(1)\cdot\hat{k}_1 |\vec{W}_{31}(1)\cdot\hat{k}_2 \sum_{m=1}^{3} \sum_{n=1}^{3} \{ [\vec{W}_m S_1^{(k)}(W_m^2), \vec{W}_n S_1^{(\ell)}(W_n^2)]_R + \\ & [\vec{W}_m S_1^{(k)}(W_m^2), \vec{W}_n S_1^{(\ell)}(W_n^2)]_C - [\vec{W}_m S_1^{(k)}(W_m^2), \vec{W}_n S_1^{(\ell)}(W_n^2)]_H \} \,, \end{aligned} \tag{3.3-11}$$

with a similar expression for $\tilde{b}^{(1)}_{k\ell}$ in terms of $\vec{W}\circ\vec{W}\, S_2^{(\;)}(W^2)$. For convenience, we have introduced the abbreviated notation

$$[\Phi, \Psi]_R = [\Phi(0) - \Phi(1)].[\Psi(3_R) - \Psi(2)] \;,$$

$$[\phi, \Psi]_C = [\phi(0) - \phi(1)].[\Psi(3_C) - \Psi(2)] \;, \qquad (3.3\text{-}12)$$

$$[\phi, \Psi]_H = [\phi(0) - \phi(1)].[\Psi(3_H) - \Psi(1)] \;,$$

where $\Phi(i) = \Phi(\vec{W}(i))$ and $\psi(i) = \psi(\vec{W}(i))$ are vector or tensor functions of the velocities $\vec{W}(i)$ and the product $\phi.\psi$ is a scalar product. The three terms in (3.3-11) should be integrated over those phase points leading, respectively, to a recollision R, a cyclic collision C and a hypothetical cyclic collision H (see Fig. 8). These integration regions are specified by the conditions (μ-2) through (μ-5) of Table IV.

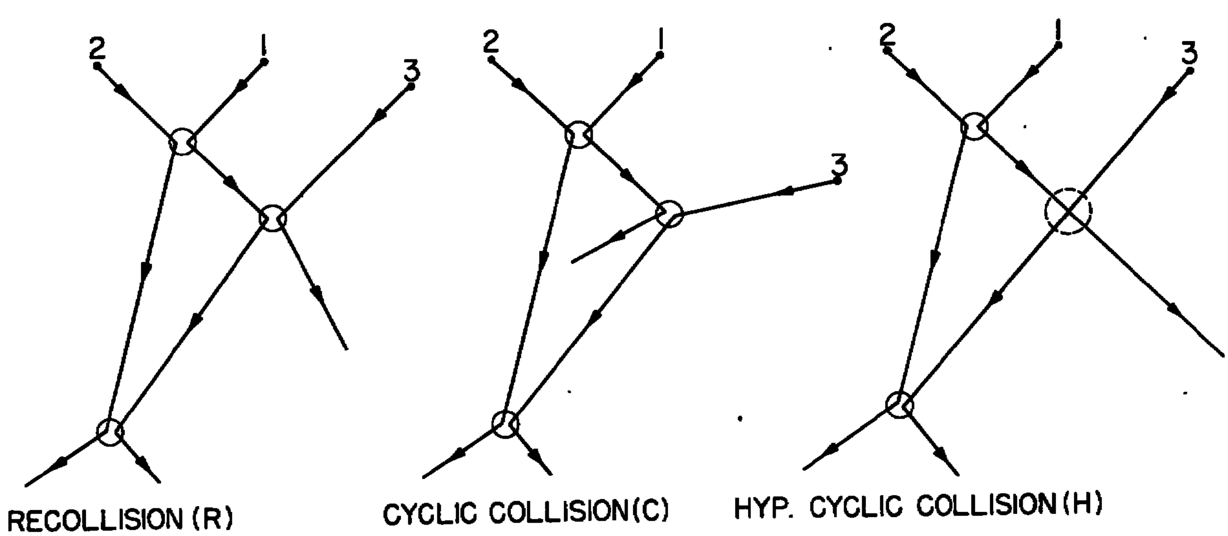

Figure 8. The three triple collision events for the collision integrals determining the coefficient of the term logarithmic in the density

The leading term in $1/\tau^*$ can be evaluated analytically. To illustrate the procedure we consider the recollision contribution $\tilde{a}^{(1)}_{k\ell}(R)$ in some detail. Just as in three dimensions we first integrate over the total velocity $\vec{W}_o = \frac{1}{3}(\vec{W}_1 + \vec{W}_2 + \vec{W}_3)$ and over all directions and the magnitude of $\vec{W}_{21}(1)$. To evaluate the remaining integral we take $\hat{W}_{21}(1)$ in the direction of the Z-axis and specify the perihelion vectors $\vec{k}_1$ and $\vec{k}_2$ by the angles θ_1 and θ_2 as indicated in Fig. 7. The velocity $\vec{W}_{31}(1)$ (strictly speaking the scaled velocity $\vec{W}_{31}(1)/W_{21}(1)$ [15]) is specified by its length w and its polar angle θ_3. Thus,

$$\tilde{a}^{(1)}_{k\ell}(R) = -\frac{1}{\pi^4}\sqrt{\frac{2}{\pi}} \int d\tau \int d\vec{W}_o \int d\vec{W}_{21}(1) W^2_{21}(1) \int_{-\pi/2}^{+\pi/2} d\theta_1 \int_{-\pi/2}^{+\pi/2} d\theta_2 \int_{-\pi/2}^{+\pi/2} d\theta_3 \int_{\frac{1}{\cos\theta_3}}^{\infty} dw$$

$$\cdot \exp[-(W^2_1(1) + W^2_2(1) + W^2_3(1))] w^2 \cos\theta_1 \cos(\theta_2 - \theta_3) \sum_{m=1}^{3} \sum_{n=1}^{3} [\vec{W}_m S^{(k)}_1(W^2_m), \vec{W}_n S^{(\ell)}_1(W^2_n)]_R \cdot \tag{3.3-13}$$

Just as in (2.7-1) τ is the scaled dimensionless time $\tau^* W_{21}(1)$. It is convenient to consider the perihelion vector $\vec{k}_3$ of the third collision as a new integration variable. We specify $\vec{k}_3$ by an angle θ_4 as indicated in Fig. 9. After the first collision (between 1 and 2) particle 1 is at the origin of the coordinate system and particle 2 is moving in the Z-direction with the unit velocity, as shown in Fig. 7. After the second collision (between 1 and 3) particle 1 will move in the direction of $\vec{k}_2$. A singularity will occur when $\theta_2 \to 0$, because for small values of θ_2 particle 1 will move approximately in the Z-direction and be able to collide again with 2 even for large values of τ. At the time of the second collision 2 will have travelled a distance τ in the Z-direction. After the collision between 1 and 3 the velocity of particle 1 is equal to $w\cos\theta_3$ in the limit considered. Therefore, the time τ' required for 1 to overhaul 2 is approximately $\tau/(w\cos\theta_3 - 1)$, so that the total time $\tau + \tau'$ between the first and the last collision becomes

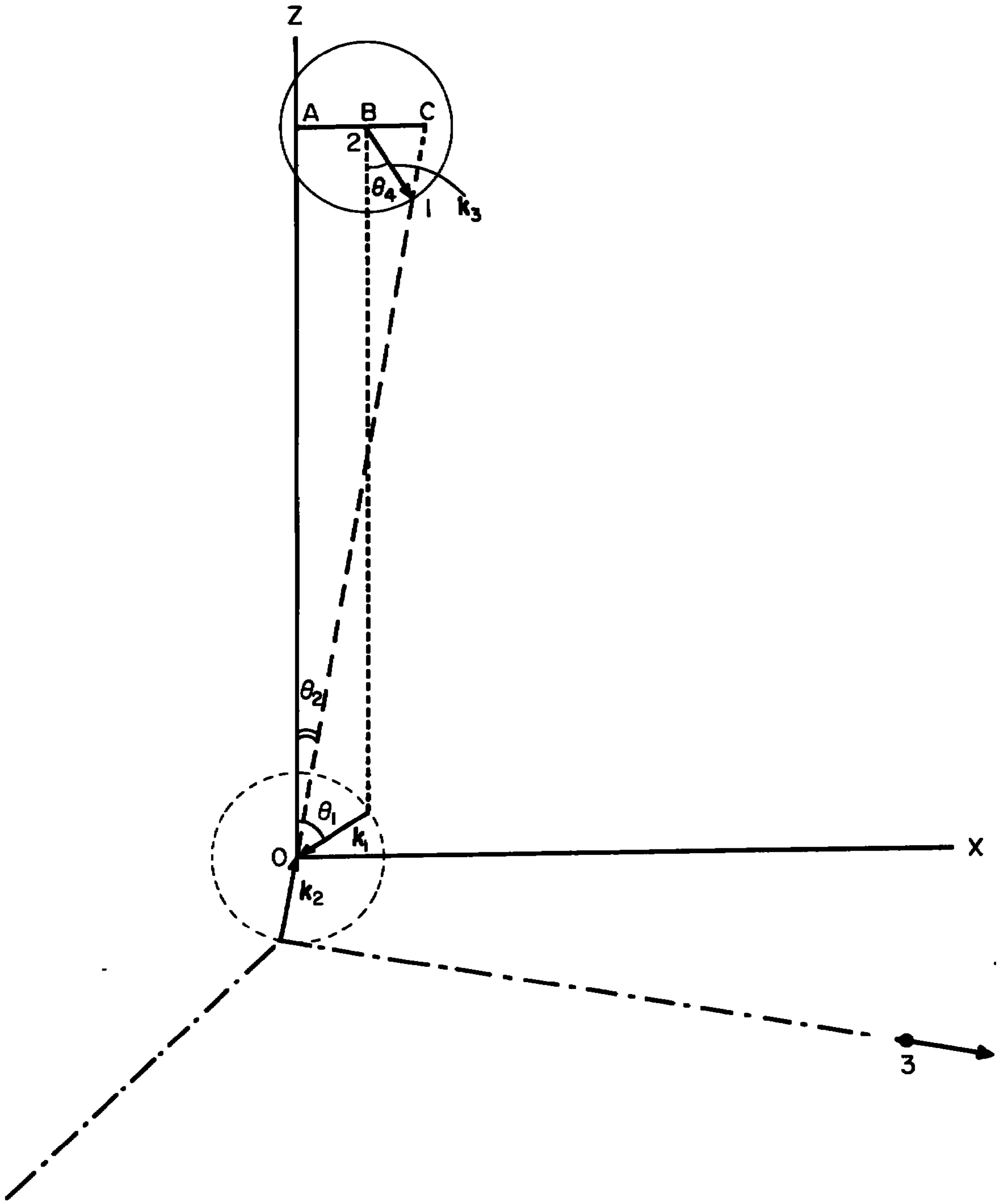

Figure 9. A recollision. The figure represents the situation at the time of the third collision

$$\tau + \tau' = \frac{w\cos\theta_3}{w\cos\theta_3 - 1}\,\tau \quad . \tag{3.3-14}$$

The positions of the particles at the time of the third collision are indicated in Fig. 9. Particle 2 is at B and has travelled a distance $\tau + \tau'$ in the Z-direction when colliding with 1 again. Neglecting terms of order θ_2 and constant terms when compared with τ, we have $AC \approx \theta_2 \times OC \approx \theta_2\,(\tau + \tau')$. The distance BC is essentially $k_{3x} = \sin\theta_4$. Since $AB = \sin\theta_1$, we obtain

$$\sin\theta_4 = -\sin\theta_1 + \frac{w\cos\theta_3}{w\cos\theta_3 - 1}\,\tau\theta_2 \quad , \tag{3.3-15}$$

so that

$$d\theta_2 = \frac{1}{\tau}\,\frac{w\cos\theta_3 - 1}{w\cos\theta_3}\,\cos\theta_4 d\theta_4 \quad . \tag{3.3-16}$$

In (3.3-13) we replace the integration over θ_2 by an integration over θ_4. Since the Jacobian (3.3-16) is proportional to $1/\tau$, it is sufficient to evaluate the remaining part of the integrand for $\theta_2 = 0$ (terms of order θ_2 are equivalent to terms of order $1/\tau$). We can indicate this formally by introducing a δ-function $\delta(\theta_2)$ and integrating again over θ_2. Thus

$$\tilde{a}^{(1)}_{k\ell}(R) = -\frac{1}{\pi^4}\sqrt{\frac{2}{\pi}}\int\frac{d\tau}{\tau}\int d\vec{W}_o\int d\vec{W}_{21}(1)W^2_{21}(1)\int_{-\pi/2}^{+\pi/2} d\theta_1\cos\theta_1\int_{-\pi/2}^{+\pi/2} d\theta_4\cos\theta_4\int_{-\pi/2}^{+\pi/2} d\theta_2\int_{-\pi/2}^{+\pi/2} d\theta_3\int_{\frac{1}{\cos\theta_3}}^{\infty} dw$$

$$\cdot\ \exp[-W^2_1(1)+W^2_2(1)+W^2_3(1))]\,w(w\cos\theta_3 - 1)\,\frac{\cos(\theta_2-\theta_3)}{\cos\theta_3} \tag{3.3-17}$$

$$\cdot\sum_{m=1}^{3}\sum_{n=1}^{3}[\vec{W}_m S^{(k)}(W^2_m),\ \vec{W}_n S^{(\ell)}_1(W^2_n)]_R\ \delta(\theta_2) + \int d\tau\, O(1/\tau^2)\ .$$

The first term in this expansion is proportional to $1/\tau$. As mentioned in Section 3.1 we take as the upper limit for the time integral a mean free time $\bar{\tau}$ inversely proportional to the density $b\rho$. Thus writing

$$\begin{aligned} \bar{a}_{k\ell}^{(1)} &= \alpha_{k\ell}^{(1)} \ln b\rho + a_{k\ell}^{(1)} , \\ \bar{b}_{k\ell}^{(1)} &= \beta_{k\ell}^{(1)} \ln b\rho + b_{k\ell}^{(1)} , \end{aligned} \tag{3.3-18}$$

we obtain for the recollision contribution $\alpha_{k\ell}^{(1)}(R)$ to the coefficient of the logarithm:

$$\alpha_{k\ell}^{(1)}(R) = \frac{1}{\pi^4}\sqrt{\frac{2}{\pi}} \int d\vec{W}_o \int d\vec{W}_{21}(1) W_{21}^2(1) \int_{-\pi/2}^{+\pi/2} d\theta_1 \cos\theta_1 \int_{-\pi/2}^{+\pi/2} d\theta_4 \cos\theta_4 \int_{-\pi/2}^{+\pi/2} d\theta_2 \int_{-\pi/2}^{+\pi/2} d\theta_3 \int_{\frac{1}{\cos\theta_3}}^{\infty} dw$$

$$\cdot \exp[-(W_1^2(1)+W_2^2(1)+W_3^2(1))] \; w(w\cos\theta_3-1) \frac{\cos(\theta_2-\theta_3)}{\cos\theta_3}$$

$$\cdot \sum_{m=1}^{3} \sum_{n=1}^{3} [\vec{W}_m S_1^{(k)}(W_m^2), \vec{W}_n S_1^{(\ell)}(W_n^2)]_R \, \delta(\theta_2) . \tag{3.3-19}$$

The contributions from the cyclic and hypothetical cyclic collisions can be evaluated in a similar manner. We first introduce again the perihelion vecotr $\vec{k}_3$ of the third collision as a new variable. The asymptotic recollisions occurred when $\theta_2 \to 0$. The asymptotic cyclic collisions will occur when $\theta_2 \to -\pi/2$ and $\theta_2 \to +\pi/2$; both limits give an equal contribution.[31] The asymptotic hypothetical cyclic collisions occur when $\theta_3 \to 0$. The velocity functions to be evaluated before and after the third collision are symmetric in all three particles. Therefore, this difference before and after the third collision is the same function of $\vec{k}_3$ regardless of the fact between which two particles the third collision actually occurs. As a result the contributions from cyclic and hypothetical cyclic collisions can be simply related to the expression found

for recollisions. After introducing $\vec{k}_3$ as a new variable, in the case of recollisions the remaining integrand had to be evaluated for $\theta_2=0$. For cyclic and hypothetical cyclic collisions we have to consider the same integrand for $\theta_2 = -\pi/2$, and $\theta_3=0$, respectively. Thus the total contribution reduces to

$$\alpha_{k\ell}^{(1)} = \frac{1}{\pi^4}\sqrt{\frac{2}{\pi}} \int d\vec{W}_o \int d\vec{W}_{21}(1) W_{21}^2(1) \int_{-\pi/2}^{+\pi/2} d\theta_1 \cos\theta_1 \int_{-\pi/2}^{+\pi/2} d\theta_4 \cos\theta_4 \int_{-\pi/2}^{+\pi/2} d\theta_2 \int_{-\pi/2}^{+\pi/2} d\theta_3 \int_{\frac{1}{\cos\theta_3}}^{\infty} dw$$

$$\cdot \exp[-(W_1^2(1) + W_2^2(1) + W_3^2(1))] \; w(w\cos\theta_3 - 1) \frac{|\cos(\theta_2-\theta_3)|}{\cos\theta_3} \tag{3.3-20}$$

$$\cdot \sum_{m=1}^{3} \sum_{n=1}^{3} [\vec{W}_m S_1^{(k)}(W_m^2), \vec{W}_n S_1^{(\ell)}(W_n^2)]_R \; [\delta(\theta_2) + \delta(\theta_2 - \tfrac{\pi}{2}) - \delta(\theta_3)] .$$

The three delta functions pick out the contributions from recollisions, cyclic collisions and hypothetical cyclic collisions, respectively.+) For the matrix elements $\beta_{k\ell}^{(1)}$ in (3.3-18) we obtain similarly

$$\beta_{k\ell}^{(1)} = \frac{1}{\pi^4}\sqrt{\frac{2}{\pi}} \int d\vec{W}_o \int d\vec{W}_{21}(1) W_{21}^2(1) \int_{-\pi/2}^{+\pi/2} d\theta_1 \cos\theta_1 \int_{-\pi/2}^{+\pi/2} d\theta_4 \cos\theta_4 \int_{-\pi/2}^{+\pi/2} d\theta_2 \int_{-\pi/2}^{+\pi/2} d\theta_3 \int_{\frac{1}{\cos\theta_3}}^{\infty} dw$$

$$\cdot \exp[-(W_1^2(1) + W_2^2(1) + W_3^2(1))] \; w(w\cos\theta_3 - 1) \frac{|\cos(\theta_2-\theta_3)|}{\cos\theta_3} \tag{3.3-21}$$

$$\cdot \sum_{m=1}^{3} \sum_{n=1}^{3} [\vec{W}_m^{\circ} \vec{W}_m S_2^{(k)}(W_m^2), \vec{W}_n^{\circ} \vec{W}_n S_2^{(\ell)}(W_n^2)]_R \; [\delta(\theta_2) + \delta(\theta_2 - \tfrac{\pi}{2}) - \delta(\theta_3)] .$$

+) When integrating the delta function $\delta(\theta_2 - \frac{\pi}{2})$ the lower limit of θ_2 should be taken as $-(\frac{\pi}{2} + \varepsilon)$.

The logarithmic density dependence (3.3-18) of the matrix elements $\tilde{a}_{k\ell}^{(1)}$ and $\tilde{b}_{k\ell}^{(1)}$ implies $\tilde{\lambda}_1 = \lambda_1' \ell n b\rho + \lambda_1$ and $\tilde{\eta}_1 = \eta_1' \ell n b\rho + \eta_1$ so that the expansion (3.3-1) for the transport coefficients should be replaced with

$$\lambda = \lambda_o + \lambda_1' b\rho \ell n b\rho + \lambda_1 b\rho + \ldots \quad ,$$

$$\eta = \eta_o + \eta_1' b\rho \ell n b\rho + \eta_1 b\rho + \ldots \quad . \tag{3.3-22}$$

The coefficients λ_1' and η_1' are determined by the new asymptotic triple collision integrals $\alpha_{k\ell}^{(1)}$ and $\beta_{k\ell}^{(1)}$:

$$\frac{\lambda_1'(N)}{\lambda_o(1)} = - \sum_{k=1}^{N} \sum_{\ell=1}^{N} a_k^{(o)}(N) a_\ell^{(o)}(N) \alpha_{k\ell}^{(1)} \quad ,$$

$$\frac{\eta_1'(N)}{\eta_o(1)} = - \sum_{k=o}^{N-1} \sum_{\ell=o}^{N-1} b_k^{(o)}(N) b_\ell^{(o)}(N) \beta_{k\ell}^{(1)} \quad . \tag{3.3-23}$$

The coefficients λ_1' and η_1' can be considered as the sum of three contributions associated with the three triple collision events of Fig. 8. We note, however, that in (3.3-20) and (3.3-21) the matrix elements $\alpha_{k\ell}^{(1)}$ and $\beta_{k\ell}^{(1)}$ are reduced to triple collision integrals containing the dynamics of recollisions only. In these integrals the velocities $\vec{W}_{ij}(0)$ and $\vec{W}_{ij}(2)$ are related to the integration variables by (2.6-25) and (2.6-26). The final velocities $\vec{W}_{ij}(3_R)$ are related to the variable $\vec{k}_3$ (or θ_4) by

$$\vec{W}_{21}(3_R) = \vec{W}_{21}(2) - 2\vec{W}_{21}(2).\vec{k}_3\vec{k}_3 \quad ,$$

$$\vec{W}_{31}(3_R) = \vec{W}_{31}(2) - \vec{W}_{21}(2).\vec{k}_3\vec{k}_3 \quad . \tag{3.3-24}$$

3.4 LOGARITHMIC DENSITY DEPENDENCE OF THE TRANSPORT COEFFICIENTS IN THE FIRST ENSKOG APPROXIMATION

The logarithmic density dependence of the transport coefficients in the first Enskog approximation is determined by the matrix elements $\alpha_{11}^{(1)}$ and $\beta_{oo}^{(1)}$. If we carry out the integration over $\vec{W}_o$ and $\vec{W}_{21}(1)$ we obtain similarly to (2.7-1)[31]

$$\alpha_{11}^{(1)} = \frac{2}{3}\beta_{oo}^{(1)} + \frac{8505}{1024}\frac{\sqrt{3}}{\pi^2}\int_{-\pi/2}^{+\pi/2} d\theta_1 \cos\theta_1 \int_{-\pi/2}^{+\pi/2} d\theta_4 \cos\theta_4 \int_{-\pi/2}^{+\pi/2} d\theta_2 \int_{-\pi/2}^{+\pi/2} d\theta_3 \int_{\frac{1}{\cos\theta_3}}^{\infty} dw$$
$$\frac{w(w\cos\theta_3-1)}{E^{11/2}} \frac{|\cos(\theta_2-\theta_3)|}{\cos\theta_3} [\vec{K},\vec{K}]_R [\delta(\theta_2)+\delta(\theta_2-\tfrac{\pi}{2})-\delta(\theta_3)] , \qquad (3.4\text{-}1)$$

$$\beta_{oo}^{(1)} = \frac{315}{64}\frac{\sqrt{3}}{\pi^2}\int_{-\pi/2}^{+\pi/2} d\theta_1 \cos\theta_1 \int_{-\pi/2}^{+\pi/2} d\theta_4 \cos\theta_4 \int_{-\pi/2}^{+\pi/2} d\theta_2 \int_{-\pi/2}^{+\pi/2} d\theta_3 \int_{\frac{1}{\cos\theta_3}}^{\infty}$$
$$\frac{w(w\cos\theta_3-1)}{E^{9/2}} \cdot \frac{|\cos(\theta_2-\theta_3)|}{\cos\theta_3} [\overleftrightarrow{L},\overleftrightarrow{L}]_R [\delta(\theta_2)+\delta(\theta_2-\tfrac{\pi}{2})-\delta(\theta_3)] , \qquad (3.4\text{-}2)$$

where E, $\vec{K}$ and $\overleftrightarrow{L}$ are again defined by (2.7-2), (2.7-3) and (2.7-4). In the coordinate system under consideration E is given by (2.7-14):

$$E = w^2 + 1 - w\cos\theta_3 . \qquad (3.4\text{-}3)$$

The components of the various velocities $\vec{W}_{ij}(n)$ to be substituted in $\vec{K}(n)$ and $\overleftrightarrow{L}(n)$ are listed in Table XI.

Table XI

The velocities to be substituted in the triple collision integrals $\alpha_{k\ell}^{(1)}$ and $\beta_{k\ell}^{(1)}$.

	X-component	Z-component
$\vec{W}_{21}(0)$	$-2\sin\theta_1\cos\theta_1$	$1-2\cos^2\theta_1$
$\vec{W}_{31}(0)$	$w\sin\theta_3-\sin\theta_1\cos\theta_1$	$w\cos\theta_3-\cos^2\theta_1$
$\vec{W}_{21}(1)$	0	1
$\vec{W}_{31}(1)$	$w\sin\theta_3$	$w\cos\theta_3$
$\vec{W}_{21}(2)$	0	$1-w\cos\theta_3$
$\vec{W}_{31}(2)$	$w\sin\theta_3$	$-w\cos\theta_3$
$\vec{W}_{21}(3_R)$	$2(1-w\cos\theta_3)\sin\theta_4\cos\theta_4$	$(1-w\cos\theta_3)(1-2\cos^2\theta_4)$
$\vec{W}_{31}(3_R)$	$w\sin\theta_3+(1-w\cos\theta_3)\sin\theta_4\cos\theta_4$	$-w\cos\theta_3-(1-w\cos\theta_3)\cos^2\theta_4$

Omitting terms odd in the integration variables θ_1 and θ_4 we obtain

$$[\vec{\vec{K}}, \vec{\vec{K}}]_R = \{\vec{\vec{K}}(0) - \vec{\vec{K}}(1)\}.\{\vec{\vec{K}}(3_R) - \vec{\vec{K}}(2)\} = \tag{3.4-4}$$

$$= 4(1-w\cos\theta_3)^2[4w^2\sin^2\theta_3 + (1+w\cos\theta_3)(1-2w\cos\theta_3)]\sin^2\theta_1\cos^2\theta_1\sin^2\theta_4\cos^2\theta_4 ,$$

$$[\vec{\vec{L}}, \vec{\vec{L}}]_R = \{\vec{\vec{L}}(0) - \vec{\vec{L}}(1)\}:\{\vec{\vec{L}}(3_R) - \vec{\vec{L}}(2)\} = \tag{3.4-5}$$

$$= 18(1-w\cos\theta_3)^2\sin^2\theta_1\cos^2\theta_1\sin^2\theta_4\cos^2\theta_4 .$$

Introducing these results into (3.4-1) and carrying out the integrations over θ_1 and θ_4, we obtain

$$\alpha_{11}^{(1)} = \frac{2}{3}\beta_{oo}^{(1)} + \frac{\sqrt{3}}{\pi^2}\frac{189}{80}\int_{-\pi/2}^{+\pi/2} d\theta_2 \int_{-\pi/2}^{+\pi/2} d\theta_3 \int_{\frac{1}{\cos\theta_3}}^{\infty} dw \frac{w(w\cos\theta_3-1)^3}{E^{11/2}} \frac{|\cos(\theta_2-\theta_3)|}{\cos\theta_3} \tag{3.4-6}$$

$$\cdot[4w^2\sin^2\theta_3 - 2w^2\cos^2\theta_3 - (w\cos\theta_3-1)]\,[\delta(\theta_2) + \delta(\theta_2 - \tfrac{\pi}{2}) - \delta(\delta_3)] ,$$

$$\beta_{oo}^{(1)} = \frac{\sqrt{3}}{\pi^2}\frac{63}{10}\int_{-\pi/2}^{+\pi/2} d\theta_2 \int_{-\pi/2}^{+\pi/2} d\theta_3 \int_{\frac{1}{\cos\theta_3}}^{\infty} dw \frac{w(w\cos\theta_3-1)^3}{E^{9/2}} \frac{|\cos(\theta_2-\theta_3)|}{\cos\theta_3} \tag{3.4-7}$$

$$\cdot[\delta(\theta_2) + \delta(\theta_2 - \tfrac{\pi}{2}) - \delta(\theta)] .$$

The remaining integrals can be readily evaluated.[31] Thus we obtain in the first Enskog approximation

$$\frac{\lambda_1'(1)}{\lambda_o(1)} = - \alpha_{11}^{(1)} = - \frac{1}{1800} \frac{\sqrt{3}}{\pi^2} (8276 - 1920 \frac{\pi}{\sqrt{3}} - 4185 \ \ell n 3) , \qquad (3.4\text{-}8)$$

$$\frac{\eta_1'(1)}{\eta_o(1)} = - \beta_{oo}^{(1)} = - \frac{1}{225} \frac{\sqrt{3}}{\pi^2} (820 - 224 \frac{\pi}{\sqrt{3}} - 405 \ \ell n 3) . \qquad (3.4\text{-}9)$$

The contributions of the three triple collision events individually are presented in Table XII.

Table XII

Contributions to the coefficient of the logarithm in the first Enskog approximation.

diagram (Fig. 8)	$\lambda_1'(1)/\lambda_o(1)$
R	$-\frac{48}{25}\frac{\sqrt{3}}{\pi^2}\left(1-\frac{5}{9}\frac{\pi}{\sqrt{3}}\right)$
C	$-\frac{1}{1080}\frac{\sqrt{3}}{\pi^2}(2764-2511\ \ln 3)$
H	$-\frac{16}{135}\frac{\sqrt{3}}{\pi^2}$
R + C + H	$-\frac{1}{1800}\frac{\sqrt{3}}{\pi^2}\left(8276-1920\frac{\pi}{\sqrt{3}}-4185\ \ln 3\right)$
diagram	$\eta_1'(1)/\eta_o(1)$
R	$-\frac{48}{25}\frac{\sqrt{3}}{\pi^2}\left(1-\frac{14}{27}\frac{\pi}{\sqrt{3}}\right)$
C	$-\frac{1}{225}\frac{\sqrt{3}}{\pi^2}(452-405\ \ln 3)$
H	$+\frac{64}{225}\frac{\sqrt{3}}{\pi^2}$
R + C + H	$-\frac{1}{225}\frac{\sqrt{3}}{\pi^2}\left(820-224\frac{\pi}{\sqrt{3}}-405\ \ln 3\right)$

3.5 LOGARITHMIC DENSITY DEPENDENCE OF THE VISCOSITY IN THE SECOND ENSKOG APPROXIMATION+)

From the results obtained in the preceding Section we conclude that the transport properties do depend logarithmically on the density with non-vanishing coefficients λ_1' and η_1'. Nevertheless, one may wonder whether the first Enskog approximation provides a reasonable estimate for these coefficients. From the fact that the Sonine polynomial expansion (3.2-10) of the solutions $A^{(o)}(V_1)$ and $B^{(o)}(V_1)$ of the linearized Boltzmann equation is a convergent one, we may expect that the resulting expansion for the density correction (3.3-6) to the transport coefficients converges as well, provided, of course, that $\tilde{I}_3$ is replaced with a finite operator I_3 by taking the collisional damping into account. However, in order to conclude that a reliable estimate has been obtained for λ_1' and η_1', it is not sufficient to know that the expansion procedure converges, but we need to verify whether the next correction terms are small, as was the case for the dilute gas values λ_o and η_o (see Table X). For this purpose we have extended the analysis to determine the corrections in the second Enskog approximation. In this report we discuss the results obtained for the viscosity.

The second Enskog approximation $\eta_1'(2)$ is given by

$$\frac{\eta_1'(2)}{\eta_o(1)} = -\left[\{b_o^{(o)}(2)\}^2\beta_{oo}^{(1)} + b_o^{(o)}(2)b_1^{(o)}(2)\{\beta_{01}^{(1)} + \beta_{10}^{(1)}\} + \{b_1^{(o)}(2)\}^2\beta_{11}^{(1)}\right] . \quad (3.5\text{-}1)$$

It can be easily demonstrated that the matrix elements $\alpha_{k\ell}^{(1)}$ and $\beta_{k\ell}^{(1)}$ are symmetric

$$\alpha_{k\ell}^{(1)} = \alpha_{\ell k}^{(1)} \quad ; \quad \beta_{k\ell}^{(1)} = \beta_{\ell k}^{(1)} . \quad (3.5\text{-}2)$$

+) The research of this Section was carried out in cooperation with Dr. H. T. Wood at the National Bureau of Standards, Washington, D. C.

The reason is that in Fig. 8 the same triple collision events are obtained whether the diagrams are read from top to bottom or from bottom to top (except for a permutation of the particle numbers).

For the matrix element $\beta_{10}^{(1)}$, given by (3.3-21), we need to consider

$$\sum_{m=1}^{3}\sum_{n=1}^{3}[\vec{W}_m{}^{\circ}\vec{W}_m S_2^{(1)}(W_m^2),\ \vec{W}_n{}^{\circ}\vec{W}_n S_2^{(o)}(W_n^2)]_R = \sum_{m=1}^{3}\sum_{n=1}^{3}[\vec{W}_m{}^{\circ}\vec{W}_m(3 - W_m^2),\ \vec{W}_n{}^{\circ}\vec{W}_n]_R =$$

$$\sum_{m=1}^{3}\sum_{n=1}^{3} 3[\vec{W}_m{}^{\circ}\vec{W}_m,\ \vec{W}_n{}^{\circ}\vec{W}_n]_R - [\vec{W}_m{}^{\circ}\vec{W}_m W_m^2,\ \vec{W}_n{}^{\circ}\vec{W}_n]_R \ .$$

Thus

$$\beta_{10}^{(1)} = 3\beta_{oo}^{(1)} - \frac{1}{\pi^4}\sqrt{\frac{2}{\pi}}\int d\vec{W}_o\int d\vec{W}_{21}(1)W_{21}^2(1)\int_{-\pi/2}^{+\pi/2} d\theta_1\cos\theta_1\int_{-\pi/2}^{+\pi/2} d\theta_4\cos\theta_4\int_{-\pi/2}^{+\pi/2} d\theta_2\int_{-\pi/2}^{+\pi/2} d\theta_3\int_{\frac{1}{\cos\theta_3}}^{\infty} dw$$

$$\cdot\ \exp[-(W_1^2(1)+W_2^2(1)+W_3^2(1)]\ w(w\cos\theta_3-1)\ \frac{|\cos(\theta_2-\theta_3)|}{\cos\theta_3} \tag{3.5-3}$$

$$\cdot \sum_{m=1}^{3}\sum_{n=1}^{3}[\vec{W}_m{}^{\circ}\vec{W}_m W_m^2,\ \vec{W}_n{}^{\circ}\vec{W}_n]_R[\delta(\theta_2) + \delta(\theta_2 - \tfrac{\pi}{2}) - \delta(\theta_3)] \ .$$

As in the preceding Sections we express the velocity functions in terms of the total velocity $\vec{W}_o = \frac{1}{3}(\vec{W}_1 + \vec{W}_2 + \vec{W}_3)$ and the relative velocities $\vec{W}_{21}$ and $\vec{W}_{31}$.

$$\sum_{n=1}^{3}\vec{W}_n\vec{W}_n = 3\vec{W}_o\vec{W}_o + \frac{2}{3}\overset{\leftrightarrow}{L} \ , \tag{3.5-4}$$

$$\sum_{m=1}^{3}\vec{W}_m\vec{W}_m W_m^2 = \frac{1}{9}[9\vec{W}_o\vec{W}_o(3W_o^2 + \tfrac{2}{3}E) + (6W_o^2 + 2E)\overset{\leftrightarrow}{L} - \overset{\leftrightarrow}{N} \ ,$$

$$+ 24\overline{\overline{(\vec{W}_o . \overset{\leftrightarrow}{L})\vec{W}_o}} - 6\vec{W}_o\overset{\leftrightarrow}{K} + 4\vec{W}_o . \overset{\leftrightarrow}{M}] \ , \tag{3.5-5}$$

where we have introduced two new tensors[+)]

$$\overleftrightarrow{\overleftrightarrow{M}} = \vec{W}_{21}\vec{W}_{21}\vec{W}_{21} + \vec{W}_{31}\vec{W}_{31}\vec{W}_{31} +$$

$$- \tfrac{1}{2}[\vec{W}_{21}\vec{W}_{21}\vec{W}_{31} + \vec{W}_{21}\vec{W}_{31}\vec{W}_{21} + \vec{W}_{31}\vec{W}_{21}\vec{W}_{21} + \vec{W}_{21}\vec{W}_{31}\vec{W}_{31} + \vec{W}_{31}\vec{W}_{21}\vec{W}_{31} + \vec{W}_{31}\vec{W}_{31}\vec{W}_{21}] ,$$

$$\overleftrightarrow{N} = W_{21}^2\vec{W}_{31}\vec{W}_{31} + W_{31}^2\vec{W}_{21}\vec{W}_{21} - \vec{W}_{21}.\vec{W}_{31}(\vec{W}_{21}\vec{W}_{31} + \vec{W}_{31}\vec{W}_{21}) . \tag{3.5-7}$$

Note that

$$\overleftrightarrow{I}:\overleftrightarrow{\overleftrightarrow{M}} = -\frac{3}{2}\vec{K} \qquad \text{and} \qquad \mathrm{Tr}\ \overleftrightarrow{A}.\overleftrightarrow{\overleftrightarrow{M}} = -\frac{3}{2}\overleftrightarrow{A}.\vec{K} . \tag{3.5-8}$$

In two dimensions

$$\overleftrightarrow{N} = 0 . \tag{3.5-9}$$

In (3.5-5) terms odd in $\vec{W}_o$ vanish after integration over $\vec{W}_o$. The terms that contain only $\vec{W}_o$ and E are constants of the motion and vanish also. The remaining terms in (3.5-3) contain $[\overleftrightarrow{L}, \overleftrightarrow{L}]_R$ and as a consequence they can be related to the expression (3.4-2) for $\beta_{oo}^{(1)}$. As a result we obtain after integration over $\vec{W}_o$ and $\vec{W}_{21}$ (1)

$$\boxed{\beta_{10}^{(1)} = \beta_{01}^{(1)} = -\frac{1}{4}\beta_{oo}^{(1)} .} \tag{3.5-10}$$

For the matrix element $\beta_{11}^{(1)}$ we consider

$$\sum_{m=1}^{3}\sum_{n=1}^{3} [\vec{W}_m^o\vec{W}_m S_2^{(1)}(W_m^2),\ \vec{W}_n^o\vec{W}_n S_2^{(1)}(W_n^2)] =$$

$$\sum_{m=1}^{3}\sum_{n=1}^{3} 9[\vec{W}_m^o\vec{W}_m,\vec{W}_n^o\vec{W}_n]_R - 3\ [\vec{W}_m^o\vec{W}_m W_m^2,\vec{W}_n^o\vec{W}_n]_R$$

$$-3[\vec{W}_m^o\vec{W}_m,\vec{W}_n^o\vec{W}_n W_n^2]_R + [\vec{W}_m^o\vec{W}_m W_m^2,\vec{W}_n^o\vec{W}_n W_n^2] ,$$

+) $\overleftrightarrow{\overleftrightarrow{M}}$ is a two dimensional tensor of the third rank. The scalar product $\overleftrightarrow{\overleftrightarrow{M}}\vdots\overleftrightarrow{\overleftrightarrow{M}}'$ is defined as $\sum_\alpha \sum_\beta \sum_\gamma M_{\alpha\beta\gamma} M'_{\gamma\beta\alpha}$. Symmetrized dyadics are indicated by $\overline{\overline{AB}} = \frac{1}{2}(\vec{A}\vec{B} + \vec{B}\vec{A})$.

so that

$$\beta_{11}^{(1)} = 3\beta_{01}^{(1)} + 3\beta_{10}^{(1)} - 9\beta_{00}^{(1)} +$$

$$+ \frac{1}{\pi^4}\sqrt{\frac{2}{\pi}}\int d\vec{W}_o \int d\vec{W}_{21}(1) W_{21}^2(1) \int_{-\pi/2}^{+\pi/2} d\theta_1 \cos\theta \int_{-\pi/2}^{+\pi/2} d\theta_4 \cos\theta_4 \int_{-\pi/2}^{+\pi/2} d\theta_2 \int_{-\pi/2}^{+\pi/2} d\theta_3 \int_{\frac{1}{\cos\theta_3}}^{\infty} dw$$

$$\cdot \exp[-(W_1^2(1) + W_2^2(1) + W_3^2(1))]\ w(w\cos\theta_3 - 1)\ \frac{|\cos(\theta_2-\theta_3|}{\cos\theta_3} \tag{3.5-11}$$

$$\cdot \sum_{m=1}^{3}\sum_{n=1}^{3} [\vec{W}_m^o\vec{W}_m W_m^2,\ \vec{W}_n^o\vec{W}_n W_n^2]_R[\delta(\theta_2) + \delta(\theta_2 - \frac{\pi}{2}) - \delta(\theta_3)] \ .$$

To evaluate this integral we substitute (3.5-5) into (3.5-11). We see that upon integration over $\vec{W}_o$ several terms can be related again to $[\overset{\Rightarrow}{L}, \overset{\Rightarrow}{L}]_R$. Moreover, as a result of relations (3.5-8) most terms involving $\vec{K}$ and $\overset{\Rightarrow}{M}$ can be related to $[\vec{K}, \vec{K}]_R$ and, therefore, to the expression (3.4-1) for $\alpha_{11}^{(1)} - \frac{2}{3}\beta_{oo}^{(1)}$. Thus we obtain after integrating over $\vec{W}_o$ and $\vec{W}_{21}(1)$

$$\beta_{11}^{(1)} = \frac{73}{48}\cdot\beta_{oo}^{(1)} + \alpha_{11}^{(1)} + \frac{315}{128}\ \frac{\sqrt{3}}{\pi^2}\int_{-\pi/2}^{+\pi/2} d\theta_1 \cos\theta_1 \int_{-\pi/2}^{+\pi/2} d\theta_4 \cos\theta_4 \int_{-\pi/2}^{+\pi/2} d\theta_2 \int_{-\pi/2}^{+\pi/2} d\theta_3 \int_{\frac{1}{\cos\theta_3}}^{\infty} dw$$

$$\cdot\ \frac{w(w\cos\theta_3-1)}{E^{11/2}}\ \frac{|\cos(\theta_2-\theta_3)|}{\cos\theta_3}\ [\overset{\Rightarrow}{M}, \overset{\Rightarrow}{M}]_R[\delta(\theta_2) + \delta(\theta_2 - \frac{\pi}{2}) - \delta(\theta_3)] \ , \tag{3.5-12}$$

where the energy E is again given by (3.4-3). To evaluate the last term we substitute the velocities of Table XI into

$$[\overset{\Rightarrow}{M}, \overset{\Rightarrow}{M}]_R = \{\overset{\Rightarrow}{M}(0) - \overset{\Rightarrow}{M}(1)\} \ \vdots\ \{\overset{\Rightarrow}{M}(3_R) - \overset{\Rightarrow}{M}(2)\} \ .$$

Upon comparing with (3.4-4) we find

$$\int_{-\pi/2}^{+\pi/2} d\theta_1 \cos\theta_1 \int_{-\pi/2}^{+\pi/2} d\theta_4 \cos\theta_4 [\overset{\Rightarrow}{M}, \overset{\Rightarrow}{M}]_R = \frac{27}{4}\int_{-\pi/2}^{+\pi/2} d\theta_1 \cos\theta_1 \int_{-\pi/2}^{+\pi/2} d\theta_4 \cos\theta_4 [\vec{K}, \vec{K}]_R \tag{3.5-13}$$

so that this term can also be related to $\alpha_{11}^{(1)} - \frac{2}{3}\beta_{oo}^{(1)}$. We obtain finally

$$\boxed{\beta_{11}^{(1)} = \frac{3}{16}\beta_{oo}^{(1)} + 3\,\alpha_{11}^{(1)}\,.} \tag{3.5-14}$$

Substitution of the results for $\beta_{01}^{(1)}$ and $\beta_{11}^{(1)}$ into (3.5-1) yields for the first density coefficient

$$\frac{\eta_1'(2)}{\eta_o(1)} = -\frac{1251\beta_{oo}^{(1)} + 24\alpha_{11}^{(1)}}{1250}\,. \tag{3.5-15}$$

Thus the second Enskog approximation $\eta_1'(2)$ can be expressed in terms of the known results (3.4-8) and (3.4-9) for $\lambda_1'(1)/\lambda_o(1)$ and $\eta_1'(1)/\eta_o(1)$:

$$\frac{\eta_1'(2)}{\eta_o(1)} = \frac{1251}{1250}\frac{\eta_1'(1)}{\eta_o(1)} + \frac{12}{625}\frac{\lambda_1'(1)}{\lambda_o(1)}\,. \tag{3.5-16}$$

3.6 DISCUSSION OF THE RESULTS

As indicated in Section 3.1, we expect on general grounds that the successive correlated binary collisions will cause a logarithmic density dependence of the transport properties. For a two dimensional gas of hard disks the density dependence of the transport properties can be represented by

$$\begin{aligned} \lambda &= \lambda_o + \lambda_1' b\rho \ln b\rho + \lambda_1 b\rho + \ldots \;, \\ \eta &= \eta_o + \eta_1' b\rho \ln b\rho + \eta_1 b\rho + \ldots \;. \end{aligned} \tag{3.6-1}$$

In this chapter we developed a method to determine the coefficients λ_1' and η_1'. Although the procedure was carried out for hard disks in particular, the method can be used to predict the logarithmic contribution to the transport properties for any two dimensional gas of molecules with short range, spherically

symmetric, forces. The coefficients λ_1' and η_1' were expressed in terms of (asymptotic) collision integrals related to the recollisions (R), the cyclic collisions (C) and the hypothetical cyclic collisions (H) of Fig. 8.

The numerical values obtained for λ_1' and η_1' of hard disks are presented in Table XIII. The Table includes also the contributions from the three diagrams R, C and H individually. The values $\lambda_1'(1)$ and $\eta_1'(1)$ obtained in the first Enskog approximation are listed in the second and third columns. The values obtained for the viscosity coefficient $\eta_1'(2)$ in the second Enskog approximation are presented in the fourth column. It turns out that the second Enskog approximation modifies the values found in the first approximation by about 1% only. Thus we expect that we have found the correct order of magnitude for the logarithmic density dependence of thermal conductivity and viscosity for the model considered.

From the last column of Table XIII we see that the second Enskog approximation affects the three contributions to η_1' by the same relative amount of $\approx$ 1%. Since the total value for $\eta_1'(1)$ is of the same order as the contribution from the most important diagrams (R and H in this case), approximately the same correction is obtained for the total contribution. However, this is not necessarily true in general. For instance, if we evaluate the logarithmic contribution to the self diffusion in the first Enskog approximation,[32] the total coefficient turns out to be an order smaller than the contributions of the individual diagrams, due to some cancellations between these contributions. Although in this case the first Enskog approximation leads again to a reasonable estimate for these individual contributions, it is no longer evident that it will lead to a good estimate of the total effect. This will be discussed in a future report.

From the results of Table XIII we conclude that the coefficients of the term logarithmic in the density is non vanishing. However, the fact that these coefficients are different from zero, can be expected on much more general grounds. Inspection of the collision integrals (3.3-20) and (3.3-21) shows that in <u>any</u> Enskog approximation, the three collision events R, C and H will lead to a contribution of the form $\pi^{-2}\sqrt{3}\ (a_R - b_R\frac{\pi}{\sqrt{3}})$, $\pi^{-2}\sqrt{3}\ (a_C - b_C \ln 3)$ and $\pi^{-2}\sqrt{3}\ a_H$, respectively. Thus the three collision events lead to three different irrational numbers and a cancellation is therefore unlikely in any higher order Enskog approximation.

The results of Table XIII also reveal that the sign of the logarithmic density contribution depends on the particular form of the collision integrals and is not the same for the thermal conductivity and viscosity. Thus it could be that both the sign and the magnitude of the logarithmic density dependence would be sensitive to the intermolecular potential as well, and it does not seem possible to predict the sign from a priori considerations.

As discussed in Section 3.1, the same physical effects encountered in the triple collisions of a two dimensional gas, will occur in the quadruple collisions of a three dimensional gas. Thus we submit that our results for the two dimensional model gas provide significant evidence that also in an actual three dimensional gas a logarithmic density dependence must be expected, as expressed in equation (3.1-4).

Table XIII

Coefficient of the logarithmic density dependence for the transport coefficients of hard disks.

diagram	$\frac{\lambda_1'(1)}{\lambda_o(1)}$	$\frac{\eta_1'(1)}{\eta_o(1)}$	$\frac{\eta_1'(2)}{\eta_o(1)}$	$\frac{\eta_1'(2) - \eta_1'(1)}{\eta_1'(1)}$
R	+0.00258	-0.02005	-0.02002	-0.2%
C	-0.00088	-0.00551	-0.00553	+0.4%
H	-0.02080	+0.04992	+0.04956	-0.7%
R+C+H	-0.01909	+0.02436	+0.02401	-1.4%

CHAPTER IV
DENSITY DEPENDENCE OF EXPERIMENTAL TRANSPORT COEFFICIENTS+)

4.1 INTRODUCTION

In this Chapter we want to investigate whether the theoretically predicted density dependence of the transport properties can represent the experimental data. Up to the present experimental transport properties have usually been represented by a power series in the density (3.1-1).

$$\begin{aligned} \lambda &= \lambda_o + \lambda_1\rho + \tilde{\lambda}_2\rho^2 + \ldots , \\ \eta &= \eta_o + \eta_1\rho + \tilde{\eta}_2\rho^2 + \ldots . \end{aligned} \tag{4.1-1}$$

Our analysis of the two dimensional model gas demonstrated that such a power series cannot be justified theoretically and we provided substantial evidence that instead one should expect a density dependence that contains terms logarithmic in the density

$$\begin{aligned} \lambda &= \lambda_o + \lambda_1\rho + \lambda_2'\rho^2 \ln\rho + \lambda_2\rho^2 + \ldots , \\ \eta &= \eta + \eta_1\rho + \eta_2'\rho^2 \ln\rho + \eta_2\rho^2 + \ldots . \end{aligned} \tag{4.1-2}$$

It is the purpose of this Chapter to establish some criteria to test whether meaningful density coefficients λ_k and η_k can be deduced from the experimental data. In particular we shall try to determine the first density coefficients λ_1 and η_1 and make an assessment of the precision with which they can be obtained from the presently available experimental data.

In order to determine the first density coefficients, one initially looks at the experimental data in the linear region. But to decide which data are actually in the linear range, an estimate of the higher order terms

---

+) This Chapter was prepared in collaboration with Dr. H. J. M. Hanley and Dr. R. D. McCarty of the National Bureau of Standards, Boulder, Colorado.[33]

in the density expansion is desirable. Moreover, it is not evident *a priori* that the best value for this coefficient is obtained from the data in the linear region alone. For example to determine the second virial coefficient B in the equation of state (1.1-1) it is often advantageous to include experimental pVT data in the quadratic range.[34] For these reasons we try to assess the effect of higher order terms on the determination of the first density coefficient. We use equation (4.1-2) for this purpose, since it represents the density expansion suggested by the theory. However, for comparison we shall make a few remarks concerning the results obtained when the data are fitted to a simple power series (4.1-1).

In Section 4.2 we outline a general procedure to analyze experimental transport properties as a function of density. In Section 4.3 we apply this method to the thermal conductivity of neon. In Section 4.4 we present first density coefficients λ_1 and η_1 deduced from the experimental viscosities and thermal conductivities of a number of gases. In Section 4.5 we summarize and discuss these results.

4.2 CRITERIA FOR A CONSISTENT REPRESENTATION OF THE EXPERIMENTAL DATA AS A FUNCTION OF DENSITY

We assume that the theory predicts a density representation (not necessarily a power series) with finite coefficients

$$\lambda(T,\rho) = \sum_{k=o}^{\infty} \lambda_k(T) f_k(\rho) \; ,$$
$$\eta(T,\rho) = \sum_{k=o}^{\infty} \eta_k(T) f_k(\rho) \; , \qquad (4.2\text{-}1)$$

where the density coefficients λ_k and η_k are a function of the temperature alone. The functions $f_k(\rho)$ are ordered such that

$$\lim_{\rho\to 0} f_{k+1}(\rho)/f_k(\rho) = 0 \; . \qquad (4.2\text{-}2)$$

Theoretically, (4.2-1) contains an infinite number of terms representing the density variation around $\rho=0$. In practice, one uses a finite number of terms to represent the transport properties in a finite density interval

$$\lambda(T,\rho) = \sum_{k=o}^{N-1} \lambda_k(T) f_k(\rho) \; ,$$
$$\eta(T,\rho) = \sum_{k=o}^{N-1} \eta_k(T) f_k(\rho) \; . \qquad (4.2\text{-}3)$$

As pointed out in Chapter II, the present theory suggests $f_o(\rho) = 1$ (excluding Knudsen effects), $f_1(\rho) = \rho$, $f_2(\rho) = \rho^2 \ell n\rho$ and $f_3(\rho) = \rho^2$. However, we shall also include in the discussion a power series for which $f_k(\rho) = \rho^k$.

Recently, investigators have discussed some of the factors affecting the precision with which the virial coefficients of the equation of state can be deduced from the experimental pVT data.[34,35] In trying to determine

the experimental values for the coefficients λ_k and η_k in (4.2-3) several additional complications present themselves. The precision of the second virial coefficient B in (1.1-1) can be enhanced by an independent knowledge of the temperature, so that the first virial coefficient RT no longer represents a degree of freedom in analyzing the pVT data. However, the Chapman-Enskog values λ_o and η_o cannot be predicted with an accuracy significantly better than the experimental accuracy, presumably due to insufficient independent information on the intermolecular potential. This is despite the fact that a detailed theory is available for their description. In practice, therefore, the low density values λ_o and η_o have to be extracted from the experimental data themselves.

Furthermore, in order to deduce physically meaningful coefficients from experimental data with a given accuracy, one ideally needs to know a priori whether the chosen function is a correct representation of the data. This requires not only a theoretical knowledge of the form of the functions $f_k(\rho)$, but also an estimate of the magnitude of the coefficients, so that one can decide which terms can be neglected in a given density interval. Again, this condition is satisfied for the equation of state of simple gases.[34] For the transport properties, however, we do not know the functions $f_k(\rho)$ for $k>3$, nor do we have reliable a priori estimates of the magnitude of the coefficients for $k=1,2,3$. As a result we shall be forced to conclude that at the present we cannot determine the coefficients for $k\geq 2$ with enough confidence to make them amendable to theoretical interpretation.

Nevertheless, in order to proceed, one can lay down some minimum criteria which have to be satisfied if (4.2-3) is to be compatible with the

data. The first criterion is

(i) The standard deviation of the fitted data points. When the standard deviation of the points fitted with (4.2-3) exceeds the experimental error of the data, and/or when a curve representing the difference between experimental and calculated points shows systematic deviations, the proposed function cannot be a correct representation of the given experimental data. Although this criterion rules out certain possibilities, it is rather weak in that it still allows many interpolation formulas to represent the data. In particular, we shall see that in a given density interval the transport coefficients can always be fitted to a polynomial with or without a term logarithmic in the density.

To reduce the class of possible correct functions we consider two additional requirements:

(ii) The coefficients of the fitted equation should be independent of the size of the density interval. If (4.2-3) is the correct equation to represent the data in a given density interval, one may fit it to the data and return values for the coefficients. When the equation is fitted to data in a subinterval the values of the coefficients then obtained must be equal to (within their standard deviation) to the corresponding coefficients found from the fit for the complete density interval. This should be true for any subinterval as long as all coefficients are significant.

(iii) The coefficients should be independent of the number of terms in the equation. Assume that equation (4.2-3) is the correct equation to represent the data in a given density interval and that one determines values for all coefficients ($0 \leq k \leq N-1$). When the density interval is sufficiently reduced so that the last term ($k = N-1$) is no longer significant, a refit in the reduced interval with the equation $\sum_{k=o}^{N-2} \lambda_k f_k(\rho)$ or $\sum_{k=o}^{N-2} \eta_k f_k(\rho)$

must return the same values (within their standard deviations) for the first N-1 coefficients ($0 \le k \le N-2$) as are returned from the fit with the full equation (4.2-3) in the complete density interval.

We shall call any function (4.2-3) satisfying the criteria i, ii and iii consistent with the experimental data. In addition to these criteria, we shall also require that

(iv) All coefficients are to be significant for a proper fit. Violation of this condition does not exclude the possibility that the function under consideration is theoretically correct. However, the presence of insignificant terms affects the values returned for the significant coefficients.

Our analysis of the transport data is thus to investigate whether (4.2-3) is consistent with the experimental data so as to return reliable estimates of the coefficients λ_1 and η_1. If a certain function of the density, linear in the coefficients, is a correct representation of the data, the best estimates of the values of the coefficients can be obtained by the method of least squares. Of course, when the data are correlated and of unequal variance, these factors should be properly taken into account.[36]

In practice, we proceed as follows. Suppose we have several isotherms for λ and η. To reduce the effects from internal inconsistencies, we consider a set of data from only one experimental source at a time. We have n data points $\lambda(\rho_i)$ or $\eta(\rho_i)$ ($i = 1, \ldots n$) at a given temperature T, ordered such that $\rho_{i+1} \ge \rho_i$. To ensure equal variance of the data points we decide whether or not weighting of the data is desirable, basing our decision on the experimental estimates of the possible errors in λ or η and the density ρ. It turns out that the effect of errors in the independent variable ρ is usually negligible compared to that of the errors in the experimental transport properties.

We first consider the linear equation+) .

$$\lambda = \lambda_o + \lambda_1 \rho \ ,$$
$$\eta = \eta_o + \eta_1 \rho \ , \qquad (4.2\text{-}4)$$

and determine λ_o, λ_1 or η_o, η_1 from a least squares fit for the first few data points ($i \approx 3$ or 4). We then add the next datum point and redetermine the coefficients and note the criteria i-iv. This procedure is repeated, the criteria noted for each fit, until at a certain number of points, corresponding to densities up to a density ρ_ℓ, equation (4.2-4) no longer represents the experimental data correctly. Such a conclusion can be drawn when the criteria are not satisfied, i.e., when the standard deviation begins to increase and/or when the deviation curve begins to indicate a systematic deviation. Furthermore, the values returned for the coefficients begin to change systematically with the size of the density interval.

At this point, that is when (4.2-4) ceases to be valid, the next density dependent term $\lambda_2 f_2(\rho)$ or $\eta_2 f_2(\rho)$ is added to the fitting equation and the procedure is repeated. Once again, the criteria are noted after each fit and, in addition, the significance test on the new coefficients λ_2 or η_2 is used to recheck that the original estimate for the limiting density ρ_ℓ for a linear fit is valid (λ_2 or η_2 should not be significant for $\rho \le \rho_\ell$).

In principle, when enough experimental data are available, this procedure can be continued until all terms in equation (4.2-3) are significant.

From the results obtained by this procedure we can obtain some insight, whether a proposed density expansion (4.2-3) is consistent with the experimental

---

+) Strictly, we should, and did on occasion, fit the data first to the equation $\lambda=\lambda_o$ or $\eta=\eta_o$. However, usually there are not enough data as a function of density in the Chapman-Enskog regime to warrant this extra step.

data. Specifically, here we shall fit the data to (a) the linear equation (4.2-4), (b) to a quadratic polynomial, (c) to a cubic polynomial and (d) to the equation

$$\begin{aligned} \lambda &= \lambda_o + \lambda_1\rho + \lambda_2'\rho^2\ell n\rho + \lambda_2\rho^2 \ , \\ \eta &= \eta_o + \eta_1\rho + \eta_2'\rho^2\ell n\rho + \eta_2\rho^2 \ , \end{aligned} \tag{4.2-5}$$

which contains the first four terms of the theoretically predicted density expansion.

4.3 ANALYSIS OF THE THERMAL CONDUCTIVITY OF NEON

We discuss in some detail the results of this procedure for the set of thermal conductivity data of neon obtained by Bolk, Stigter and the author.[37] In the experiment care was taken to measure the data points at regularly spaced density intervals in an appreciable density range. The variation of the thermal conductivity of neon as a function of density is shown in Fig. 10. The actual experimental values are listed in Table XIV[+)].

+) Tables XIV through XVIII can be found at the end of this Section. In this report the thermal conductivity is expressed in cal/cm.s.K, since most authors have presented their experimental data in this unit. For the same reason the viscosity is expressed in g/cm.s or poise. The presently recommended SI values for λ and η are W/m.K and N.s/m^2, resp. The conversion factors are: 1 cal/cm.s.K = 418.68 W/m.K; 1 poise = 0.1 N.s/m^2.

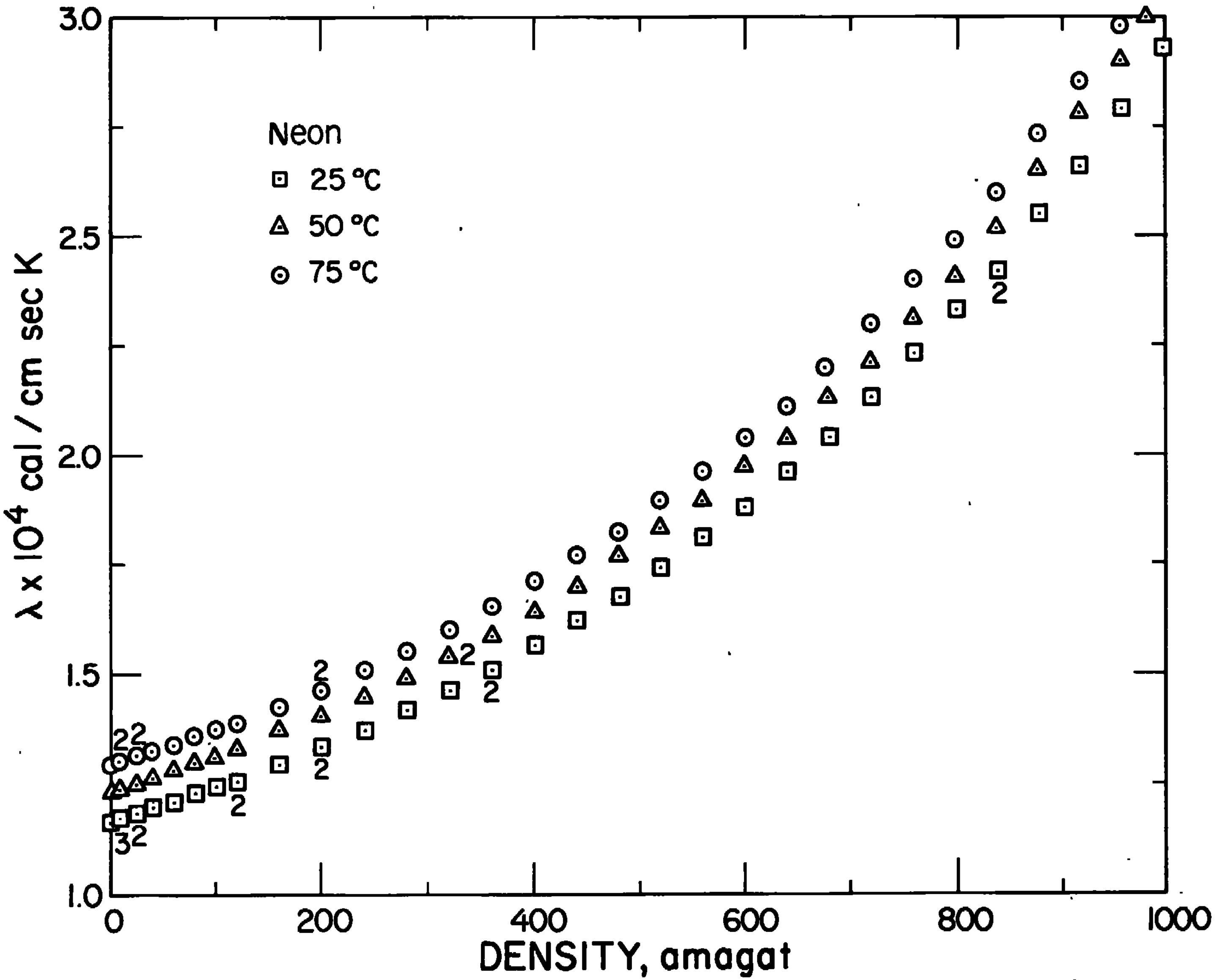

Figure 10. Experimental thermal conductivities of neon as a function of density.

Because equation (4.1-2) contains a term logarithmic in the density, we prefer to express the density in dimensionless units. Therefore, we have retained the amagat unit of density used in the original experimental tables.[37] The density in amagat represents the ratio of the actual density to the density ρ_{STP} of the gas at standard temperature and pressure (0^{o}C and 1 atm.). For neon one amagat corresponds to 0.00089979 g/cm^3.

Three thermal conductivity isotherms are available, namely at 25.1^{o}C 50.1^{o}C and 75.0^{o}C. The experimental method[38] suggests that any random error is due to errors in the measurement of the temperature difference across the gas layer or of the heat current through the gas layer, and is therefore most likely a relative error, that is, an error proportional to λ. This suggests a weight factor $\lambda(\rho_i)^{-2}$ for the least squares analysis.[36] Actually, we chose $[\lambda(\rho_i)/100]^{-2}$ as the weighting factors, so that the method of least squares returns the estimated standard deviation σ_λ of the data points as a percentage.

Linear fit. The results obtained by fitting the data to the linear equation (4.2-4) are presented in Table XV for the three isotherms. The second column gives the density interval $0<\rho<\rho_{max}$ and the third column the number n of data points from Table XIV used in fitting the equation. In columns four and five the values returned for the coefficients λ_o and λ_1 are presented together with their standard deviation σ_{λ_o} and σ_{λ_1}. The last column shows the estimated standard deviation of the data points. It turns out that up to a density of 120 amagat the coefficients within their standard deviation do not depend on the size of the density interval. The standard deviation σ_λ does not increase with density. The

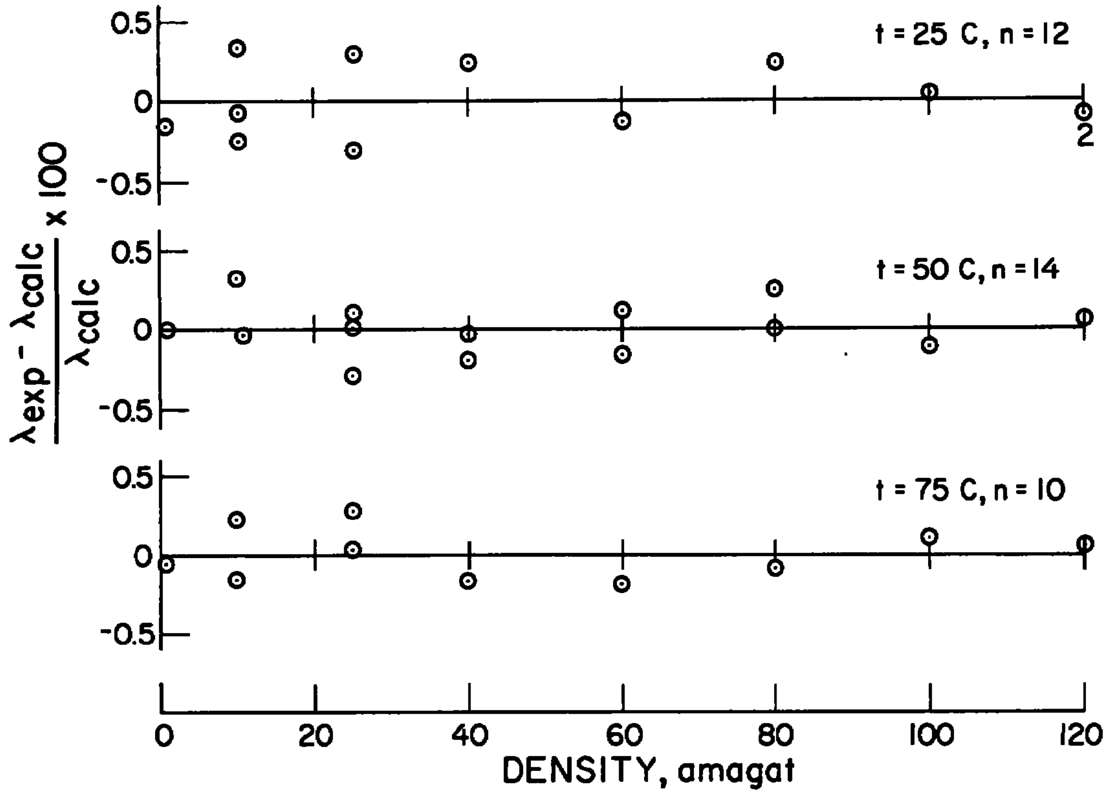

Figure 11. Plot of deviations $(\lambda_{exp} - \lambda_{calc})/\lambda_{calc}$ in % for the thermal conductivity of neon in the linear region.

deviation curves (shown in Fig. 11 for the largest density interval) confirm that the linear equation fits the data to within their experimental precision. Thus the linear equation satisfies the criteria i, ii and iv of Section 4.2. However, when data points at densities beyond 120 amagat are included, (not shown here), the standard deviation σ_λ begins to increase and the coefficients λ_o and λ_1 begin to change systematically. Thus we conclude that the linear equation (4.2-4) is consistent with the experimental data at densities up to 120 amagat. The most probable value for the first density coefficient λ_1, virtually independent of the temperature, deduced by fitting the data to

a linear equation is 0.77×10^{-7} cal/cm.s.K.am with a standard deviation of 0.02×10^{-7} in the same units.

Quadratic fit. We then first tried to represent the data over a wider density range by a polynomial, as has been the general practice in the literature up to now. For this purpose we consider the quadratic equation

$$\lambda = \lambda_o + \lambda_1\rho + \tilde{\lambda}_2\rho^2 . \tag{4.3-1}$$

The results obtained when the data are fitted to this equation are presented in Table XVI. The quadratic term does not become significant+) until $\rho = 200$ amagat, in agreement with our previous conclusion that at $\rho = 120$ amagat a linear equation is still sufficient. We note that in the units chosen $\tilde{\lambda}_2$ is about 10^{-3} times λ_1. Up to a density $\rho = 440$ amagat the quadratic equation satisfies conditions i, ii and iv; that is, the coefficients are independent of the density interval and the standard deviation σ_λ does not increase with density. (At densities beyond 440 amagat we begin to detect systematic deviations.) However, the estimate for the first density coefficient λ_1 obtained by fitting the quadratic equation, varies from 0.64×10^{-7} cal/cm.s.K.am to 0.71×10^{-7} cal/cm.s.K.am, in distinct disagreement with the value $(0.77 \pm 0.02)\times10^{-7}$ cal/cm.s.K.am deduced from the linear fit. Thus the quadratic equation is the density interval considered violates condition iii.

Cubic fit. Next we consider the cubic equation

$$\lambda = \lambda_o + \lambda_1\rho + \tilde{\lambda}_2\rho^2 + \tilde{\lambda}_3\rho^3 , \tag{4.3-2}$$

results for which are presented in Table XVII. The cubic term does not become significant until $\rho = 560$ amagat. Up to $\rho = 800$ amagat the coefficients do not vary with the density interval and the standard deviation σ_λ is constant.

+) As a test of significance for a linear coefficient λ_k we require that the quantity $T = (\lambda_k^2/\sigma_{\lambda_k}^2)$ is larger than the value of the $F_{.975}$ distribution for the corresponding degrees of freedom.[36]

(The fact that σ_λ is the same for all equations reinforces our original assumption that the random error is approximately a relative error independent of the density). However, the cubic equation again does not reproduce for the first density coefficient λ_1 the value of 0.77×10^{-7} cal/cm.s.K.am suggested by the linear fit, nor does it reproduce for $\tilde{\lambda}_2$ the value $\approx 0.8 \times 10^{-10}$ cal/cm.s.K.am^2 estimated from the quadratic equation in Table XVI.

From these results we conclude that neither a quadratic equation in a density interval up to ρ = 400 amagat, nor a cubic equation in a density interval up to ρ = 800 amagat, is consistent with the experimental data.

One could relax conditions ii and iii by allowing for variations of the coefficients within a 95% confidence interval Δ which is related to the standard deviation by

$$\Delta = \sigma t_{.025} \quad , \tag{4.3-3}$$

where $t_{.025}$ is the 2.5 percent point of the "student t" distribution for the corresponding degrees of freedom.[36+)] But, even so, the values $(0.77 \pm 0.06) \times 10^{-7}$ cal/cm.s.K.am and $(0.67 \pm 0.06) \times 10^{-7}$ cal/cm.s.K.am for $\lambda_1 \pm \Delta_{\lambda_1}$, returned from the linear and quadratic fit, do not agree very well, while the values returned for $\tilde{\lambda}_2$ from the quadratic and cubic fit are well outside each other's 95% confidence interval.

A serious problem is, of course, the possible effect of systematic errors in the data. A statistical analysis can only account for the effects of random errors and not of systematic errors. The effect of systematic errors could be estimated, e.g., by comparing sets of data from a number of different experimental sources for the same gas at the same temperature. A

+) When the degrees of freedom are large, $t_{.025} \cong 2$.

more decisive check could be made if the results were compared with those from experimental data with an appreciably higher precision, so that the various terms would become significant at other (lower) densities. The effect of two simple systematic errors can be easily assessed. A systematic error independent of the density (e.g. an error in the radiation constant[38]) would only modify the value returned for λ_o equally for all equations. If there is a systematic error proportional to λ (e.g. an error in the distance between the hot and the cold plate[38]), all coefficients will have this same percentage error. Thus, systematic errors of these kinds would not affect the conclusions of this analysis.

Logarithmic fit. After these negative results for the polynomial equations, we fitted the data with equation (4.2-5) that includes a term logarithmic in the density as predicted by the theory. The presence of this logarithmic term leads to some complications not encountered when fitting polynomials. It does not seem desirable to consider the $\rho^2 \ln\rho$ and the ρ^2 terms separately. For instance, if we change the density units such that $\bar{\rho} = \rho/\rho_o$, the coefficients $\bar{\lambda}_2'$ and $\bar{\lambda}_2$ of

$$\lambda = \lambda_o + \bar{\lambda}_1\bar{\rho} + \bar{\lambda}_2'\bar{\rho}^2 \ln\bar{\rho} + \bar{\lambda}_2\bar{\rho}^2 \quad , \tag{4.3-4}$$

are related to λ_2' and λ_2 in (4.2-5) by

$$\bar{\lambda}_2' = \lambda_2'\rho_o^{\,2} \; ; \; \bar{\lambda}_2 = \lambda_2'\rho_o^{\,2}\ln\rho_o + \lambda_2\rho_o^2 \; . \tag{4.3-5}$$

Therefore, the relative contribution of the two individual terms depends on the particular unit chosen for the density. In fact, if we had chosen ρ_o such that $\ln\rho_o = -\lambda_2/\lambda_2'$, the quadratic term in (4.3-4) would have

disappeared completely. This problem could be avoided by using the equation

$$\lambda = \lambda_o + \lambda_1\rho + \lambda_2'\rho^2 \ell n \frac{\rho}{\rho_o} , \tag{4.3-6}$$

where (in addition to λ_o, λ_1, λ_2') ρ_o is a constant to be determined. However, equation (4.3-6) is nonlinear in the coefficient ρ_o and therefore, less suitable to least squares analysis. Thus, in practice we prefer equation (4.2-5) and test the sum $\lambda_2'\rho^2 \ell n\rho + \lambda_2\rho^2$ for significance.

The results when the thermal conductivity data are fitted to this equation are presented in Table XVIII. The sum $\lambda_2'\rho^2 \ell n\rho + \lambda_2\rho^2$ becomes significant at ρ = 240 amagat similar to the quadratic results given in Table XVI. However, since (4.2-5) still contains four degrees of freedom, the individual terms become significant at much higher densities, comparable to the densities where all terms in the cubic polynomial became significant. The fit is within the experimental error up to ρ = 720 amagat; at densities beyond 720 amagat we detect systematic deviations.

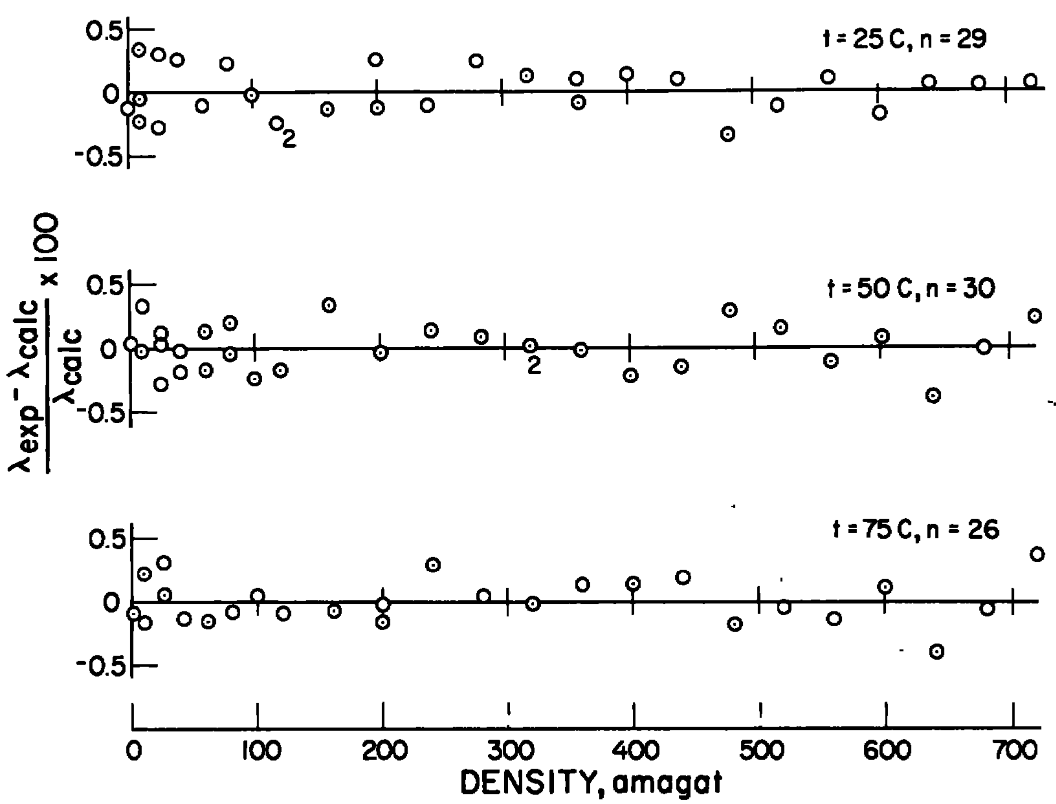

Figure 12. Plot of deviations $(\lambda_{exp} - \lambda_{calc})/\lambda_{calc}$ in % for the thermal conductitity of neon using equation (4.2-5)

We note that in the density interval considered σ_λ is again approximately constant and the deviations of the data points are random, as shown in Fig. 12. The value returned for the coefficient λ_1 does not vary with the density interval; this is also true for the coefficients λ_2' and λ_2 when they become significant individually+). Thus the equation satisfies criteria i, ii and iv. The results for the 75°C isotherm are slightly out of line; here the coefficients become significant at a later stage. But even here, when finally at ρ = 720 amagat all coefficients are significant, the coefficients are similar to those at the other temperatures.

Furthermore, from the fit up to ρ = 720 amagat we note that, on the average, $\lambda_1 = 0.79 \times 10^{-7}$ cal/cm.s.K.am with a standard deviation of 0.03×10^{-7}, in agreement with the value $(0.77\pm0.02)\times10^{-7}$ cal/cm.s.K.am deduced for λ_1 from the linear fit in Table XV. Thus, condition iii is satisfied as well. We therefore, conclude that equation (4.2-5) is consistent with the experimental data. Of course, any physical conclusions from this result should be considered with the same caution as mentioned earlier when discussing the results for the polynomial fits.

To obtain a realistic error estimate for λ_1, we prefer to replace the standard deviation σ_{λ_1} with a 95% confidence interval Δ_{λ_1}. From the agreement between Tables XV and XVIII we conclude that these tables yield

---

+) Upon a density transformation $\rho=\bar{\rho}\rho_o$, the standard deviation of the coefficient $\bar{\lambda}_2$ in (4.3-5) transforms as

$$\sigma^2_{\bar{\lambda}_2} = \rho_o^4(\sigma^2_{\lambda_2'}\ln^2\rho_o + 2\sigma^2_{\lambda_2',\lambda_2}\ln\rho_o + \sigma^2_{\lambda_2} ,$$

where $\sigma^2_{\lambda_2',\lambda_2}$ is the related off-diagonal element of the variance-covariance matrix of the coefficients.[36]

a meaningful value for the first density coefficient λ_1. On the other hand, it seems that a quadratic polynomial would have underestimated this coefficient λ_1 by as much as 10 percent.

We cannot draw a similar conclusion about the significance of the values returned for λ_2' and λ_2. To check the reliability of these coefficients by our procedure, we would have to add the next term (or combination of terms) beyond the ρ^2 term to the equation and compare the results for the new equation with those of Table XVIII. The character of these terms have not been investigated theoretically in sufficient detail as yet, nor are there enough experimental data to investigate their effect. However, we think it reasonable to assume that such higher order terms will no longer affect the value returned for the coefficient λ_1 of the linear term.

Table XIV

Experimental Thermal Conductivity data for neon[37]

	25.1°C		50.1°C		75.0°C	
n	ρ amagat	λx10^4 cal/cm.s.K	ρ amagat	λx10^4 cal/cm.s.K	ρ amagat	λx10^4 cal/cm.s.K
1	0.92	1.166	0.86	1.236	0.83	1.296
2	10.01	1.174	10.06	1.247	10.06	1.302
3	10.03	1.172	10.62	1.243	10.06	1.307
4	10.31	1.179	24.97	1.255	25.02	1.316
5	25.00	1.183	25.01	1.256	25.76	1.320
6	25.02	1.190	25.06	1.251	40.06	1.325
7	40.01	1.201	39.97	1.264	60.06	1.340
8	59.96	1.212	39.99	1.266	80.06	1.357
9	79.99	1.232	59.95	1.280	100.06	1.375
10	100.01	1.245	60.02	1.284	120.06	1.390
11	120.31	1.259	79.96	1.301	159.99	1.426
12	120.34	1.259	80.21	1.298	199.99	1.463
13	160.41	1.295	100.00	1.312	199.99	1.465
14	200.23	1.337	119.96	1.330	239.99	1.511
15	200.33	1.332	159.91	1.373	279.94	1.552
16	240.53	1.372	199.85	1.406	319.99	1.599
17	279.93	1.419	239.89	1.450	360.02	1.653
18	319.94	1.463	278.63	1.492	399.72	1.708
19	359.94	1.509	319.89	1.540	439.81	1.768
20	359.98	1.512	319.89	1.540	479.73	1.824
21	399.74	1.565	359.90	1.590	519.68	1.893
22	439.88	1.621	400.02	1.641	559.7	1.962
23	479.91	1.674	440.05	1.700	599.7	2.042
24	519.92	1.742	480.03	1.769	639.7	2.110
25	559.84	1.814	520.03	1.832	676.5	2.194
26	599.69	1.881	560.04	1.896	719.7	2.298
27	640.0	1.963	600.1	1.973	759.7	2.398
28	680.0	2.044	640.2	2.041	799.6	2.493
29	720.0	2.130	680.2	2.130	839.6	2.602
30	760.0	2.230	720.2	2.221	879.7	2.725
31	799.6	2.327	760.1	2.307	919.6	2.851
32	839.5	2.422	800.2	2.408	959.6	2.981
33	840.0	2.422	840.1	2.524		
34	879.9	2.547	880.1	2.654		
35	920.0	2.661	920.0	2.777		
36	960.1	2.792	960.1	2.903		
37	1000.0	2.928	984.6	2.996		

Table XV

Coefficients of $\lambda = \lambda_o + \lambda_1\rho$ for neon

(λ in cal/cm.s.K; ρ in amagat)

t	ρ_{max}	n	$(\lambda_o \pm \sigma_{\lambda_o})\mathrm{x}10^4$	$(\lambda_1 \pm \sigma_{\lambda_1})\mathrm{x}10^7$	σ_λ
°C	am				%
25	40	7	1.166 ± 0.002	0.86 ± 0.10	0.27
25	60	8	1.167 ± 0.002	0.79 ± 0.06	0.27
25	80	9	1.166 ± 0.002	0.81 ± 0.04	0.25
25	100	10	1.167 ± 0.001	0.79 ± 0.03	0.24
25	120	12	1.167 ± 0.001	0.77 ± 0.02	0.23
50	40	8	1.237 ± 0.002	0.71 ± 0.06	0.18
50	60	10	1.236 ± 0.001	0.75 ± 0.04	0.18
50	80	12	1.235 ± 0.001	0.79 ± 0.03	0.19
50	100	13	1.235 ± 0.001	0.78 ± 0.02	0.18
50	120	14	1.235 ± 0.001	0.78 ± 0.02	0.18
75	40	6	1.297 ± 0.002	0.79 ± 0.09	0.22
75	60	7	1.297 ± 0.002	0.73 ± 0.05	0.20
75	80	8	1.297 ± 0.001	0.74 ± 0.03	0.19
75	100	9	1.297 ± 0.001	0.77 ± 0.03	0.19
75	120	10	1.296 ± 0.001	0.77 ± 0.02	0.18

Table XVI

Coefficients of $\lambda = \lambda_o + \lambda_1\rho + \tilde{\lambda}_2\rho^2$ for neon

(λ in cal/cm.s.K; ρ in amagat)

t	ρ_{max}	n	$(\lambda_o \pm \sigma_{\lambda_o})\times 10^4$	$(\lambda_1 \pm \sigma_{\lambda_1})\times 10^7$	$(\tilde{\lambda}_2 \pm \sigma_{\tilde{\lambda}_2})\times 10^{10}$	σ_λ
°C	am					%
25	200	15	1.168 ± 0.002	0.71 ± 0.04	0.57 ± 0.22	0.26
25	240	16	1.168 ± 0.002	0.71 ± 0.04	0.57 ± 0.16	0.25
25	280	17	1.168 ± 0.001	0.68 ± 0.03	0.72 ± 0.12	0.25
25	320	18	1.169 ± 0.001	0.68 ± 0.03	0.75 ± 0.09	0.24
25	360	20	1.169 ± 0.001	0.68 ± 0.02	0.76 ± 0.06	0.23
25	400	21	1.169 ± 0.001	0.67 ± 0.02	0.79 ± 0.05	0.23
25	440	22	1.169 ± 0.001	0.66 ± 0.02	0.82 ± 0.04	0.23
50	200	16	1.236 ± 0.001	0.71 ± 0.04	0.73 ± 0.20	0.20
50	240	17	1.236 ± 0.001	0.71 ± 0.03	0.75 ± 0.14	0.19
50	280	18	1.236 ± 0.001	0.71 ± 0.03	0.75 ± 0.10	0.18
50	320	20	1.236 ± 0.001	0.71 ± 0.02	0.75 ± 0.06	0.17
50	360	21	1.236 ± 0.001	0.71 ± 0.02	0.76 ± 0.05	0.17
50	400	22	1.236 ± 0.001	0.71 ± 0.02	0.76 ± 0.04	0.16
50	440	23	1.237 ± 0.001	0.70 ± 0.01	0.79 ± 0.04	0.16
75	200	13	1.297 ± 0.001	0.69 ± 0.03	0.69 ± 0.16	0.16
75	240	14	1.298 ± 0.001	0.66 ± 0.03	0.90 ± 0.14	0.18
75	280	15	1.298 ± 0.001	0.66 ± 0.03	0.87 ± 0.10	0.17
75	320	16	1.298 ± 0.001	0.67 ± 0.02	0.86 ± 0.07	0.16
75	360	17	1.298 ± 0.001	0.66 ± 0.02	0.90 ± 0.05	0.16
75	400	18	1.298 ± 0.001	0.65 ± 0.02	0.92 ± 0.04	0.16
75	440	19	1.299 ± 0.001	0.64 ± 0.01	0.95 ± 0.03	0.16

Table XVII

Coefficients of $\lambda = \lambda_o + \lambda_1\rho + \tilde{\lambda}_2\rho^2 + \tilde{\lambda}_3\rho^3$ for neon

(λ in cal/cm.s.K; ρ in amagat)

t	ρ_{max}	n	$(\lambda_o \pm \sigma_{\lambda_o})\times10^4$	$(\lambda_1 \pm \sigma_{\lambda_1})\times10^7$	$(\tilde{\lambda}_2 \pm \sigma_{\tilde{\lambda}_2})\times10^{10}$	$(\tilde{\lambda}_3 \pm \sigma_{\tilde{\lambda}_3})\times10^{13}$	σ_λ
°C	am						%
25	560	25	1.168 ± 0.001	0.72 ± 0.03	0.44 ± 0.13	0.59 ± 0.17	0.22
25	600	26	1.168 ± 0.001	0.71 ± 0.02	0.47 ± 0.11	0.54 ± 0.13	0.22
25	640	27	1.168 ± 0.001	0.72 ± 0.02	0.45 ± 0.10	0.58 ± 0.11	0.21
25	680	28	1.168 ± 0.001	0.72 ± 0.02	0.45 ± 0.08	0.58 ± 0.09	0.21
25	720	29	1.168 ± 0.001	0.71 ± 0.02	0.46 ± 0.07	0.56 ± 0.08	0.20
25	760	30	1.168 ± 0.001	0.72 ± 0.02	0.43 ± 0.07	0.61 ± 0.06	0.20
25	800	31	1.168 ± 0.001	0.72 ± 0.02	0.42 ± 0.06	0.61 ± 0.05	0.20
50	560	26	1.236 ± 0.001	0.74 ± 0.03	0.51 ± 0.12	0.53 ± 0.15	0.18
50	600	27	1.236 ± 0.001	0.73 ± 0.02	0.51 ± 0.10	0.52 ± 0.10	0.18
50	640	28	1.236 ± 0.001	0.72 ± 0.02	0.61 ± 0.10	0.38 ± 0.11	0.19
50	680	29	1.236 ± 0.001	0.72 ± 0.02	0.59 ± 0.09	0.41 ± 0.09	0.19
50	720	30	1.236 ± 0.001	0.73 ± 0.02	0.54 ± 0.08	0.47 ± 0.08	0.19
50	760	31	1.236 ± 0.001	0.73 ± 0.02	0.56 ± 0.07	0.45 ± 0.06	0.19
50	800	32	1.236 ± 0.001	0.73 ± 0.02	0.55 ± 0.06	0.46 ± 0.05	0.18
75	560	22	1.298 ± 0.001	0.67 ± 0.02	0.77 ± 0.11		0.15
75	600	23	1.298 ± 0.001	0.69 ± 0.02	0.69 ± 0.11	0.38 ± 0.11	0.15
75	640	24	1.298 ± 0.001	0.67 ± 0.02	0.77 ± 0.09	0.27 ± 0.10	0.16
75	680	25	1.298 ± 0.001	0.68 ± 0.02	0.72 ± 0.08	0.33 ± 0.08	0.16
75	720	26	1.297 ± 0.001	0.70 ± 0.02	0.64 ± 0.08	0.44 ± 0.08	0.18
75	760	27	1.297 ± 0.001	0.71 ± 0.02	0.57 ± 0.07	0.52 ± 0.07	0.19
75	800	28	1.297 ± 0.001	0.71 ± 0.02	0.57 ± 0.06	0.52 ± 0.06	0.19

Table XVIII

Coefficients of $\lambda=\lambda_o + \lambda_1\rho + \lambda_2'\rho^2 \ln\rho + \lambda_2\rho^2$ for neon

(λ in cal/cm.s.K; ρ in amagat)

t °C	ρ_{max} am	n	$(\lambda_o \pm \sigma_{\lambda_o})x10^4$	$(\lambda_1 \pm \sigma_{\lambda_1})x10^7$	$(\lambda_2' \pm \sigma_{\lambda_2'})x10^{10}$	$(\lambda_2 \pm \sigma_{\lambda_2})x10^{10}$	σ_λ %
25	240	16	1.166 ± 0.002	0.9 ± 0.1	[1.1 ± 0.8]	[-6 ± 5]	0.24
25	320	18	1.167 ± 0.002	0.83 ± 0.09	[0.7 ± 0.4]	[-4 ± 3]	0.23
25	400	21	1.167 ± 0.001	0.79 ± 0.07	[0.4 ± 0.2]	[-2 ± 2]	0.22
25	480	23	1.168 ± 0.001	0.75 ± 0.05	[0.3 ± 0.2]	[-1 ± 1]	0.22
25	520	24	1.167 ± 0.001	0.76 ± 0.04	0.31 ± 0.12	[-1.3 ± 0.9]	0.21
25	560	25	1.167 ± 0.001	0.78 ± 0.04	0.39 ± 0.11	-1.8 ± 0.7	0.21
25	600	26	1.167 ± 0.001	0.78 ± 0.04	0.38 ± 0.09	-1.7 ± 0.6	0.21
25	640	27	1.167 ± 0.001	0.79 ± 0.03	0.42 ± 0.08	-2.0 ± 0.6	0.21
25	680	28	1.167 ± 0.001	0.79 ± 0.03	0.44 ± 0.07	-2.1 ± 0.5	0.20
25	720	29	1.167 ± 0.001	0.80 ± 0.03	0.45 ± 0.06	-2.2 ± 0.4	0.20
50	240	17	1.236 ± 0.002	0.7 ± 0.1	[-0.1 ± 0.6]	[1 ± 5]	0.20
50	320	20	1.236 ± 0.001	0.70 ± 0.07	[-0.0 ± 0.3]	[1 ± 2]	0.18
50	400	22	1.236 ± 0.001	0.71 ± 0.05	[0.0 ± 0.2]	[1 ± 1]	0.17
50	480	24	1.235 ± 0.001	0.78 ± 0.05	0.33 ± 0.14	[-1.4 ± 0.9]	0.19
50	520	25	1.235 ± 0.001	0.79 ± 0.04	0.37 ± 0.11	[-1.6 ± 0.8]	0.19
50	560	26	1.235 ± 0.001	0.78 ± 0.04	0.32 ± 0.10	[-1.3 ± 0.7]	0.18
50	600	27	1.235 ± 0.001	0.79 ± 0.04	0.34 ± 0.09	-1.4 ± 0.6	0.18
50	640	28	1.236 ± 0.001	0.77 ± 0.03	0.28 ± 0.08	-1.0 ± 0.5	0.19
50	680	29	1.235 ± 0.001	0.78 ± 0.03	0.31 ± 0.07	-1.3 ± 0.5	0.19
50	720	30	1.235 ± 0.001	0.80 ± 0.03	0.36 ± 0.06	-1.6 ± 0.5	0.19
75	240	14	1.296 ± 0.002	0.8 ± 0.1	[1.1 ± 0.6]	[-6 ± 4]	0.16
75	320	16	1.297 ± 0.001	0.71 ± 0.08	[0.2 ± 0.3]	[-0 ± 2]	0.17
75	400	18	1.297 ± 0.001	0.73 ± 0.05	[0.3 ± 0.2]	[-1 ± 1]	0.16
75	480	20	1.298 ± 0.001	0.70 ± 0.04	[0.2 ± 0.1]	[-0.1 ± 0.9]	0.16
75	520	21	1.297 ± 0.001	0.70 ± 0.04	[0.2 ± 0.1]	[-0.2 ± 0.7]	0.15
75	560	22	1.297 ± 0.001	0.71 ± 0.04	[0.2 ± 0.1]	[-0.3 ± 0.6]	0.15
75	600	23	1.297 ± 0.001	0.73 ± 0.03	0.26 ± 0.08	[-0.8 ± 0.6]	0.16
75	640	24	1.297 ± 0.001	0.71 ± 0.03	0.21 ± 0.07	[-0.5 ± 0.5]	0.16
75	680	25	1.297 ± 0.001	0.73 ± 0.03	0.25 ± 0.06	[-0.8 ± 0.5]	0.16
75	720	26	1.297 ± 0.001	0.76 ± 0.03	0.34 ± 0.07	-1.4 ± 0.5	0.19

Note: When λ_2' and/or λ_2 are not significant <u>individually</u> we place the value between brackets.

4.4 THE FIRST DENSITY COEFFICIENT OF THERMAL CONDUCTIVITY AND VISCOSITY FOR A NUMBER OF GASES

Hanley, McCarty and the author applied the techniques described in Sections 4.2 and 4.3 to the thermal conductivity and viscosity of a number of gases and tried to determine experimental first density coefficients λ_1 and η_1.[33] Unfortunately, data for a single gas that are accurate and extensive enough to yield reliable values for this density coefficient over a wide temperature range do not exist. Therefore, to obtain a more general picture of the temperature dependence of the first density coefficient, one needs to coordinate the results obtained for different gases using the principle of corresponding states. For this purpose we considered the noble gases: helium, neon, argon, krypton and xenon. Hydrogen and nitrogen were also included to obtain additional information at more extreme reduced temperatures.

Whenever possible, we prepared a set of tables similar to those shown for the thermal conductivity of neon, but, of course, such a complete analysis was only possible in a limited number of cases. In most cases we again noted a tendency for the logarithmic equation (4.2-5) to be more consistent with the experimental data than a pure polynomial. In particular, the data of LeNeindre et.al.[39] exhibited parallel behavior to that shown for neon. In many cases the scatter of the data was large enough to mask the difference between (4.2-5) and a polynomial, but, even then, we preferred the equations (4.2-4) and (4.2-5), since they contain the first terms of the theoretically predicted density expansion.

The final estimates for λ_1 and η_1 are presented in Tables XIX and XX. The references to the sources of the experimental data used in the analysis are given in the first column. For experimental data that were

given as a function of pressure, the pressures were converted to densities. A reference to the equation of state data, when such a conversion was needed, is also included. Column 6 indicates whether the final estimate of λ_1 and η_1 is based on the linear equation (4.2-4) or the logarithmic equation (4.2-5). This choice was usually dictated by the number and the range of the data at a given isotherm.

The estimated λ_1 and η_1 together with their standard deviation are listed in column 4 of Tables XIX and XX. The values for the corresponding 95% confidence interval are included in column 5. When the data were extensive enough to permit a test of equation (4.2-5), empirical values were obtained for the higher order coefficients. However, they have not been included here, since, as mentioned in the previous Section, their physical meaning is uncertain.

If the molecules interact with a spherically symmetric two-parameter potential, if the internal degrees of freedom of the molecules do not contribute to the transport of momentum and energy, and if the translational motion of the molecules can be described by classical mechanics, the transport properties in dimensionless form should be universal functions of the reduced state variables.[2] Thus, λ_1 and η_1 of the noble gases should obey a law of corresponding states, certainly within the precision with which these coefficients can be determined at the present.[6,58] One may also expect that the corresponding states relation for the transport properties of the noble gases can be extended to include the viscosity of nitrogen without introducing too large an error.[33,59] However, it is doubtful whether hydrogen will satisfy a corresponding states relation with the noble gases.[59] So any results for hydrogen should be interpreted with caution.

Dimensionless first density coefficients are obtained by defining

$$\lambda_1^* = \lambda_1 \frac{1}{r\rho_{STP}} \frac{m}{k}\sqrt{\frac{m}{\varepsilon}} \quad ; \quad \eta_1^* = \eta_1 \frac{1}{r\rho_{STP}}\sqrt{\frac{m}{\varepsilon}} \quad , \tag{4.4-1}$$

where m is the molecular mass, and r and ε are length and energy reducing parameters deduced for the Lennard-Jones potential.[3,60] The values of these reduced first density coefficients are presented in the last column of Tables XIX and XX, as a function of the reduced temperature $T^* = kT/\varepsilon$. The reduction parameters used are given in Table XXI.

Table XIX

The first density coefficient λ_1 of thermal conductivity

ref	gas	T	$(\lambda_1 \pm \sigma_{\lambda_1})\times 10^7$	$(\lambda_1 \pm \Delta_{\lambda_1})\times 10^7$	eq.	T*	$\lambda_1^* \pm \Delta_{\lambda_1^*}$
		K	cal/cm.s.K.am				
39	He	303.0	2.33 ± 0.08	2.33 ± 0.15	(4.2-5)	30.3	6.94 ± 0.45
40,41	He	195.2	1.22 ± 0.07	1.22 ± 0.14	(4.2-4)	19.5	3.63 ± 0.42
		126.6	1.40 ± 0.08	1.40 ± 0.15	(4.2-4)	12.7	4.17 ± 0.45
		77.9	0.99 ± 0.06	0.99 ± 0.26	(4.2-4)	7.79	2.95 ± 0.77
		43.15	1.01 ± 0.11	1.01 ± 0.24	(4.2-5)	4.32	3.01 ± 0.71
42	He	260.0	2.86 ± 0.07	2.86 ± 0.17	(4.2-4)	26.0	8.52 ± 0.51
		240.0	2.51 ± 0.22	2.51 ± 0.61	(4.2-4)	24.0	7.45 ± 1.82
		220.0	2.35 ± 0.20	2.35 ± 0.51	(4.2-4)	22.0	7.00 ± 1.52
		200.7	2.05 ± 0.15	2.05 ± 0.48	(4.2-4)	20.1	6.11 ± 1.43
		180.0	1.37 ± 0.06	1.37 ± 0.15	(4.2-4)	18.0	4.08 ± 0.45
		100.5	0.88 ± 0.02	0.88 ± 0.05	(4.2-4)	10.1	2.62 ± 0.15
		87.5	0.91 ± 0.04	0.91 ± 0.11	(4.2-4)	8.75	2.71 ± 0.33
		21.15	0.442 ± 0.003	0.44 ± 0.01	(4.2-4)	2.12	1.31 ± 0.03
37	Ne	348.15	0.76 ± 0.03	0.76 ± 0.06	(4.2-5)	7.41	2.26 ± 0.18
		323.15	0.79 ± 0.04	0.79 ± 0.08	(4.2-5)	6.87	2.35 ± 0.24
		298.15	0.79 ± 0.03	0.79 ± 0.07	(4.2-5)	6.34	2.35 ± 0.21
43	Ar	831.15	0.99 ± 0.07	0.99 ± 0.22	(4.2-4)	6.65	2.02 ± 0.45
		775.15	0.84 ± 0.05	0.84 ± 0.16	(4.2-4)	6.20	1.72 ± 0.33
		683.15	1.18 ± 0.02	1.18 ± 0.06	(4.2-4)	5.47	2.41 ± 0.12
		674.15	1.02 ± 0.09	1.02 ± 0.19	(4.2-5)	5.39	2.09 ± 0.39
		475.15	1.24 ± 0.07	1.24 ± 0.15	(4.2-5)	3.80	2.54 ± 0.31
		413.15	1.18 ± 0.08	1.18 ± 0.16	(4.2-5)	3.31	2.41 ± 0.33
		370.15	1.20 ± 0.04	1.20 ± 0.09	(4.2-4)	2.96	2.45 ± 0.18

Table XIX (continued)

The first density coefficient λ_1 of thermal conductivity

ref	gas	T	$(\lambda_1 \pm \sigma_{\lambda_1})\times10^7$	$(\lambda_1 \pm \Delta_{\lambda_1})\times10^7$	eq.	T*	$\lambda_1^* \pm \Delta_{\lambda_1}^*$
		K	cal/cm.s.K.am				
43	Ar	298.15	1.06 ± 0.08	1.06 ± 0.17	(4.2-5)	2.39	2.17 ± 0.35
44	Ar	348.15	1.00 ± 0.06	1.00 ± 0.13	(4.2-5)	2.79	2.05 ± 0.27
		323.15	1.02 ± 0.08	1.02 ± 0.34	(4.2-4)	2.59	2.09 ± 0.70
		298.15	1.02 ± 0.08	1.02 ± 0.30	(4.2-4)	2.39	2.09 ± 0.61
45,46	Ar	193.15	1.03 ± 0.04	1.03 ± 0.50	(4.2-4)	1.55	2.11 ± 1.02
		183.15	1.15 ± 0.04	1.15 ± 0.15	(4.2-4)	1.47	2.35 ± 0.31
		173.15	1.71 ± 0.12	1.71 ± 0.31	(4.2-4)	1.40	3.50 ± 0.63
		153.15	1.95 ± 0.28	1.95 ± 3.56	(4.2-4)	1.23	3.99 ± 7.28
39	N_2	298.15	1.21 ± 0.06	1.21 ± 0.12	(4.2-5)	3.28	2.25 ± 0.22
47,48	N_2	973.15	1.36 ± 0.29	1.36 ± 0.68	(4.2-5)	10.7	2.53 ± 1.27
		873.15	1.41 ± 0.20	1.41 ± 0.47	(4.2-5)	9.83	2.63 ± 0.88
		673.15	1.35 ± 0.01	1.35 ± 0.13	(4.2-4)	7.41	2.51 ± 0.24
		573.15	1.22 ± 0.07	1.22 ± 0.22	(4.2-5)	6.31	2.27 ± 0.41
		473.15	1.25 ± 0.01	1.25 ± 0.17	(4.2-4)	5.21	2.33 ± 0.32
		398.15	1.34 ± 0.01	1.34 ± 0.13	(4.2-4)	4.38	2.50 ± 0.24
		348.15	1.31 ± 0.02	1.31 ± 0.20	(4.2-4)	3.83	2.44 ± 0.37
45,48	N_2	200.0	0.98 ± 0.14	0.98 ± 0.44	(4.2-5)	2.20	1.82 ± 0.82
		180.0	0.89 ± 0.22	0.89 ± 0.70	(4.2-5)	1.98	1.66 ± 1.30
		170.0	0.96 ± 0.04	0.96 ± 0.51	(4.2-4)	1.87	1.79 ± 0.95
		160.0	1.02 ± 0.05	1.02 ± 0.62	(4.2-4)	1.76	1.90 ± 1.15
		130.0	2.61 ± 0.25	2.61 ± 1.07	(4.2-4)	1.43	4.86 ± 1.99

Table XX

The first density coefficient η_1 of viscosity

Ref	gas	T K	$(\eta_1 \pm \sigma_{\eta_1})\times 10^7$ g/cm.s.am	$(\eta_1 \pm \Delta_{\eta_1})\times 10^7$	eq.	T*	$(\eta_1^* \pm \Delta_{\eta_1^*})\times 10$
49	He	293.15	-0.024 ± 0.007	-0.024 ± 0.015	(4.2-4)	29.3	-0.36 ± 0.22
50	He	373.15	-0.21 ± 0.03	-0.21 ± 0.13	(4.2-4)	37.3	-3.10 ± 1.92
		298.15	-0.05 ± 0.01	-0.05 ± 0.13	(4.2-4)	29.8	-0.74 ± 1.92
		223.15	0.021 ± 0.005	0.021 ± 0.020	(4.2-4)	22.3	0.31 ± 0.30
51	Ne	348.15	0.48 ± 0.07	0.48 ± 0.14	(4.2-5)	7.41	1.36 ± 0.40
		323.15	0.43 ± 0.04	0.43 ± 0.13	(4.2-4)	6.88	1.22 ± 0.37
		298.15	0.55 ± 0.05	0.55 ± 0.14	(4.2-4)	6.34	1.56 ± 0.40
50	Ne	373.15	0.52 ± 0.05	0.52 ± 0.64	(4.2-4)	7.93	1.47 ± 1.81
		298.15	0.66 ± 0.04	0.66 ± 0.50	(4.2-4)	6.34	1.87 ± 1.41
		248.15	0.68 ± 0.05	0.68 ± 0.20	(4.2-4)	5.28	1.92 ± 0.56
		223.15	0.76 ± 0.07	0.76 ± 0.89	(4.2-4)	4.75	2.15 ± 2.52
49	Ne	293.15	0.48 ± 0.07	0.48 ± 0.19	(4.2-4)	6.24	1.36 ± 0.54
49	Ar	298.17	2.15 ± 0.07	2.15 ± 0.30	(4.2-4)	2.39	2.19 ± 0.31
		293.17	2.03 ± 0.09	2.03 ± 0.22	(4.2-5)	2.35	2.07 ± 0.22
52	Ar	298.15	2.20 ± 0.05	2.20 ± 0.12	(4.2-5)	2.39	2.24 ± 0.12
50	Ar	298.15	2.14 ± 0.30	2.14 ± 1.29	(4.2-5)	2.39	2.18 ± 1.31
		248.0	2.13 ± 0.50	2.13 ± 2.15	(4.2-5)	1.98	2.17 ± 2.19
		223.0	2.48 ± 0.50	2.48 ± 2.15	(4.2-5)	1.78	2.53 ± 2.19
53	Ar	348.15	2.80 ± 0.08	2.80 ± 0.34	(4.2-4)	2.79	2.85 ± 0.35
		323.15	2.74 ± 0.40	2.74 ± 0.92	(4.2-5)	2.59	2.79 ± 0.94
		298.15	2.31 ± 0.20	2.31 ± 0.46	(4.2-5)	2.39	2.35 ± 0.47

Table XX (continued)

The first density coefficient η_1 of viscosity

Ref	gas	T	$(\eta_1 \pm \sigma_{\eta_1})\times 10^7$	$(\eta_1 \pm \Delta_{\eta_1}) \times 10^7$	eq.	T*	$(\eta_1^* \pm \Delta_{\eta_1^*})\times 10$
		K	g/cm.s.am				
54	Kr	348.15	3.69 ± 0.30	3.69 ± 0.67	(4.2-5)	1.90	2.02 ± 0.37
		323.15	4.81 ± 0.24	4.81 ± 0.76	(4.2-4)	1.77	2.63 ± 0.42
		298.15	3.36 ± 0.19	3.36 ± 0.41	(4.2-5)	1.63	1.84 ± 0.22
49	Kr	293.15	3.47 ± 0.15	3.47 ± 0.64	(4.2-5)	1.60	1.90 ± 0.35
49	Xe	298.15	3.36 ± 0.30	3.36 ± 3.81	(4.2-4)	1.19	1.14 ± 1.30
50	N_2	373.15	2.08 ± 0.15	2.08 ± 1.90	(4.2-4)	4.11	2.75 ± 2.51
		298.15	1.18 ± 0.14	1.18 ± 0.36	(4.2-5)	3.28	1.56 ± 0.48
		248.15	2.10 ± 0.30	2.10 ± 1.29	(4.2-5)	2.73	2.78 ± 1.71
		223.15	1.95 ± 0.03	1.95 ± 0.13	(4.2-5)	2.45	2.58 ± 0.17
49	N_2	298.15	1.48 ± 0.10	1.48 ± 0.32	(4.2-5)	3.28	1.96 ± 0.42
		293.15	1.36 ± 0.25	1.36 ± 0.59	(4.2-5)	3.22	1.80 ± 0.78
55	N_2	323.15	1.61 ± 0.30	1.61 ± 1.29	(4.2-5)	3.56	2.13 ± 1.71
		298.15	1.70 ± 0.07	1.70 ± 0.14	(4.2-5)	3.28	2.25 ± 0.19
56	H_2	423.15	0 ± ?	0 ± ?	-	12.8	0 ± ?
		348.15	0.16 ± 0.013	0.16 ± 0.05	(4.2-4)	10.6	1.68 ± 0.52
57	H_2	348.15	0.173 ± 0.004	0.173 ± 0.016	(4.2-4)	10.6	1.82 ± 0.17

Table XXI

Reduction parameters used to express λ_1^* and η_1^* in dimensionless units.

gas	ρ_{STP}	r	ε/k	$\frac{1}{r\rho_{STP}}\frac{m}{k}\sqrt{\frac{m}{\varepsilon}}\times10^{-7}$	$\frac{1}{r\rho_{STP}}\sqrt{\frac{m}{\varepsilon}}\times10^{-7}$
	g/cm^3	Å	K	cal/cm.s.K.am	g/cm.s.am
He	0.00017845	2.63	10.0	2.979	14.78
Ne	0.00089979	2.72	47.0	2.980	2.828
Ar	0.0017834	3.41	125.0	2.045	1.019
Kr	0.0037481	3.62	183.0	2.306	0.547
Xe	0.0058974	3.96	250.0	2.248	0.340
N_2	0.0012506	3.68	90.9	1.862	1.323
H_2	0.00008994	2.87	33.0	1.065	10.511

4.5 DISCUSSION OF THE RESULTS

We have proposed some criteria to check whether a given density function is a possible correct representation of experimental data for the transport properties of gases. According to these criteria, the density function suggested by the theory, which involves a term logarithmic in the density, is shown to be consistent with experimental data.

In particular, by investigating whether the coefficient of the linear term does not change upon adding additional terms to the linear equation, we verified whether meaningful values for the first density coefficient are deduced from the experimental transport data. Based on this analysis we report experimental values for the first density coefficients λ_1 and η_1 for a number of gases. The reduced first density coefficients λ_1^* and η_1^* are plotted in Figs. 13 and 14 as a function of the reduced temperature T*, up to T* = 30.

Both λ_1^* and η_1^* appear insensitive to the temperature in the approximate range $2 < T^* < 10$. The theoretical predictions for λ_1 and η_1 developed in Chapter II were limited to a gas of hard spheres and, therefore, cannot be used legitimately to describe λ_1 and η_1 for a real gas. Nevertheless, we could make such an attempt by attributing an effective hard sphere diameter σ to the real molecules. The most natural choice for such a diameter σ is the requirement that the dilute gas values λ_o and η_o should reduce to the hard sphere expressions (2.2-13). For such a hypothetical hard sphere gas the first density coefficients are given by (2.8-1) (together with the appropriate collisional transfer contribution). If we apply this procedure at temperatures corresponding to T* = 4 we obtain $\lambda_1^* \sim 1.9$ for helium,

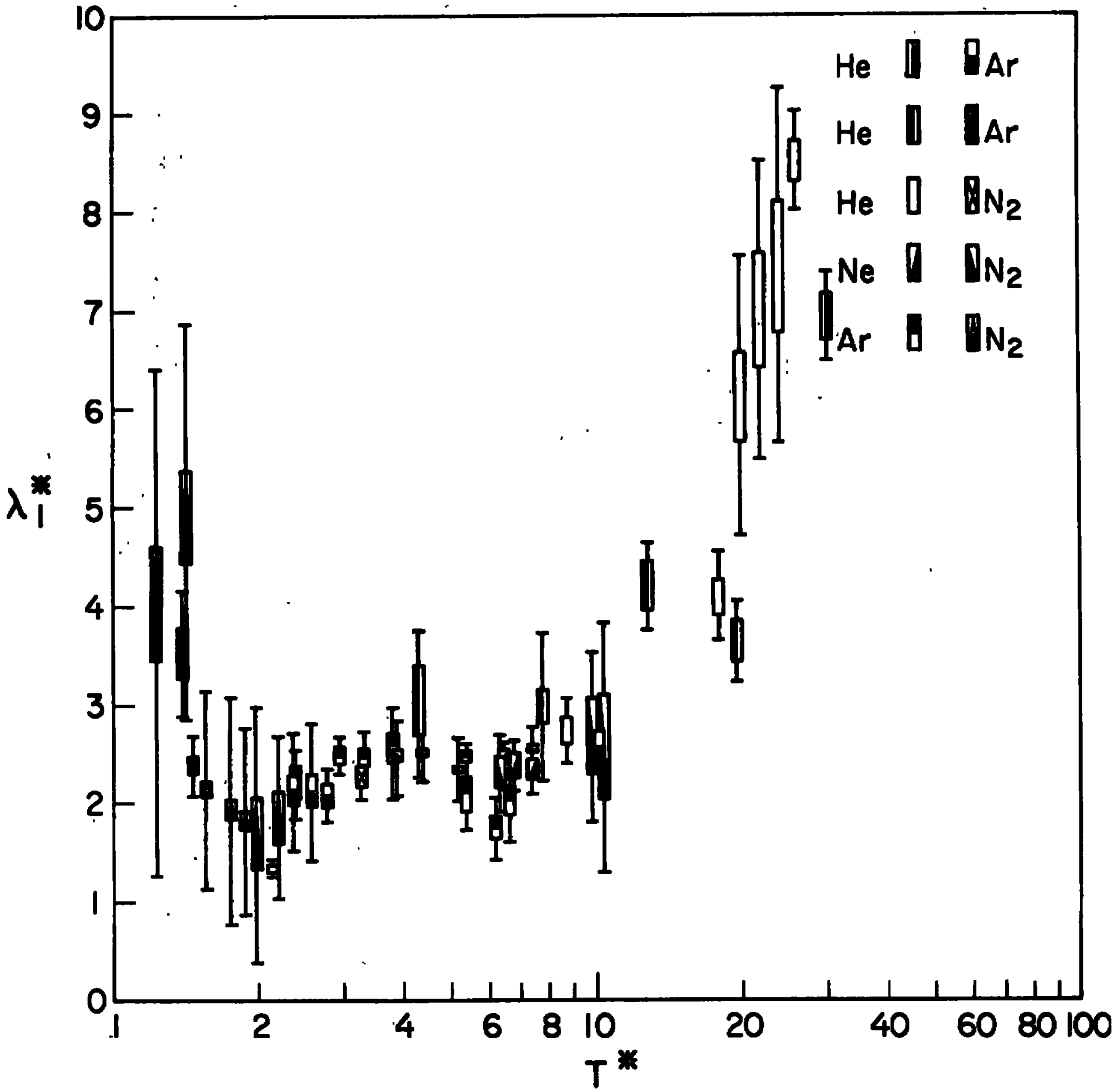

Figure 13. The reduced first density coefficient λ_1^* of thermal conductivity as a function of the reduced temperature T*.

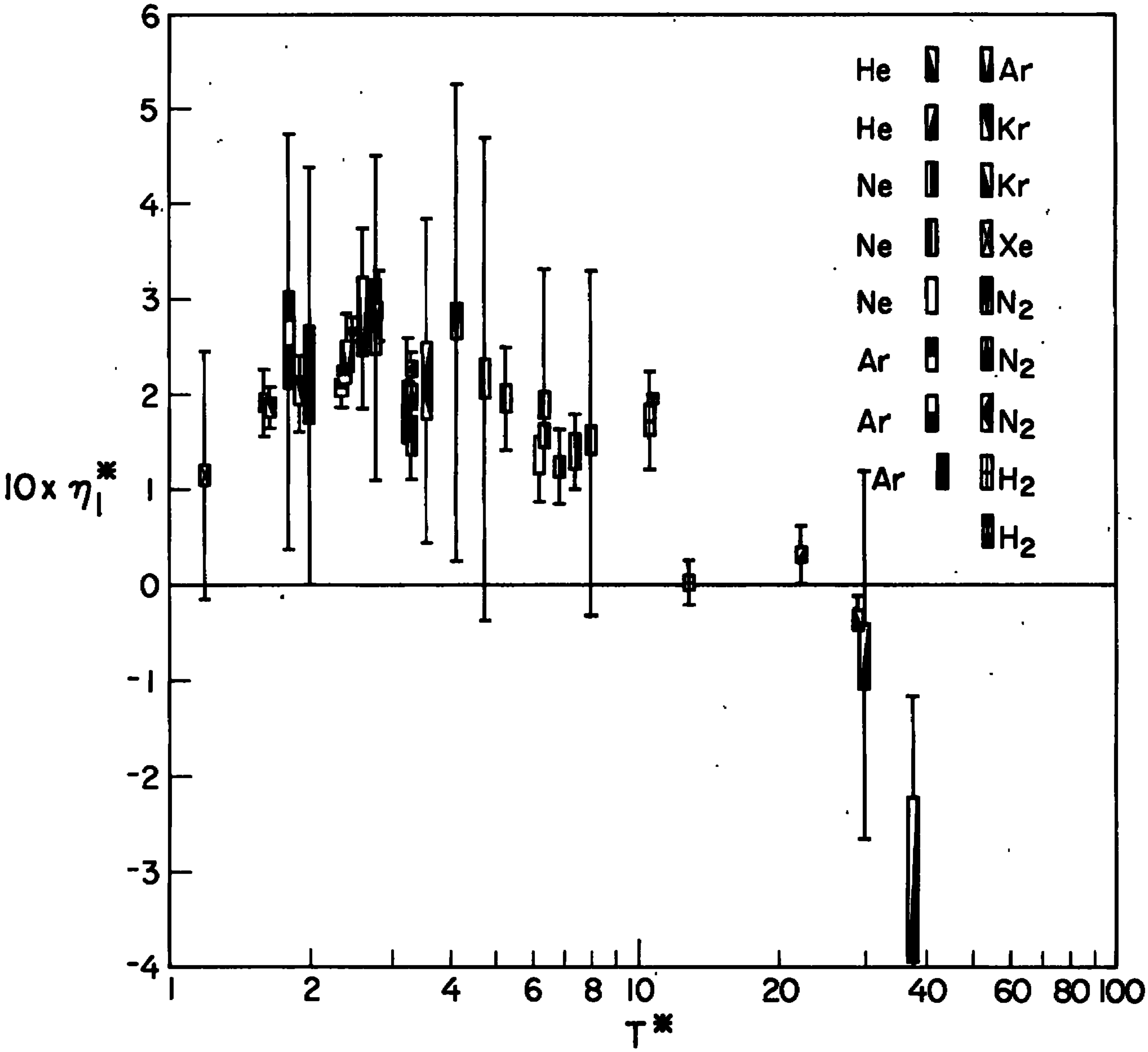

Figure 14. The reduced first density coefficient η_1^* of viscosity as a function of the reduced temperature T*.

$\lambda_1^* \sim 1.8$ for neon, $\lambda_1^* \sim 1.7$ for argon and $\lambda_1^* \sim 1.8$ for nitrogen. Corresponding values obtained for η_1^* are $\eta_1^* \sim 0.17$ for helium, $\eta_1^* \sim 0.16$ for neon, $\eta_1^* \sim 0.15$ for argon, $\eta_1^* \sim 0.17$ for krypton, $\eta_1^* \sim 0.17$ for xenon, $\eta_1^* \sim 0.15$ for nitrogen and $\eta_1^* \sim 0.13$ for hydrogen.

From Figs. 13 and 14 we see that these estimates have a reasonable order of magnitude in the insensitive temperature range.

The first density coefficients appear sensitive to temperature when $T^* < 2$ and when $T^* > 10$. In fact, it is clear that η_1^* will pass through zero.[7,58] Since this observation is based largely on experimental data for helium (recently Kao and Kobayashi have presented further evidence that η_1 becomes negative for helium[61]), some estimated values for η_1^* for hydrogen[56,57] are included in Fig. 14. However, it does not seem possible to determine accurately the reduced temperature at which $\eta_1^* = 0$. By contrast, Fig. 13 shows that in the same temperature range λ_1^* does not change sign.

The existence of the insensitive temperature range means that it is imperative to have reliable experimental data for temperatures outside the range, if we are to make any sensitive comparisons of theory with experiment. At this time we rely heavily on the data of Ziebland and Burton[45] for λ_1^* at low reduced temperatures, and we are very dependent on the preliminary work at NBS[42] for λ_1^* at high temperatures. It is obvious from the spread of the confidence interval bars in Figs. 13 and 14, that the coefficients λ_1 and η_1 should be known with a better precision. Thus, more reliable data are required for the whole temperature range. The precision of λ_1 and η_1 can only be improved if the individual data points

are determined with a standard deviation of about 0.5% for λ and 0.2% or less for η. Furthermore, the data points on an individual isotherm should be numerous and well-spaced,[34] in particular, in the linear region. It goes without saying that systematic errors should be minimized as much as possible.

APPENDIX A. SURFACE INTEGRAL FORM OF THE TRIPLE COLLISION INTEGRAL

The fact that the six dimensional configurational triple collision integral can be converted into a five dimensional surface integral was pointed out by Green.[16]

The streaming operators $\mathcal{S}(1. . .s)$ are mathematically defined as[8]

$$\mathcal{S}(1. .s) = \lim_{\tau\to\infty} \mathcal{S}_\tau(1. .s) = \lim_{\tau\to\infty} e^{-\tau\mathcal{H}_s} . e^{+\tau\mathcal{H}_s^{(o)}} , \tag{A-1}$$

where $\mathcal{H}_s(1. .s)$ is a "Hamilton" operator

$$\mathcal{H}_s(1. .s) = \sum_{i=1}^{s} \vec{v}_i \cdot \frac{\partial}{\partial \vec{r}_i} - \sum_{i<j}^{s} \theta_{ij} , \tag{A-2}$$

and $\mathcal{H}_s^{(o)}$ that part of $\mathcal{H}_s$ which is associated with the free streaming of s particles

$$\mathcal{H}_s^{(o)} (1. .s) = \sum_{i=j}^{s} \vec{v}_i \cdot \frac{\partial}{\partial \vec{r}_i} . \tag{A-3}$$

We assume that for large values of τ the streaming operators become independent of τ +)

$$\lim_{\tau\to\infty} \frac{d}{d\tau}\mathcal{S}_\tau(1. .s) = \mathcal{H}_s(1. .s)\mathcal{S}(1. .s) - \mathcal{S}(1. .s)\mathcal{H}_s^{(o)}(1. .s) = 0 , \tag{A-4}$$

so that [62]

$$\mathcal{H}_s^{(o)}(1. .s)\mathcal{S}(1. .s) - \mathcal{S}(1. .s)\mathcal{H}_s^{(o)}(1. .s) = \sum_{i<j}^{s} \theta_{ij}(1. .s) . \tag{A-5}$$

+) In this assumption we neglect the collisions which are taking place exactly at the time $-\tau$. Therefore, we make an error, referred to as the "initial" error term by Dorfman and Cohen.[25] This initial error term is less divergent than the asymptotic error term discussed in Section 3.1 and does not contribute to the first density coefficients, nor to the coefficient of the logarithm.

In particular

$$\mathcal{H}_3^{(o)}(123)\,\mathcal{S}(123) - \mathcal{S}(123)\,\mathcal{H}_3^{(o)}\,123) = (\theta_{12} + \theta_{13} + \theta_{23})\,\mathcal{S}(123)\,, \qquad \text{(A-6)}$$

and

$$\mathcal{H}_3^{(o)}(123)\,\mathcal{S}(\alpha) - \mathcal{S}(\alpha)\,\mathcal{H}_3^{(o)}(123) = \theta_\alpha \mathcal{S}(\alpha)\,, \qquad \text{(A-7)}$$

where α is either 12, 13 or 23. Using these relations the operator 0(123) given by (2.4-15) can be rewritten into the form[16]

$$0(123 = \int d\vec{r}_{21}d\vec{r}_{31}\Big[\mathcal{H}_3^{(o)}U(123) - U(123)\mathcal{H}_3^{(o)}$$
$$- \sum_{\alpha\neq\beta}\sum\{\mathcal{H}_3^{(o)}U(\alpha) - U(\alpha)\,\mathcal{H}_3^{(o)}\}U(\beta)\Big]\,. \qquad \text{(A-8)}$$

For convenience we have introduced the Ursell operators

$$U(\alpha) = \mathcal{S}(\alpha) - 1\,,$$
$$U(123) = \mathcal{S}(123) - \mathcal{S}(12) - \mathcal{S}(13) - \mathcal{S}(23) + 2\,. \qquad \text{(A-9)}$$

The summations over α and β are to be taken over the pairs 12, 13 and 23. The integrand depends only on the relative positions and the integration can be carried out over any two relative position vectors, for which we have chosen $\vec{r}_{21}$ and $\vec{r}_{31}$. Since in (2.4-14) the operator 0(123) operates on a function of the velocities alone, the term $U(123)\mathcal{H}_3^{(o)}$ vanishes in (A-8).

In order to define an appropriate transformation for the integration variables, we consider for fixed $\vec{V}_1$, $\vec{V}_2$, $\vec{V}_3$ the positions of particles 1, 2 and 3 which are related to each other by free particle motion. This is schematically illustrated in Fig. A1, where the time t associated with the free motion of the particles is taken to increase when the diagram is read from bottom to top.

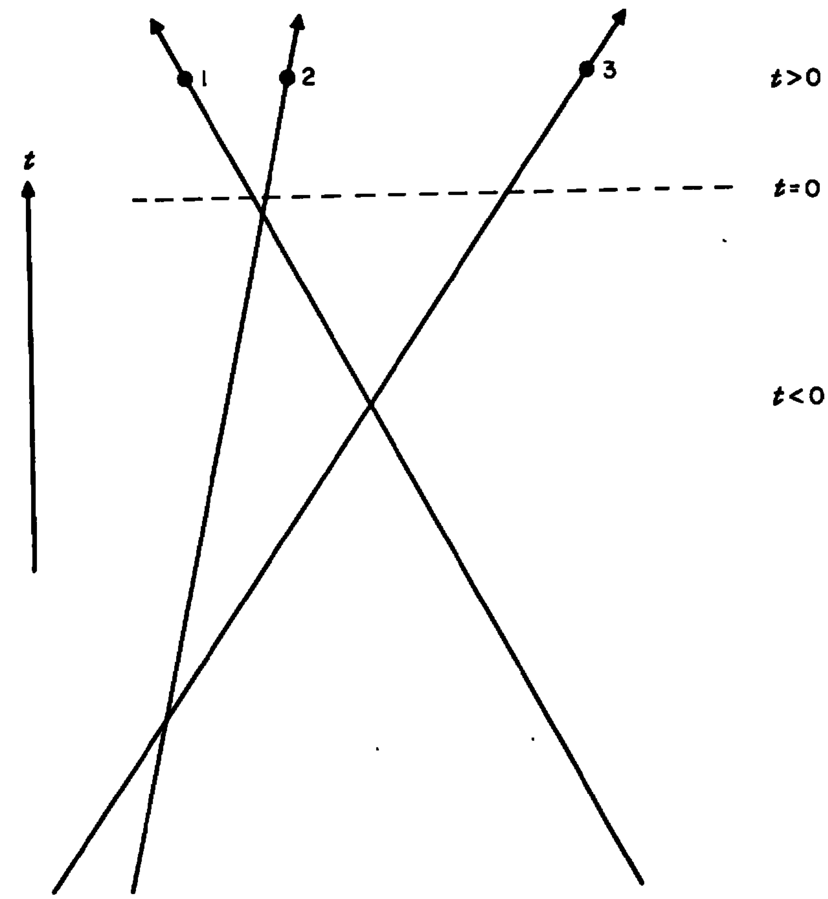

Figure A 1. Diagram representing the free trajectories of particles 1, 2 and 3.

However, since the $\mathcal{S}$ operators transform the present phases of the particles to phases in the previous history of the motion, we shall retrace the trajectories backwards in time and always read the diagrams from top to bottom as in the main text.

We remark that the three free particle trajectories have at least one "intersection", by which we mean that along the free trajectories the relative distance of at least one pair of particles becomes equal to σ for some value of t. Otherwise, the particles are not dynamically correlated

and the Ursell operators in (A-8) would vanish for all positions along these trajectories. Suppose that when the trajectories in Fig. A1 are retraced from top to bottom, the distance r_{21} is the first distance which becomes equal to σ. Then, the positions of the particles along the free trajectories can be characterized by

$$\vec{r}_{21} = \vec{r}_{21}(t) = \exp(t\mathcal{H}_3^{(o)})\ \hat{\vec{r}}_{21}(0) = \hat{\vec{r}}_{21}(0) + t\vec{V}_{21} \ ,$$

$$\vec{r}_{31} = \vec{r}_{31}(t) = \exp(t\mathcal{H}_3^{(o)})\ \vec{r}_{31}(0) = \vec{r}_{31}(0) + t\vec{V}_{31} \ , \tag{A-10}$$

where the notation $\hat{\vec{r}}_{21}(0)$ indicates that the distance $r_{21}(t)$ is equal to σ for $t = 0$. We take $\hat{\vec{r}}_{21}(0)$, $\vec{r}_{31}(0)$ and t as the new integration variables. In this new coordinate system $d\hat{\vec{r}}_{21}(0)$ is a two dimensional surface element. The Jacobian of this transformation is

$$d\vec{r}_{21}d\vec{r}_{31} = \vec{V}_{21}.\hat{\vec{r}}_{21}(0)d\hat{\vec{r}}_{21}(0)d\vec{r}_{31}(0)dt \ . \tag{A-11}$$

From the expression (2.4-15) for 0(123) we see that the integrand will give contributions in the three regions for which, respectively, $r_{21}<\sigma$, $r_{31}<\sigma$ and $r_{32}<\sigma$. Therefore, the upper limit for the integration over t can be taken at any value $t > 0$ corresponding to phases of receding particles. The lower limit has to be taken at a sufficiently negative value of t, so that the free trajectories will no longer intersect when retraced further backwards in time. As a consequence, all Ursell operators vanish at the lower limit of the t-integration.

In this new coordinate system

$$\mathcal{H}_3^{(o)} = \frac{\partial}{\partial t} \ , \tag{A-12}$$

since for any function $g(\vec{r}_{21},\vec{r}_{31},\vec{V}_1,\vec{V}_2,\vec{V}_3)$:

$$\mathcal{H}_3^{(o)} g(\vec{r}_{21},\vec{r}_{31},\vec{V}_1,\vec{V}_2,\vec{V}_3) = \mathcal{H}_3^{(o)} e^{\tau \mathcal{H}_3^{(o)}} g(\hat{\vec{r}}_{21}(0),\vec{r}_{31}(0),\vec{V}_1,\vec{V}_2,\vec{V}_3) =$$

$$= \frac{\partial}{\partial t} e^{t \mathcal{H}_3^{(o)}} g(\hat{\vec{r}}_{21}(0),\vec{r}_{31}(0),\vec{V}_1,\vec{V}_2,\vec{V}_3) = \frac{\partial}{\partial t} g(\vec{r}_{21},\vec{r}_{31},\vec{V}_1,\vec{V}_2,\vec{V}_3) \; .$$

Therefore, as pointed out by Green,[16] equation (A-8) transforms to

$$0(123) = \int d\hat{\vec{r}}_{21}(0) d\vec{r}_{31}(0) \vec{V}_{21}\cdot\hat{\vec{r}}_{21}(0) \int dt \left[\frac{\partial}{\partial t}U(123) - \sum_{\alpha\neq\beta}\sum\{\frac{\partial}{\partial t}U(\alpha) - U(\alpha)\frac{\partial}{\partial t}\}U(\beta)\right] . \tag{A-13}$$

In the first term of (A-13) the t-integration can be carried out immediately. The second term can be simplified by partial integration.

$$0(123) = \int d\hat{\vec{r}}_{21}(0) d\vec{r}_{31}(0) \vec{V}_{21}\cdot\hat{\vec{r}}_{21}(0) \left[U(123) - \sum_{\alpha\neq\beta}\sum\int dt \left\{\frac{\partial}{\partial t}U(\alpha)\right\}U(\beta)\right] . \tag{A-14}$$

To elucidate the result for the second time integral we shall consider as an example

$$0' = \int dt[\frac{\partial}{\partial t}U(13)]U(23) + \int dt[\frac{\partial}{\partial t}U(23)]U(13) \; . \tag{A-15}$$

We consider the three possible successions of two binary collisions in Figs. A2, A3 and A4 separately. We first evaluate (A-15) for phase points for which one encounters along the free trajectories the two collisions indicated in Fig. A2+). In the figure a circle indicates a collision between

+) In diagram A2 (when read from top to bottom) we disregard the possibility that the collision between 2 and 3 may cause a deflected path of 3 to collide with the original path of 1. The contribution of such an event is taken into account by diagram A3 (upon interchanging 1 and 2).

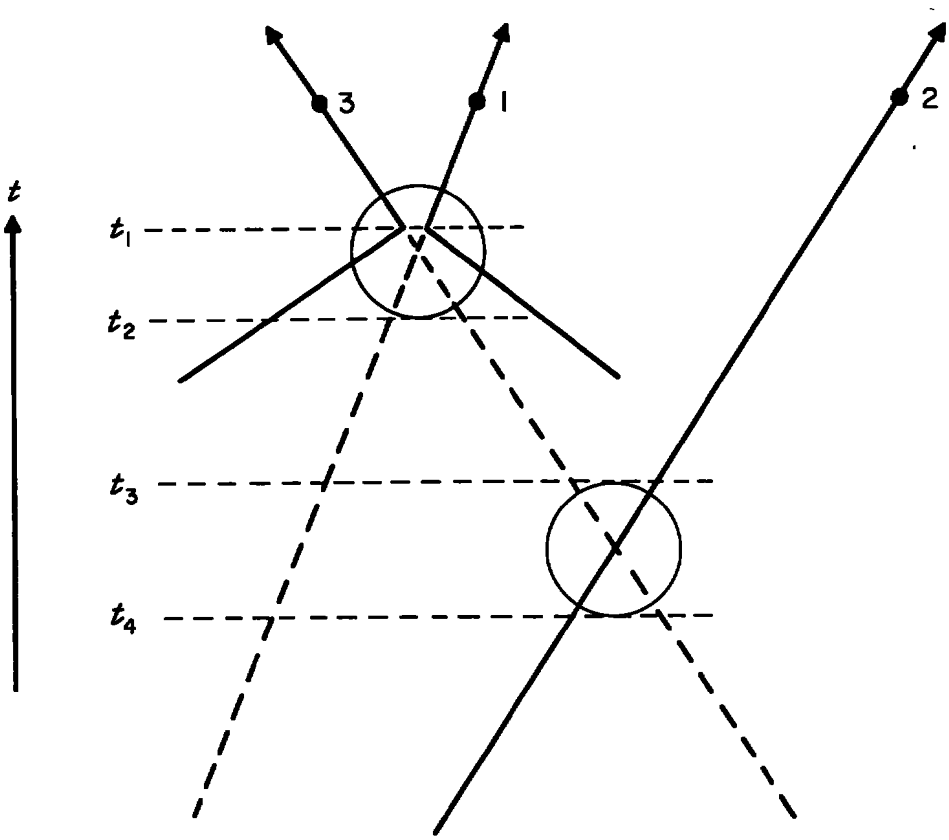

Figure A 2. Diagram of successive collisions leading to a contribution U(13)U(23) to the surface integral.

the particles whose trajectories are enclosed. In the case under consideration both particles 1 and 3 and particles 2 and 3 are aimed to collide. We have indicated the free trajectories by dotted lines when they have to be distinguished from the actual trajectories, if we would take into account the interaction between 1 and 3. Following the particles along their free trajectories, particles 1 and 3 are inside each other ($r_{31}(t)<\sigma$) during the time interval $t_2<t<t_1$ and particles 2 and 3 are inside each other during the time interval $t_4<t<t_3$.

For the evaluation of the first integral in (A-15) we have to study the variation of U(13) as a function of t along the free trajectories. For $t>t_1$ U(13) has a certain value which is constant, since the operators ultimately operate on functions of the velocities alone. For $t_2<t<t_1$ the operator $\mathcal{S}(13)$ creates infinite velocities; this contribution vanishes as a result of the normalization of the distribution function and U(13) can be taken as -1. Finally, for $t<t_2$, particles 1 and 3 are no longer aimed to collide and U(13) = 0. Thus

$$
\begin{aligned}
t>t_1 &: \quad U(13) = U(13) \\
t_2<t<t_1 &: \quad U(13) = -1 \\
t<t_2 &: \quad U(13) = 0 \quad .
\end{aligned}
\tag{A-16}
$$

Similarly

$$
\begin{aligned}
t>t_3 &: \quad U(23) = U(23) \\
t_4<t<t_3 &: \quad U(23) = -1 \\
t<t_4 &: \quad U(23) = 0 \quad .
\end{aligned}
\tag{A-17}
$$

It follows from (A-16) that the first integrand in (A-15) only contributes for $t = t_1$ and $t = t_2$:

$$
\int dt[\frac{\partial}{\partial t}U(13)]U(23) =
$$

$$
\lim_{\delta\to+0} \int_{t_1-\delta}^{t_1+\delta} dt[\frac{\partial}{\partial t}U(13)]U(23) + \lim_{\delta\to+0} \int_{t_2-\delta}^{t_2+\delta} dt[\frac{\partial}{\partial t}U(13)]U(23) .
$$

For hard spheres we can take δ arbitrarily small, so that U(23) does not vary during the interval δ. Thus

$$
\int dt[\frac{\partial}{\partial t}U(13)]U(23) = U(13)U(23)\Big|_{t_1-\delta}^{t_1+\delta} + U(13)U(23)\Big|_{t_2-\delta}^{t_2+\delta} \quad .
$$

The second term in (A-15) can be integrated in a similar way so that we obtain

$$0' = U(13)U(23)_{t_1+\delta} - U(13)U(23)_{t_1-\delta} + U(13)U(23)_{t_2+\delta} - U(13)U(23)_{t_2-\delta}$$

$$+ U(23)U(13)_{t_3+\delta} - U(23)U(13)_{t_3-\delta} + U(23)U(13)_{t_4+\delta} - U(23)U(13)_{t_4-\delta} \, , \qquad \text{(A-18)}$$

where the indices denote the values of t for which the operators have to be evaluated. From (A-16) and (A-17)

$$U(13)U(23)_{t_1+\delta} = U(13)U(23) \, ,$$

$$U(13)U(23)_{t_1-\delta} = U(23) \, ,$$

$$U(13)U(23)_{t_2-\delta} = U(23)U(13)_{t_4-\delta} = 0 \, ,$$

so that (A-18) reduces to

$$0' = U(13)U(23) + U(23) + U(13)U(23)_{t_2+\delta} + U(23)U(13)_{t_3+\delta}$$

$$- U(23)U(13)_{t_3-\delta} + U(23)U(13)_{t_4+\delta} \, . \qquad \text{(A-19)}$$

In order to evaluate the remaining terms in (A-19) we distinguish three different cases.

Case I: $t_4 < t_3 < t_2 < t_1$

In this case the two collisions are spatially separated. From (A-16) and (A-17) we conclude

$$U(13)U(23)_{t_2+\delta} = - U(23) \, ,$$

$$U(23)U(13)_{t_3+\delta} = U(23)U(13)_{t_3-\delta} = U(23)U(13)_{t_4-\delta} = 0 \, ,$$

so that (A-19) becomes

$$O' = U(13)U(23) \,. \tag{A-20}$$

Case II: $t_4<t_2<t_3<t_1$

In this case the collision between 2 and 3 starts while 1 and 3 are still overlapping. In this case

$$U(13)U(23)_{t_2+\delta} = +1 \;\; ; \;\; U(23)U(13)_{t_3+\delta} = -U(23);$$

$$U(23)U(13)_{t_3-\delta} = +1 \;\; ; \;\; U(23)U(13)_{t_4+\delta} = 0 \,,$$

so that (A-19) reduces to (A-20).

Case III: $t_2<t_4<t_3<t_1$

In this case the collision between 2 and 3 not only begins while 1 and 3 are overlapping, but 2 and 3 have also separated before 1 and 3 leave their overlapping configurations. We have

$$U(13)U(23)_{t_2+\delta} = 0 \;\; ; \;\; U(23)U(13)_{t_3+\delta} = -U(23) \,;$$

$$U(23)U(13)_{t_3-\delta} = +1 \; ; \;\; U(23)U(13)_{t_4+\delta} = +1,$$

so that (A-19) reduces again to (A-20).

Thus we conclude that for phase points represented by Fig. A2 the integral (A-15) leads to the result (A-20) regardless whether or not the collisions are spatially separated, provided that the collision between 2 and 3 begins after the collision between 1 and 3 started, when the diagram is retraced from top to bottom.

Using the same method one can prove that also

$$O' = U(13)U(23) \,, \tag{A-21}$$

for phase points represented by the diagram of Fig. A3. When the integration is carried out for phase points represented by Fig. A4, one finds[16]

$$0' = 0 \,. \tag{A-22}$$

Thus events of this kind do not contribute to the surface integral, although the operator U(13)U(23) itself would not vanish for $t>t_o$.

The contribution of any diagram containing two other successive binary collisions is obtained by permutation of the particle numbers. Thus for hard spheres (A-14) reduces to the surface integral as given by Green[16]

$$0(123) = \int d\hat{\vec{r}}_{21}(0) d\vec{r}_{31}(0)\ \vec{V}_{21}\cdot\hat{\vec{r}}_{21}(0)\ T(123) \,, \tag{A-23}$$

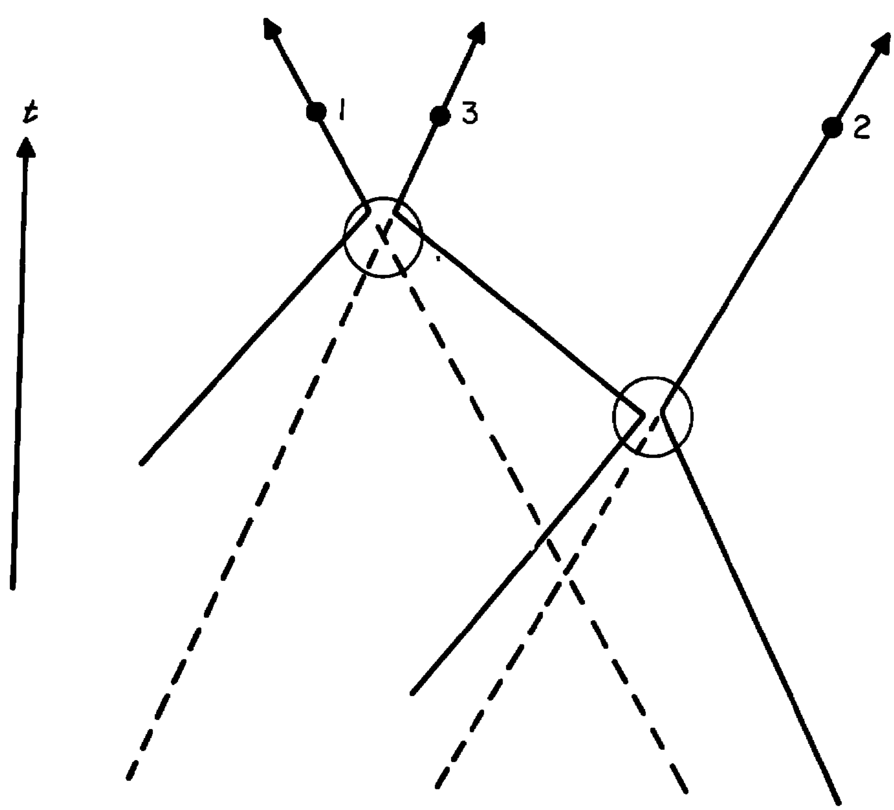

Figure A 3. Diagram of successive collisions leading to a contribution U(13)U(23) to the surface integral.

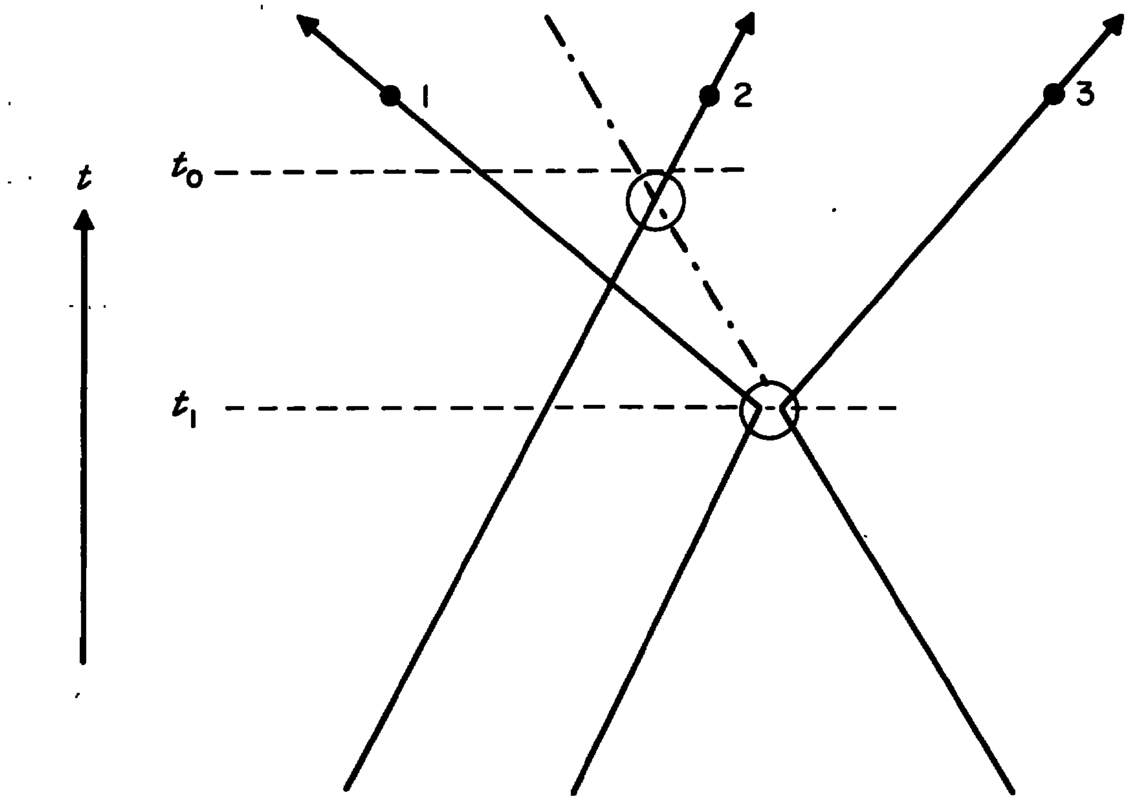

Figure A 4. Diagram of successive collisions not leading to any contribution to the surface integral, although U(13)U(23) $\neq$ 0 for $t>t_o$.

with

$$T(123) = U(123) - \sum_{\alpha>\beta}{}' \sum U(\alpha)U(\beta) . \tag{A-24}$$

The notation $\alpha>\beta$ indicates that the product $U(\alpha)U(\beta)$ should only be evaluated for successive binary collisions involving pairs α and β for which the α-collision occurs prior to the β-collision when the diagrams are retraced backwards in time. For example, if α=13 and β=23, U(13)U(23) should only be evaluated for the collision sequences shown in Fig. A2 and A3 (regardless, of course, of the occurrence of other collisions).

To evaluate the triple collision operator T(123) in more detail we introduce the following notation. Each binary collision in a collision sequence representing the dynamical history of a phase point will be indicated by listing the pairs whose interaction has to be taken into account successively for that particular collision to occur. For example, in Fig. A2 the first collision is denoted by (13) and the second collision by (23). In Fig. A3 the first collision is again denoted by (13), but the second collision is now denoted by (13)(23), since the collision between 2 and 3 occurs after the interaction between 1 and 3 has been taken into account. With this notation (A-24) can be written more specifically as

$$T(123) = U(123) - \sum_{(\alpha)>(\alpha)(\beta)}\sum \mathcal{S}(\alpha)U(\beta) + \sum_{(\alpha)>(\beta)}\sum U(\beta)\quad(\alpha\neq\beta)\,, \tag{A-25}$$

where the summation in the second term is to be taken over all pairs of collisions (α) and $(\alpha)(\beta)$ for which (α) occurs prior to $(\alpha)(\beta)$, and the summation in the third term over all pairs of collision (α) and (β) such that (α) occurs prior to (β).

The triple collision operator T(123) can be decomposed into a sum of operators, each of which is associated with a particular triple collision event:

$$T(123) = \sum_{\mu}\sum_{\text{perm}} T_{\mu}(\alpha_1;\alpha_2)\,, \tag{A-26}$$

Here we have indicated the possible pairs of particles by α_i $(i = 1,2,3)$. The operators $T_{\mu}(\alpha_1;\alpha_2)$ are defined in Section 2.5 for the specific example $\alpha_1 = 12$ and $\alpha_2 = 13$; α_1, α_2 refer to the pairs of particles involved in the first, resp. second collision. The first summation in (A-26) is to be taken over the six diagrams μ = R1, R2, C1, C2, H1, H2 and the second summation

over the six permutations of the particles 1, 2 and 3.

The validity of the addition theorem (A-26) for an arbitrary phase point can be demonstrated as follows. Let (α_1) be the first real collision in the diagram representing the dynamical history. If there is a second real collision, we assume that to be $(\alpha_1)(\alpha_2)$. As a consequence, $(\alpha_1)>(\alpha_1)(\alpha_2)$. We also have to consider hypothetical collisions of the type (α) and $(\alpha)(\beta)$. If there is only one hypothetical collision of the type (α), we suppose it is (α_2). If there are two hypothetical collisions of this type, we assume $(\alpha_2)>(\alpha_3)$. Then from (A-25) T(123) can be written as

$$T(123) = [\mathcal{S}(123) - \mathcal{S}(\alpha_1) - \mathcal{S}(\alpha_1)U(\alpha_2)] - \mathcal{S}(\alpha_1)U(\alpha_3)_{(\alpha_1)>(\alpha_1)(\alpha_3)}$$
$$- \sum_{\substack{(\alpha)>(\alpha)(\beta) \\ \alpha\neq\alpha_1}} \sum \mathcal{S}(\alpha)U(\beta) + U(\alpha_3), \quad (\alpha\neq\beta), \tag{A-27}$$

in which the conditions concerning the time order of the events are indicated where necessary. The sum of the first three terms between the brackets is only different from zero if there are three or more real collisions, thus if the conditions for either $R1(\alpha_1;\alpha_2)$ or $C1(\alpha_1;\alpha_2)$ are satisfied. In that case

$$\mathcal{S}(123) - \mathcal{S}(\alpha_1) - \mathcal{S}(\alpha_1)U(\alpha_2) = \mathcal{S}(123) - \mathcal{S}(\alpha_1)\,\mathcal{S}(\alpha_2),$$

which is just the contribution $T_{R1}(\alpha_1;\alpha_2)$ or $T_{C1}(\alpha_1;\alpha_2)$. The next term $\mathcal{S}(\alpha_1)U(\alpha_3)$ is different from zero, if there is a collision $(\alpha_1)(\alpha_3)$ such that $(\alpha_1)>(\alpha_1)(\alpha_3)$. This implies also that $(\alpha_1)>(\alpha_1)(\alpha_2)>(\alpha_1)(\alpha_3)$, since otherwise $(\alpha_1)(\alpha_3)$ would be a real collision contrary to our assumption. Thus the conditions for diagram $H1(\alpha_1;\alpha_2)$ are satisfied with contribution $T_{H1}(\alpha_1;\alpha_2) = -\mathcal{S}(\alpha_1)\,U(\alpha_3)$. Similarly, one easily verifies that the terms $-\mathcal{S}(\alpha)U(\beta)$, with $(\alpha)>(\alpha)(\beta)$ and $\alpha\neq\alpha_1$, are

only different from zero if the conditions for diagram $R2(\alpha_1;\alpha)$, when $\beta=\alpha_1$, or for diagram $C2(\alpha_1;\alpha)$, when $\beta\neq\alpha_1$, are satisfied, leading to the contribution $T_{R2}(\alpha_1;\alpha) = -\mathcal{S}(\alpha)U(\alpha_1)$ or $T_{C2}(\alpha_1;\alpha) = -\mathcal{S}(\alpha)U(\beta)$. Finally, the last term $U(\alpha_3)$ does not vanish if there is a collision (α_3). As a consequence of our assumption this implies $(\alpha_2)>(\alpha_3)$, so that the conditions for diagram $H2(\alpha_1;\alpha_2)$ are satisfied with the contribution $T_{H2}(\alpha_1;\alpha_2) = U(\alpha_3)$. This concludes the proof that T(123) can be represented as a sum of operators associated with the basic triple collision diagrams, as expressed by (A-26).

The result (A-26) for T(123) has to be substituted into expression (A-23) for O(123). Since the integrals in (2.4-16) for λ_1 and η_1 are symmetric in all three particles, it is sufficient to evaluate (A-26) only for one permutation of the particles and to multiply the result by 6. Thus, we replace O(123) in (2.4-16) by

$$O(123) = 6\ O(12;13) = 6 \sum_{\mu} \int d\hat{\vec{r}}_{21}(0)d\vec{r}_{31}(0)\ \vec{V}_{21}\cdot\hat{\vec{r}}_{21}(0)\ T_{\mu}(12;13)\ . \tag{A-28}$$

In (A-28), $\hat{\vec{r}}_{21}(0)$ and $\vec{r}_{31}(0)$ represent the relative position vectors at the time of the first collision in the diagrams of Fig. 4. Let $\vec{k}_1$ be the perihelion vector of the first collision, $\vec{k}_2$ the perihelion vector of the second collision, and τ the time between the first and the second collision. To specify the collision cylinder associated with the second collision, we have to make a distinction between the diagrams of the first kind in which this collision is real and the diagrams of the second kind in which this collision is hypothetical. Therefore, we define

$$\begin{aligned} &\vec{V}_{31}(1) = \vec{V}_{31}-(\vec{V}_{21}\cdot\vec{k}_1)\vec{k}_1, && (\mu = R1,\ C1,\ H1), \\ &\vec{V}_{31}(1) = \vec{V}_{31}, && (\mu = R2,\ C2,\ H2). \end{aligned} \tag{A-29}$$

Then $\vec{V}_{31}(1)$ is the relevant relative velocity to be considered for the second collision. In terms of these new variables, (A-28) transforms to

$$O(12;13) = \sum_{\mu} \sigma^4 \int d\vec{k}_1 \int d\vec{k}_2 \int d\tau \vec{V}_{21} \cdot \vec{k}_1 \vec{V}_{31}(1) \cdot \vec{k}_2 T_{\mu}(12;13). \tag{A-30}$$

It should be kept in mind that the integral in (A-23), and consequently in (A-30), is to be carried out over phase points corresponding to receding particles. This implies that in the evaluation of (A-30) one has to verify for any given $\vec{k}_1$, $\vec{k}_2$, and τ, that the particles will not suffer any collision in the future.

APPENDIX B. DYNAMICS OF A COLLISION BETWEEN TWO HARD SPHERES

Consider two hard spheres 1 and 2 with unit diameter. The relative position of 2 with respect to 1 is $\vec{r}_{21} = \vec{r}_2 - \vec{r}_1$ and the relative velocity $\vec{v}_{21} = \vec{v}_2 - \vec{v}_1$ at the initial time t = 0. The "impact vector" $\vec{b}_{21}$ (see Fig. B1) of the collision between 1 and 2 is related to the initial position $\vec{r}_{21}$ and initial velocity $\vec{v}_{21}$ by

$$\vec{b}_{21} = \frac{(\vec{v}_{21} \times \vec{r}_{21}) \times \vec{v}_{21}}{v_{21}^2} , \tag{B-1}$$

and the perihelion vector $\vec{k}$ of the collision

$$k = -\vec{b}_{21} + \hat{\vec{v}}_{21} \sqrt{1 - b_{21}{}^2} \ . \tag{B-2}$$

The two particles will experience a collision, if they approach each other

$$\vec{v}_{21} . \vec{r}_{21} < 0 , \tag{B-3}$$

and if the impact parameter b_{21} is smaller than the diameter ($\sigma = 1$)

$$(\vec{v}_{21} \times \vec{r}_{21})^2 - v_{21}^2 < 0 . \tag{B-4}$$

The time t at which the collision will take place is

$$t = - \frac{\hat{\vec{v}}_{21} . \vec{r}_{21} + \sqrt{1 - b_{21}^2}}{v_{21}} . \tag{B-5}$$

The velocities $\vec{v}_1'$, $\vec{v}_2'$ after the collision are related to the initial velocities $\vec{v}_1$, $\vec{v}_2$ by

$$\begin{aligned} \vec{v}_1' &= \vec{v}_1 + (\vec{v}_{21} . \vec{k})\vec{k} , \\ \vec{v}_2' &= \vec{v}_2 - (\vec{v}_{21} . \vec{k})\vec{k} . \end{aligned} \tag{B-6}$$

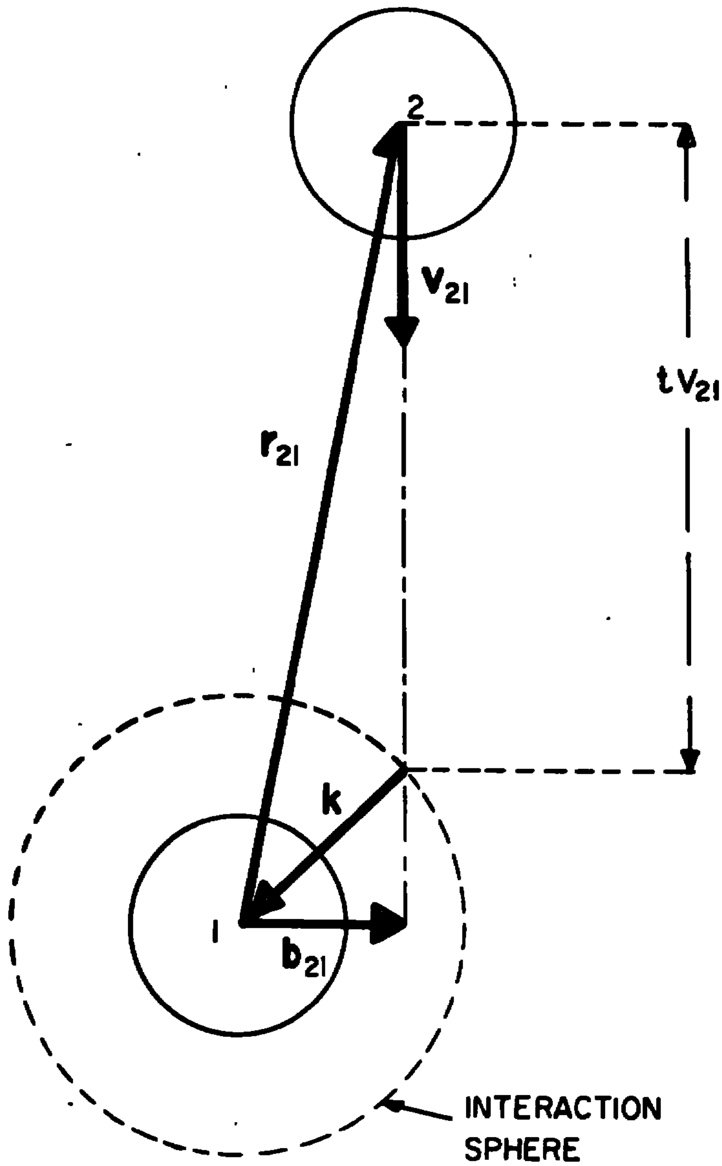

Figure B1. Geometry of a collision between two hard spheres.

REFERENCES

1. S. Chapman and T.G. Cowling, The Mathematical Theory of Nonuniform Gases, Cambridge Univ. Press, New York, 1939.

2. J.O. Hirschfelder, C.F. Curtiss and R.B. Bird, Molecular Theory of Gases and Liquids, John Wiley, New York, 1954.

3. H.J.M. Hanley and M. Klein, On the selection of the intermolecular potential function: application of statistical mechanical theory to experiment, NBS Technical Note 360, Washington, D. C., 1967.

4. Ref. 1, Chapter 16.

5. D.E. Stogryn and J.O. Hirschfelder, J. Chem. Phys. 31, 1531, 1545 (1959); 33, 942 (1960).

6. S.K. Kim and J. Ross, J. Chem. Phys. 42, 263 (1965); S.K. Kim, G.P. Flynn and J. Ross, J. Chem. Phys. 43, 4166 (1965).

7. D.K. Hoffman and C.F. Curtiss, Phys. Fluids 8, 890 (1965); C.F. Curtiss, M.B. McElroy and D.K. Hoffman, Int. J. Eng. Science 3, 269 (1965).

8. N.N. Bogoliubov, in Studies in Statistical Mechanics I, J. de Boer and G.E. Uhlenbeck, eds., North Holland Publ. Comp. Amsterdam, 1962, p. 5.

9. J.V. Sengers and E.G.D. Cohen, Physica 27, 230 (1961).

10. D. Burnett, Proc. London Math. Soc. 39, 385 (1935).

11. Ref. 1, Section 10.21.

12. S.T. Choh and G. E. Uhlenbeck, The kinetic theory of dense gases, Univ. Michigan, Ann Arbor, Michigan, Navy Theoretical Physics Contract No. Nonr 1224 (15), (1958).

13. M.S. Green, J. Chem. Phys. 25, 836 (1956); M.S. Green and R.A. Piccirelli. Phys. Rev. 132, 1388 (1963).

14. E.G.D. Cohen, Physica 28, 1025, 1045 (1962).

15. J.V. Sengers, Phys. Fluids 9, 1333 (1966).

16. M.S. Green, Phys. Rev. 136, A905 (1964).

17. G. Sandri, R.D. Sullivan and P. Norem, Phys. Rev. Letters 13, 743 (1964).

18. E.G.D. Cohen, in Boulder Lectures in Theoretical Physics 8A, Univ. Colorado Press, 1966, p. 145.

19. J. Weinstock, Phys. Rev. 132, 470 (1963).

20. G. Sandri and A.H. Kritz, Phys. Rev. 150, 92 (1966).

21. C.B. Haselgrove, Math. Computation 15, 323 (1961).

22. S. Haber, Math. Computation 20, 361 (1966).

23. B.J. Alder and T.E. Wainwright, Phys. Rev. Letters 18, 988 (1967).

24. Ref. 18, Appendix I.

25. J.R. Dorfman and E.G.D. Cohen, Phys. Letters 16, 124 (1965); J. Math. Phys. 8, 282 (1967).

26. J. Weinstock, Phys. Rev. 140, A460 (1965).

27. R. Goldman and E.A. Frieman, J. Math. Phys. 8, 1410 (1967).

28. J.V. Sengers, Phys. Rev. Letters 15, 515 (1965).

29. K. Kawasaki and I. Oppenheim, Phys. Rev. 139, A1763 (1965).

30. L.K. Haines, thesis, Univ. Maryland (1966).

31. J.V. Sengers, Phys. Fluids 9, 1685 (1966).

32. J.V. Sengers, in Lectures in Theoretical Physics, Vol. 9C, "Kinetic Theory", W. E. Brittin, editor, Gordon and Breach, New York, 1967, p. 335.

33. H.J.M. Hanley, R.D. McCarty and J.V. Sengers, J. Chem. Phys. 50, ... (1969).

34. J.M.H. Levelt Sengers, in Proc. 4th Symp. Thermophysical Properties, J.R. Moszynski, ed., ASME, New York, 1968, p. 37.

35. A. Michels, J.C. Abels, C.A. Ten Seldam and W. De Graaff, Physica 26, 381 (1960).

36. J.C.R. Li, Statistical Inference, Edwards Brothers, Inc., Ann Arbor, Michigan, 1964; A.M. Mood and F.A. Grayhill, Introduction to the Theory of Statistics, McGraw-Hill, New York, 1963.

37. J.V. Sengers, W.T. Bolk and C.J. Stigter, Physica 30, 1018 (1964).

38. A. Michels, J.V. Sengers and P.S. Van der Gulik, Physica 28, 1201 (1962).

39. B. LeNeindre, P. Bury, R. Tufeu, P. Johannin and B. Vodar, NBS Special Publ. 302, D.R. Flynn and B.A. Peavy, eds., U. S. Government Printing Office, Washington, D. C.. 1968, p. 579.

40. I.F. Golubev and I.B. Shpagina, Gaz. Prom. 11, 40 (1966).

41. D.B. Mann, NBS Technical Note 154, 1962.

42. H.M. Roder, National Bureau of Standards, private communication.

43. B. Le Neindre, private communication.

44. A. Michels, J.V. Sengers and L.J.M. Van de Klundert, Physica 29, 149 (1963).

45. H. Ziebland and J.T.A. Burton, Brit. J. Appl. Phys. 9, 52 (1958).

46. A. Gosman, thesis, Univ. Iowa, Iowa City, 1966.

47. P. Johannin, J. Rech. Centre Natl. Rech., Lab. Bellevue (Paris) 4, 116 (1958).

48. T.R. Strobridge, NBS Technical Note 129 (1962).

49. J. Kestin and W. Leidenfrost, Physica 25, 1033 (1959).

50. G.P. Flynn, R.V. Hanks, N.A. Lemaire and J. Ross, J. Chem. Phys. 38, 154 (1963).

51. N.J. Trappeniers, A. Botzen, H.R. Van den Berg and J. Van Oosten, Physica 30, 985 (1964).

52. J. Kestin and H.E. Wang, Trans. ASME 80, 11 (1958).

53. A. Michels, A. Botzen and W. Schuurman, Physica 20, 1141 (1954).

54. N.J. Trappeniers, A. Botzen, J. Van Oosten and H.R. Van den Berg, Physica 31, 945 (1965).

55. R.D. Gibson, thesis, Univ. Amsterdam, 1933.

56. A.K. Barua, M. Afzal, G.P. Flynn and J. Ross, J. Chem. Phys. 41, 374 (1964).

57. A. Michels, A.C.J. Schipper and W.H. Rintoul, Physica 19, 1011 (1953).

58. N.J. Trappeniers, A. Botzen, C.A. Ten Seldam, H.R. Van den Berg and J. Van Oosten, Physica 31, 1681 (1965).

59. J.P. Boon, J. C. Legros and G. Thomaes, Physica 33, 547 (1967).

60. H.J.M. Hanley, NBS Technical Notes 333, 350, 352.

61. J.T.F. Kao and R. Kobayashi, J. Chem. Phys. 47, 2836 (1967).

62. R.A. Piccirelli, J. Math. Phys. 7, 922 (1966).

DOCUMENT CONTROL DATA - R & D

(Security classification of title, body of abstract and indexing annotation must be entered when the overall report is classified)

1. ORIGINATING ACTIVITY *(Corporate author)*
National Bureau of Standards
Washington, D. C. 20234

2a. REPORT SECURITY CLASSIFICATION
None

2b. GROUP
N/A

3. REPORT TITLE
Triple Collision Effects in the Thermal Conductivity and Viscosity of Moderately Dense Gases

4. DESCRIPTIVE NOTES *(Type of report and inclusive dates)*
February 1, 1966, to September 1, 1968 - Final Report

5. AUTHOR(S) *(First name, middle initial, last name)*
Jan V. Sengers

6. REPORT DATE	7a. TOTAL NO. OF PAGES	7b. NO. OF REFS
March 1969	166	62

8a. CONTRACT OR GRANT NO.
DO (40-600) 66-494

b. PROJECT NO.
8951

c.
Program Element 6144501F

d. Task 02

9a. ORIGINATOR'S REPORT NUMBER(S)
AEDC-TR-69-68

9b. OTHER REPORT NO(S) *(Any other numbers that may be assigned this report)*
N/A

10. DISTRIBUTION STATEMENT
This document has been approved for public release and sale; its distribution is unlimited.

11. SUPPLEMENTARY NOTES
Available in DDC

12. SPONSORING MILITARY ACTIVITY
Arnold Engineering Development Center, Air Force Systems Command, Arnold Air Force Station, Tenn.

13. ABSTRACT

A quantitative study is made of the effect of successive correlated binary collisions on the transport properties of gases. In particular, the triple collision transport integrals determining the first density coefficients of thermal conductivity and viscosity are derived for a gas of hard spherical molecules and estimates are presented for these integrals. By applying the method to a two dimensional gas of hard disks, a logarithmic density dependence of the transport coefficients is demonstrated. In addition, an analysis is made of experimental data for the transport properties as a function of density. It is shown that the theoretically predicted density dependence is at least consistent with the experimental information. Experimental values for the first density coefficients of thermal conductivity and viscosity are reported, together with an assessment of their precision.

DD FORM 1 NOV 65 1473

14 KEY WORDS	LINK A		LINK B		LINK C	
	ROLE	WT	ROLE	WT	ROLE	WT
Transport properties						
Thermal conductivity						
Viscosity						
Triple collisions						
Dense gases						
Hard spheres						
Hard disks						

1. Gases - - -

2 " - - -

3 " - - -